Towards artifact-free auditory evoked potentials in cochlear implant users

Der Fakultät für Mathematik und Naturwissenschaften
der Carl von Ossietkzy Universität Oldenburg
angenommene Dissertation zur Erlangung
des Grades und Titels eines

Doctor rerum naturalium (Dr. rer. nat.)

von Frau Filipa Alexandra Campos Viola

geboren am 01.01.1982 in Beja, Portugal.

Gutachter: Prof. Dr. Stefan Debener

Zweitgutachter: Prof. Dr. Christoph Herrmann

Tag der Disputation: 30.11.2011

Erklärung nach § 10 Abs. 2 der Promotionsordnung der Fakultät für Mathematik und Naturwissenschaften der Carl von Ossietzky Universität Oldenburg vom 11. Dezember 2003

Hiermit erkäre ich, dass ich die Arbeit selbständig verfasst und nur die angegeben Hilfsmittle benuzt habe. Die Dissertation ist bereits in Gänze veröffentlicht.

Oldenburg, den _____ _____

Unterschrift

Erklärung nach § 10 Abs. 3 der Promotionsordnung der Fakultät für Mathematik und Naturwissenschaften der Carl von Ossietzky Universität Oldenburg vom 11. Dezember 2003

Hiermit erkäre ich, dass die Dissertation weder in ihrer Gesamtheit noch in Teilen einer anderen wissenschaftlichen Hochschule zur Begutachtung in einem Promotionsverfahren vorliegt oder vorgelegen hat.

Oldenburg, den _____ _____

Unterschrift

Abstract

Cochlear implants (CI) are neural prostheses that mimic the function of the healthy cochlea and deliver electrical stimulation to the auditory nerve, allowing individuals suffering from sensorineural hearing loss to recover a large amount of hearing function. Although CIs are regarded as one of the great achievements of modern medicine, the outcomes after implantation are variable, and it is not well understood how the auditory cortex adapts to the electrical stimulation delivered by the CI. An objective and non-invasive method for assessing auditory rehabilitation after implantation is by using electroencephalography (EEG) to measure auditory evoked potentials (AEPs). However EEG signals consist of a mixture of an unknown number of brain and non-brain contributions, the latter also called artifacts. The non-brain signals can be divided into two categories: biological and non-biological artifacts. CI devices cause non-biological electrical artifacts

These artifacts corrupt and mask the AEPs, since they are time-locked to auditory stimuli, and therefore cannot be attenuated using standard techniques such as filtering or averaging. A particularly promising technique to deal with CI artifacts is independent component analysis (ICA). This technique can disentangle multi-channel EEG signals into a number of artifacts and brain-related signals, also called independent components (ICs). When using an ICA-based attenuation approach, the ICs related to artifacts can be removed, and a corrected version of the original EEG signal can be obtained. However, the identification and interpretation of ICs is time-consuming and involves subjective decision making.

In *Study 1* a tool tailored to identify ICs representing eye blinks, lateral movements and heartbeat artifacts was developed and validated. The tool is based on the correlation of ICA inverse weights, also called IC scalp maps, with a user-defined template map, thus it was named CORRMAP. The performance of the tool was compared with the performance of 11 raters from different laboratories familiar with ICA. The overlap between ICs selected by CORRMAP and by the raters was substantial, providing evidence that the tool offers an efficient way of attenuating these particular artifacts.

In *Study 2* the effects of CI artifact attenuation on AEP quality were investigated in a sample of 18 adult post-lingually deafened individuals, using different types of CIs. Here ICs related to CI artifacts were selected by visual inspection and AEPs were reconstructed. It was found that AEPs from CI users were systematically correlated with

age, indicating that individual differences were well preserved. CI users with large signal-to-noise ratio AEPs were characterized by a significantly shorter duration of deafness. The ability of ICA in attenuating the CI artifact while preserving the AEPs was evaluated using a simulation study where datasets from normal hearing listeners were previously contaminated with CI artifacts. Results revealed very high spatial correlations between original and recovered normal hearing AEPs.

In *Study 3* a tool tailored to identify ICs related to the CI artifact was developed and validated. The CI Artifact Correction (CIAC) algorithm evaluates temporal and topographical properties of ICs, in order to objectively identify components representing the CI artifact. CIAC was tested on EEG data from two different experiments. The first consisted of datasets from the 18 CI users evaluated in *Study 2*. The second consisted of independent datasets recorded from 12 out of the 18 CI users at a different time point after implantation. CIAC sensitivity and specificity was compared to the manual IC selection performed by two experts. Results revealed both good sensitivity and specificity. A correlation between age and AEP amplitude was observed, replicating the findings from *Study 2* and confirming the algorithm's validity. High test-retest reliability for AEP N1 amplitudes and latencies also suggested that CIAC based attenuation reliably preserves plausible individual response characteristics.

Overall the results confirm that after ICA-based attenuation of CI artifacts, good quality AEPs can be recovered. This is highly important as it facilitates the objective, non-invasive study of auditory cortex function in CI users. With CORRMAP and CIAC efficient, convenient and objective tools were developed to attenuate biological and CI artifacts in EEG data. Both tools have been published and can be used by interested scientists.

Zusammenfassung

Cochlea Implantate (CI) sind Innenohrprothesen mit denen die Funktion einer gesunden Cochlea nachgeahmt wird. Dies geschieht durch eine elektrische Stimulation des auditorischen Nerven. Mit Hilfe von CIs kann bei Personen mit einem sensorineuralen Hörverlust der Höreindruck zu einem großen Teil wieder hergestellt werden. Obwohl CIs als eine der wichtigen Errungenschaften der modernen Medizin gelten, ist der Erfolg der Implantation sehr variabel. Auch ist bisher wenig darüber bekannt, inwieweit sich der auditorische Kortex an das elektrische Signal des CIs anpasst. Die Elektroenzephalographie (EEG) ist eine objektive und nicht invasive Methode mit der mittels akustisch evozierter Potenziale (AEPs) die auditorische Rehabilitation nach der Implantation eingeschätzt werden kann. Zu dem an der Kopfoberfläche gemessenen EEG Signal tragen jedoch verschiedene zerebrale und nicht zerebrale Aktivitäten bei, letztere werden auch als Artefakte bezeichnet. Diese können wiederum unterteilt werden in biologische und nicht biologische Artefakte. CIs verursachen nicht biologische, elektrische Artefakte.

CI-Artefakte verschlechtern und überdecken die AEPs. Da sie zeitlich an den akustischen Stimulus gekoppelt sind können sie jedoch nicht mittels der gängigen Techniken der Artefaktbereinigung wie z.B. Filtern oder Mittelung reduziert werden. Ein sehr vielversprechender alternativer Ansatz zur Korrektur der durch CIs verursachten elektrischen Artefakte ist die independent component analysis (ICA, unabhängige Komponenten Analyse). Mit Hilfe der ICA können verschiedene Artefakte und gehirnbezogene Signale aus einem Multikanal-EEG-Signal extrahiert werden, die sogenannten independent components (ICs, unabhängige Komponenten). Werden die artefaktbezogenen ICs aus dem EEG entfernt erhält man eine korrigierte, weitgehend artefaktfreie Version des EEGs. Ein großes Problem stellt jedoch die Identifikation und Interpretation der ICs dar, da sie einerseits sehr zeitaufwendig ist und andererseits häufig subjektive Entscheidungen beinhaltet.

In *Studie 1* wurde CORRMAP entwickelt und validiert. CORRMAP ist ein Verfahren mit dessen Hilfe die Identifikation von ICs für die häufigsten biologischen Artefakte Blinzeln, seitliche Augenbewegungen und Herzschlag möglich ist. Grundlage von CORRMAP ist die Korrelation der inversen Gewichte aller ICs einer ICA mit den inversen Gewichten einer durch den Nutzer ausgewählten, für den jeweiligen Artefakt prototypischen IC. Das inverse Gewicht einer IC reflektiert die topographische Verteilung

der IC und wird deswegen auch als IC scalp map bezeichnet. Für Die Validierung von CORRMAP wurden drei verschiedene Datensätze herangezogen. Die von CORRMAP identifizierten Artefakt-ICs wurden mit den von 11 unabhängigen Experten identifizierten Artefakt-ICs verglichen. Die Übereinstimmung zwischen CORRMAP und den Experten war beachtlich. Dies zeigt das häufige biologische EEG Artefakte mit CORRMAP effizient identifiziert und reduziert werden können.

In *Studie 2* wurden an einer Stichprobe von 18 postlingual ertaubten Erwachsenen die Effekte der CI-Artefaktreduktion auf die Qualität der AEPs untersucht. Dabei wurden die zu den CI-Artefakten gehörenden ICs manuell selektiert und entfernt, und die AEPs rekonstruiert. Das Signal-Rausch-Verhältnis der korrigierten AEPs war deutlich besser bei CI-Trägern mit kürzerer Dauer der Gehörlosigkeit. Die Amplitude der rekonstruierten AEPs der CI-Nutzer zeigte die typische systematische Korrelation mit dem Alter. Die Bewahrung individueller Unterschiede im AEP deutet auf eine gute Qualität der rekonstruierten AEPs hin. Mit Hilfe einer Simulation wurde weiterhin evaluiert inwieweit die ICA CI-Artefakte verringert und gleichzeitig die AEPs erhält. Datensätze von normal hörenden Personen wurden mit einem CI-Artefakt belegt. Der CI-Artefakt wurde mittels ICA aus den simulierten CI-Datensätzen entfernt. Rekonstruiert und originale AEPs wurden miteinander korreliert. Dabei wurden sehr hohe räumliche Korrelationen zwischen den ursprünglichen und den wiederhergestellten AEPs erzielt. Dies ist ein weiterer Beleg für die gute Qualität der rekonstruierten AEPs.

In *Studie 3* wurde ein CI-Artefakt-Korrektur-Algorithmus (CIAC, CI Artifact Correction) entwickelt und validiert. CIAC bewertet zeitliche und topographische Eigenschaften der ICs, um CI-bezogene Komponenten auf objektive Weise zu identifizieren. CIAC wurde an EEG-Daten aus zwei verschiedenen, unabhängigen Experimenten getestet. Bei dem ersten Datensatz handelt es sich um die für Studie 2 erhobenen Daten. Der zweite Datensatz enthält Daten für 12 der 18 CI-Nutzer aus Studie 2. Diese wurden in einem unabhängigen Experiment erhoben. Die Sensitivität und Spezifität von CIAC wurde verglichen mit einer manuellen IC-Selektion durch zwei Experten. Die Ergebnisse zeigen sowohl eine gute Sensitivität als auch eine gute Spezifität von CIAC. Auch in dieser Studie zeigte sich eine Korrelation zwischen dem Alter und der Amplitude der AEPs, wodurch das Ergebnis aus Studie 2 repliziert und die Validität des Algorithmus bestätigt wurde. Die hohe Test-Retest-Reliabilität zwischen den beiden Datensätzen für die N1-Amplitude und Latenz der AEPs weist darauf hin, dass bei einer Reduktion des CI-

Artefaktes basierend auf CIAC die individuellen Merkmale der Reaktionen erhalten bleiben.

Die Ergebnisse der vorliegenden Arbeit belegen, dass durch eine ICA-basierte Reduktion von CI-Artefakten AEPs in einer guten Qualität wiederhergestellt werden können. Dies ist die Voraussetzung für eine objektive, nicht invasive Untersuchung der Funktionen des auditorischen Kortex bei CI-Nutzern. Mit CORRMAP und CIAC wurden effiziente, praktische und objektive Verfahren zur Identifikation und somit Reduktion von biologischen und CI-Artefakten entwickelt. Beide Verfahren wurden veröffentlicht und sind somit für interessierte Wissenschaftler zugänglich.

Contents

Acknowledgements

This work is dedicated to my “families”, to whom I’m truly grateful.

First of all it is dedicated to my parents and my sister. Second it is dedicated to my “Doktorvater”, Stefan Debener, and my “Doktorbruder”, Jeremy Thorne. Both have been by my side since the very first day, and make it all possible.

It is also dedicated to four other “families”:

In Southampton: Jessica de Boer, Jemma Hine, Brigitte Lavoie, Roger Thornton, Angie Barks, Sue Mooney, David Olley, Stefan Bleeck, Julie Eyles, and Ragvinder Pahal.

In Jena: Janneke Terhaar, Thomas Weiss, Teresa Görtz, Ralph Huonker, Stefan Clauß, Thomas Heuchel, Christoph Kurzbuch, Ana Magina, Artur Moro, Luis Figueiredo, and Marie Fischer.

In Oldenburg: Maarten De Vos, Pascale Sandmann, Nadine Hauthal, Jolanda Janson, Janani Dhinakaran, Cornelia Kranczioch, Reiner Emkes, Alexander Förstel, and Ulrike Bayer.

My new family: Michael Groen and our future family.

I must also thank the Fundacao para a Ciencia e Tecnologia, Lisbon, Portugal for the financial support that enabled me to develop this project (SFRH/BD/37662/2007).

A special thanks to Helio Pais, who convinced me to start a “PhD”.

A special thanks to all who have inspired me.

List of figures

List of tables

List of abbreviations

ACE – Advanced combination encoders

AEP – Auditory evoked potential

ARHL – Age related hearing loss

AV – Audiovisual

BKB – Bamford-Kowal-Bench

BKB-SIN – Bamford-Kowal-Bench Speech-in-Noise (BKB-SIN)

BOLD – Blood-oxygenation-level-dependent

BTE – Behind-the-ear

CI – Cochlear implant

CIAC – Cochlear implant artifact correction

CNC – Consonant-nucleus-consonant

dB – Decibel

ECG – Electrocardiography

EEG – Electroencephalography

ERP – Event-related potential

ESS – Environmental sounds study

FDA – Food and drug administration

FSP – Fine structure processing

fMRI – Functional magnetic resonance imaging

HEP – Heartbeat evoked potential

HINT – Hearing in noise test

HiRes-S – High resolution with fidelity 120

HL – Hearing level

IC – Independent component

ICA – Independent component analysis

IHC – Inner hair cells

LE – Left ear

M – Mean

MCG – Magnetocardiography

MEG – Magnetoencephalography

Mdn – Median

MLR – Middle latency response

MMN – Mismatch negativity

MRI – Magnetic resonance imaging

NH – Normal hearing

NIRS – Near-infrared spectroscopy

OHC – Outer hair cells

ODR – Optimized differential reference

PC – Personal computer

PET – Positron emission tomography

PN – Pyramidal neuron

RE – Right ear

RF – Radio frequency

RMS – Root mean square

RV – Residual variance

SD – Standard deviation

SI – Similarity index

SNHL – Sensorineural hearing loss

SNR – Signal-to-noise ratio

SPL – Sound pressure level

SPEAK – Spectral peaking code

TNS – Tones and noise study

V – Visual

VEP – Visual evoked potential

UK – United Kingdom

USA – United States of America

WHO – World health organization

1. Overview

The structure of this thesis consists of an introduction, followed by a chapter describing the main objectives of the empirical studies, and then three independent chapters with a detailed description of each study. The last chapter consists of a general discussion that concludes the thesis. The work presented here was developed between 2008 and 2011 in the following research institutes: Medical Research Council, Institute of Hearing Research, Southampton, UK (Jan 2008 – Dec 2008); Biomagnetic Centre, Department of Neurology, Jena University Hospital, Germany (Jan 2009 – Dec 2009); Neuropsychology Laboratory, Department of Psychology, University of Oldenburg, Germany (Jan 2010 – present).

1.1. Chapter-by-chapter overview

Chapter 2

This is an introductory chapter where background information about the main techniques and methods used in the empirical studies, e.g. electroencephalography (EEG), auditory evoked potentials (AEPs), and independent component analysis (ICA), is briefly described. The assessment of AEPs in cochlear implant (CI) users is discussed. A literature overview is provided and CI technology is described.

Chapter 3

The motivation for the three empirical studies presented in the following chapters is described. Two studies focused on the improvement of signal processing tools that need to be applied when using multi-channel EEG and AEPs to investigate auditory cortical rehabilitation in CI users. The other evaluated the quality of AEPs from CI users and further validated the use of an ICA-based approach to attenuate CI artifacts from EEG recordings.

Chapter 4

This chapter describes *Study 1* where an ICA-based tool, named CORRMAP, was developed to select objectively ICs representing ocular and heartbeat activity. The main input of the tool is the scalp map from an IC representing one of the target artifacts. This template is correlated with the scalp maps from other ICs. The selected ICs are those for which the correlation value exceeds a threshold. The performance of the tool was compared with 11 independent raters familiar with ICA. Results of the validation study and the advantages of this new tool are discussed.

Chapter 5

This chapter describes *Study 2* where 68-channnel EEG was recorded from 18 adult post-lingually deafened CI users stimulated with environmental sounds. First, the ability of ICA to attenuate electrical artifacts caused by the CI was investigated. Second, the ability to preserve the brain responses of interest in the EEG data after ICA-based attenuation was investigated. Third, the quality of reconstructed AEPs was assessed using signal-to-noise ratio (SNR) measurements. The relationship between AEPs and clinical parameters was also assessed. The validity of ICA as a suitable technique to attenuate CI artifacts while preserving brain responses is discussed. The application of AEPs as an objective measurement of auditory rehabilitation in CI users is also highlighted.

Chapter 6

This chapter describes *Study 3* where an ICA-based algorithm tailored to select ICs representing the CI artifact was implemented. The algorithm, called Cochlear Implant Artifact Correction (CIAC), evaluates temporal and spatial information from the ICs, in order to find those ICs representing the CI artifact. CIAC was evaluated using two different EEG study sets. The sensitivity and specificity of CIAC was compared to the manual selection performed by two experts. AEPs were reconstructed after automatic CI artifact attenuation and evaluated. The advantages of CIAC and the AEP findings are discussed.

Chapter 7

A general discussion of the results and their implications concludes the thesis. First the main results from the three empirical studies are summarized. The tools developed in *Study 1* and *Study 3*, due to their similar frameworks, are jointly discussed. The relevance of the AEP findings from *Study 2* and *Study 3* is reviewed. Lastly the further validation and implementation of ICA-based tools to select objectively ICs is also discussed, and future directions for AEP studies with CI samples are suggested.

2. Introduction

2.1. Electroencephalography

EEG measures scalp electrical activity generated by the brain. It is a non-invasive technique since the electrical activity is recorded using electrodes attached to the scalp. EEG can be applied repeatedly to patients, healthy adults, and children, with virtually no risk or limitation (Teplan, 2002).

Hans Berger (1873-1941), a German psychiatrist, performed the first human EEG recording in the early 1920s. He was also the first to show evidence that EEG brain activity reflects functional mental states, such as attention and drowsiness (Berger, 1929). Later it was observed that neural responses associated with specific sensory, cognitive and motor events, could be extracted from the recorded signal using averaging techniques (Davis, 1939). Such averaged responses are called event-related potentials (ERPs).

The focus here is on using EEG to investigate auditory cortical functions in a clinical population of CI users. In the following sections the recording of high-density EEG in research settings is described (2.1.1), followed by the computation of ERPs with a special focus on AEPs (2.1.2). In the last section (2.1.3) the different types of artifacts that can be present in the recorded signal are described briefly, as well as procedures to minimize artifact contributions.

2.1.1. Recording the electroencephalogram

The surface of the human cortex has a very particular layout, being a convoluted, layered sheet of tissue, with a thickness of 2-3 mm but with a surface area of several hundred square cm (Shipp, 2007). As described by Schaul (1998), it is known that the electrical activity of the brain results from ionic currents generated by biochemical processes at the cellular level. The cortical cells that are thought to be the principal EEG generators are called pyramidal neurons (PNs). These neurons are arranged in columns and their apical dendritic branches are perpendicular to the cortical surface, as described first by Lorente de No (1947), and illustrated here in Figure 2.1. The synchronous activation of PNs generates coherent electric fields, which are referred to as an “open field”. This is due to the fact that PNs are akin to “current dipoles”, i.e. these neurons have two opposite charge poles. The open electrical fields are transmitted from generators, the PNs, through biological tissues. The human head acts then as a volume conductor and the electrical fields can be detected at the scalp surface by means of attached electrodes (Figure 2.1). It is also noteworthy the EEG convention of plotting the signals with negativity upward

used in Figure 2.1. This convention dates to the 1930s when ERP research started. It seems that in those days neurophysiologists plotted negative upward, possibly because this allowed an action potential to be plotted as an upward-going spike (Luck, 2005, cf. chapter 1). The negative upward convention will be used through this text.

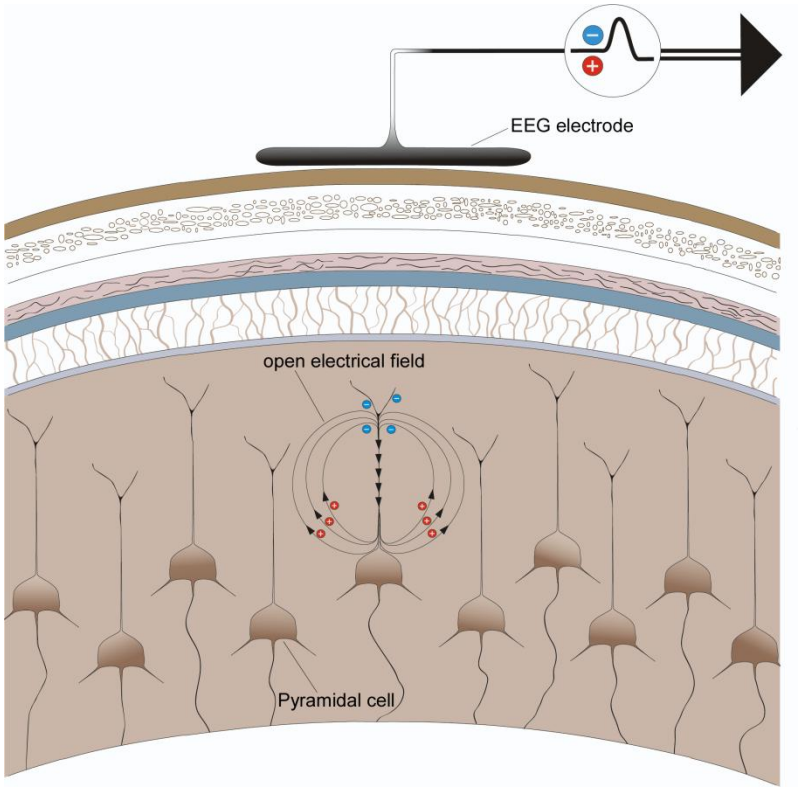

Figure 2.1 *The generation of open electrical fields by synaptic currents in pyramidal neurons. The EEG electrode (referenced to a second electrode some distance away) measures this pattern through thick tissue layers. Notice the EEG convention of plotting the signals with negativity upward (blue) (adapted from Bear, Connors, & Paradiso, 2007).* [1]

The size, shape and duration of the EEG waves are influenced by the orientation of the neural generators, their synchrony, and their distance to the recording electrode (Schaul, 1998). However the estimation of the neuronal sources responsible for a given scalp potential is not trivial, since there is no unique solution. The number of possible source configurations that give rise to a given set of measured scalp potentials is infinite and assumptions about the nature of the sources are required (Slotnick, 2005). These assumptions imply for instance *a priori* knowledge of functional neural anatomy, and conductance properties of biological tissues. This framework is called the inverse

[1] All figures reproduced or adapted in this work were reprinted with the permission from publishers or authors.

problem of EEG. Details can be found in specialized text books (Handy, 2005; Lopes da Silva, 2010; Luck, 2005).

A schematic of the different steps involved both in the EEG recording session and in the analysis of the data is shown in Figure 2.2. The first step consists of attaching electrodes to the scalp using a conductive gel or paste which establishes the connection between the electrode and the skin, while the final goal is to evaluate brain activity. The steps inbetween involve the use of electronic devices such as amplifiers with filters, analog-digital converters, recording devices, and at the last stage a computer to store the data and to perform the signal processing analysis. Briefly, the electrodes read the signal from the scalp surface, amplifiers enhance the microvolt signals into a range where they can be digitalized accurately, the converter changes signals from analog to digital form, and a computer using suitable recording software stores and displays obtained data (Teplan, 2002).

The minimum number of electrodes necessary to perform an EEG recording is three: ground, reference and active electrode. A basic electrical circuit needs to be created in order to measure potential changes over time between the pair active-ground and the pair reference-ground. There is no agreement for the placement of the reference electrode, common locations being the ear lobe or the nose tip, as neuronal activity is assumed to be low at these locations. The quality of the recorded signal is highly dependent on the proper function and preparation of the recording electrodes. For instance, it is important that the impedance at electrode sites is low. However recommendations vary according to the type of EEG system. Other authors have also investigated in detail the effects of electrode impedance on data quality (Kappenman & Luck, 2010).

Many EEG systems allow simultaneous recording from between 30 and 256 electrodes, which can be arranged in different montages. The era of high-density EEG recordings was made possible due to the rapid advances in computer technology observed in the last two decades. These high-density recordings have the advantage of allowing the computation of 2D or 3D topographic maps, which complement the high temporal resolution, and can contribute to a better estimation of the localization of neural generators. On the other hand, the larger the number of electrodes, the longer the preparation of the recording session becomes, as well as the computation time needed for the analysis. More details about recording procedures and electrode montages have been discussed in the literature (Handy, 2005; Luck, 2005; Picton, Lins, & Scherg, 1995).

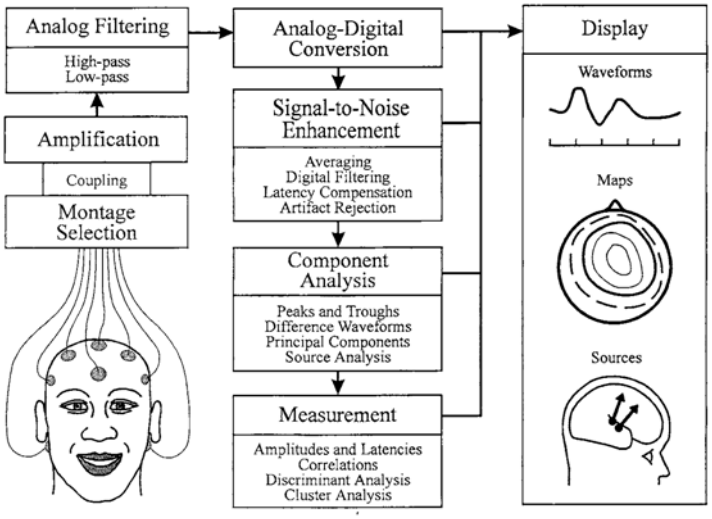

Figure 2.2 *Illustration of different procedures involved in recording human ERPs. The left column shows the procedures involved in recording the electrical activity from the scalp. The middle column shows the procedures for analyzing these signals on a digital computer. The right column shows various means displaying the measured activity (from Picton, et al., 1995).*

2.1.2. Event related potentials

ERPs are small voltage fluctuations that result from neural activity evoked by an event, and reflect the patterns of neuronal activity which are consistently associated with the stimulus processing in a time-locked way (Teplan, 2002). Examples of events are stimuli in a specific sensory modality (e.g. a sound played using loudspeakers, a picture displayed on a computer screen, a tactile stimulus using a piezoelectric device), a combination of multi-sensory stimuli, or a motor response after stimulation, i.e. a button press in a keyboard or other device.

The traditional model of ERP generation assumes that recorded data in a single epoch (trial), consist of an ERP waveform (response), plus ongoing EEG activity, as illustrated in Figure 2.3. The ongoing EEG is regarded as irrelevant background noise, and is assumed to vary randomly from trial to trial. The ERP waveforms are assumed to be independent of the state of the ongoing EEG, and to be invariant across trials. However ERP waveforms have smaller amplitudes than ongoing EEG activity, and cannot be identified at a single trial level. This can be overcome by averaging the recorded signal across trials, as the random ongoing EEG will be reduced, but the identical ERP waveforms will be preserved (see Figure 2.3, bottom).

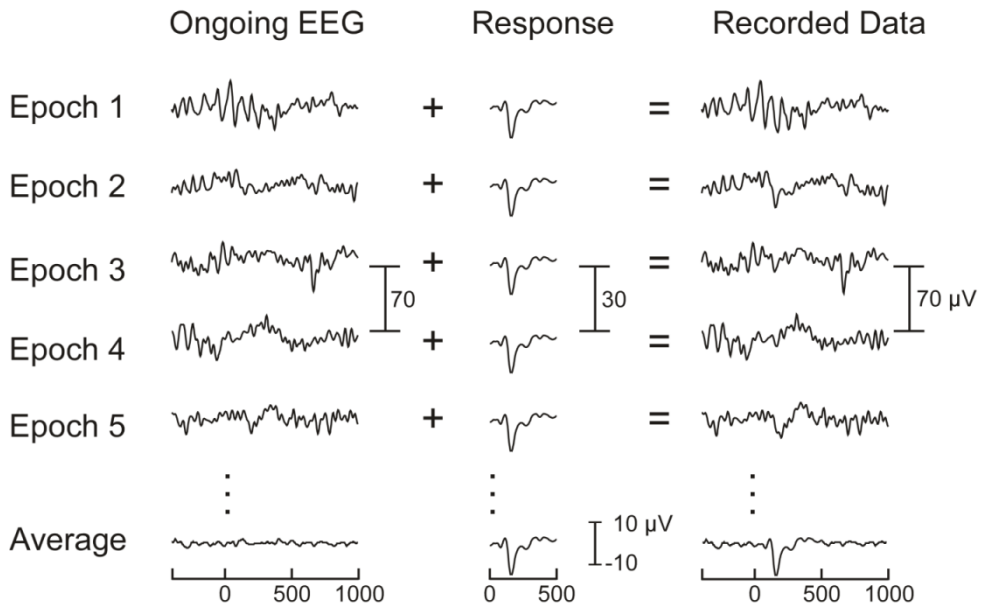

Figure 2.3 *Illustration of the ERP model. In each epoch recorded EEG consists of an ERP waveform (response) plus ongoing EEG activity. The ongoing EEG is assumed to vary randomly from epoch to epoch Thus, it is reduced by averaging, while in contrast, the assumed invariant ERP response is retained (Courtesy of S. Debener).*

It is known that the amount of noise in an average decreases as a function of the square root of the number of trials (Luck, 2005, chapter 4). As the ERP model assumes that the response, i.e. the signal, is unaffected by the averaging process, the SNR increases as a function of the square root of the number of trials. This mathematical relationship is illustrated in Figure 2.4. The curves correspond to simulations for different combinations of measured signal, i.e. ERP response of interest, and noise, i.e. ongoing EEG activity. For example, in the case of ongoing activity of 50 µV and an ERP with amplitude of 5 µV, it would be necessary to average 1000 trials to achieve a SNR of approximately 3.

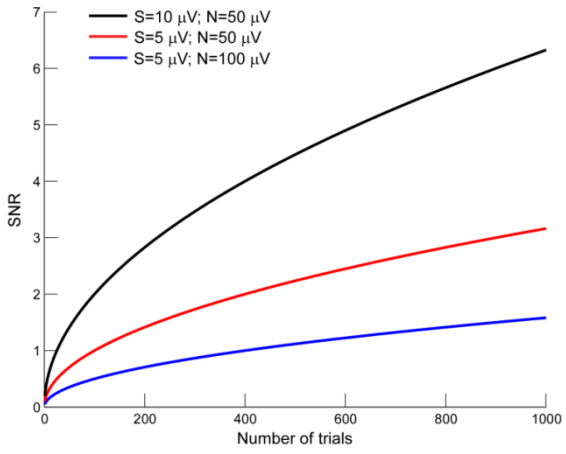

Figure 2.4 *Mathematical relationship between signal-to-noise ratio (SNR) and number of trials for three different combinations of signal (S), i.e. ERP response of interest, and noise (N), i.e. ongoing EEG activity, amplitudes (µV).*

ERP averaged waveforms comprise sequences of positive and negative deflections, which can be called, interchangeably, peaks, waves or components, since there is no convention for this nomenclature. Negative peaks are labeled with an "N" and positive ones with a "P", followed by a number which indicates the order in which the deflections occurred (e.g. N1, first negative deflection after stimulus onset) or the latency (e.g. P300, positive deflection occurring approximately 300 ms after the stimulus onset). The term ERP component usually refers to a physiological marker for a specific sensory or cognitive process, since the component is related both to the functional significance and to the underlying neural source(s). As defined by Luck: *"An ERP component is scalp-recorded neural activity that is generated in a given neuroanatomical module when a specific computation operation is performed."* (Luck, 2005, page 59). Thus ERP components are then characterized by a particular scalp distribution and also particular relationship to experimental variables (Otten & Rugg, 2005).

In a typical ERP research experiment, one of the goals is to compare a specific component between conditions (e.g. 1 kHz tone versus white noise) and/or within groups (e.g. patients versus healthy participants). These analyses can be performed in the time or in the frequency domain. The focus here is on investigating ERPs in the time domain. In this case parameters such as the amplitude, the latency, and the scalp topographical distribution are evaluated. Changes in amplitude could reflect salience, i.e. the degree of activation of generators or the degree of engagement of the associated sensory or cognitive processes. Differences in latency reflect timing, e.g. could reflect that a particular sensory or cognitive process is active at a later time in one condition than in the other. Due to the inverse problem, EEG data recorded from the scalp does not allow direct inferences about either the identity or spatial location of the underlying neural sources. Nevertheless the investigation of scalp distributions between conditions and/or within groups complements the characterization of the ERPs.

In this work the focus is on investigating cortical AEPs from CI users. It is important to clarify that AEPs have different nomenclatures according to both their origin and latency. The middle-latency responses (MLRs) consist of AEPs during the period between 10 and 50 ms after stimulus onset. The name reflects their intermediate latency between cochlear-brainstem responses and late AEPs. The brain responses evoked by sound and processed in or near the auditory cortex are called cortical AEPs. Since these responses occur after MLRs, the nomenclature late AEPs is also used (Burkard, Eggermont, & Don,

2007). For the sake of simplicity the auditory responses investigated here are referred as AEPs through this text.

Among other possible classifications AEPs can be divided into two types: exogenous or endogenous. The former are those whose presence, latency, and amplitude are determined primarily by the acoustic parameters of the stimulus, and by the integrity of the primary auditory pathway. The latter have characteristics that vary with the listener's attention and performance on assigned cognitive tasks while responses are recorded (reviewed in Cone-Wesson & Wunderlich, 2003).

Another difference is the type of stimulus that needs to be used to elicit these different responses. Exogenous AEPs can be elicited both by simple acoustic stimuli such as clicks, tonebursts, tone-complexes, and by more complex stimuli such as speech or environmental sounds. These AEPs have three early components labeled P1, N1, and P2, which reflect sensory encoding of sound that underlies perceptual events (audiologic applications reviewed in Cone-Wesson & Wunderlich, 2003; Hyde, 1997; Martin, Tremblay, & Korczak, 2008). Figure 2.5 shows a typical P1-N1-P2 complex recorded at a central electrode (vertex) from a young normal hearing (NH) woman stimulated with environmental sounds. The topographies at peak latencies are also shown. The characteristics of the P1-N1-P2 complex are reviewed briefly. P1 is the first positive peak and occurs approximately 50 ms after stimulus onset. In adults the amplitude of the P1 is small when compared to the N1-P2 complex, as can be seen in Figure 2.5. In children, on the other hand, P1 dominates the AEP response and its latency is typically used as a marker of auditory maturation. The following structures have been reported as neural generators of P1: primary auditory, hippocampus, planum temporale and lateral temporal regions (reviewed in Martin, et al., 2008). The negativity following P1 is called N1 and consists of several distinct subcomponents that peak between 80 and 150 ms (Luck, 2005, cf. chapter 1). The subcomponent shown in Figure 2.5 is the vertex-maximum potential that peaks around 100 ms after stimulus onset. N1 has multiple generators located in the primary and secondary auditory cortex (discussed in detail in Hyde, 1997; Naatanen & Picton, 1987). The positivity following the N1 is called P2. The morphology of P2 often covaries with N1 latency and amplitude. Therefore N1 and P2 are sometimes studied together as the N1-P2 complex. Generators of P2 include both primary and secondary auditory cortex (reviewed in Martin, et al., 2008).

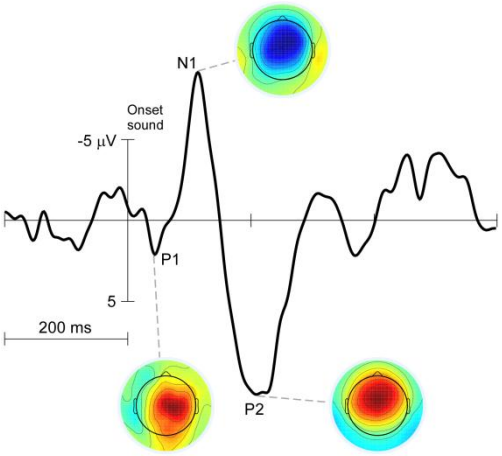

Figure 2.5 *Auditory evoked potentials recorded from a normal hearing young adult stimulated with environmental sounds. The waveform at a central electrode (vertex) is shown, as well as the respective topographic maps at P1, N1 and P2 peak latencies.*

Endogenous AEPs can be recorded only when specific experimental paradigms are used, such as an "oddball" paradigm. In these experiments the participants are required to detect a target sound within a stream of homogeneous sounds, called standards. The standard stimulus is presented with high probability (80-90%) and the deviant stimulus, used as the target, is presented with a smaller probability (10-20%). AEPs for standard and target stimuli are then compared. It has been observed that the AEPs to targets reflect not only the P1-N1-P2 complex but also a third positivity, hence it is labeled P3. This component may reflect the conscious processing of acoustic differences present in the stimuli, but its functional significance is still debated. Evidence supporting that P3 generation stems from frontal and temporal/parietal activations has been provided (Polich, 2007). Furthermore it has been shown that P3 can be modulated by attention and cognitive demands of the listening task (Polich, 2007). A detailed review about P3 was compiled by Polich (2007).

Another component that can be studied with this type of paradigm is the mismatch negativity (MMN). This component reflects an increase in negativity in the latency range of the N1-P2 complex. The MMN is observed when subtracting the response waveform for standard stimuli from the response waveform for deviant stimuli. It has been shown that it can be elicited by a variety of acoustic features of speech and other sounds (reviewed in May & Tiitinen, 2010). The MMN has also been observed in passive listening tasks, i.e. when the participants do not need to attend or respond to a particular stimulus (May & Tiitinen, 2010). The neural mechanisms underlying MMN generation are still not understood (Garrido, Kilner, Stephan, & Friston, 2009). One framework suggests that MMN reflects auditory sensory memory. This memory-based model

proposes that the MMN indexes preattentive discrimination of a sensory input deviating from the memory trace formed by the frequent standard stimuli (Naatanen, Gaillard, & Mantysalo, 1978). The "adaptation model", in contrary, suggests that the MMN is part of an amplitude- and latency-modulated N1 response (May & Tiitinen, 2010). The two models have been reviewed recently by May and Tiitinen (2010).

In this work the focus is on the N1-P2 complex, as these components can be used as an objective assessment of auditory function (Hyde, 1997). More details about AEPs and ERPs elicited by stimuli presented in other sensory modalities can be found in specialized books (Burkard, et al., 2007; Luck, 2005). Guidelines for the preparation of ERP experiments and for the interpretation of results have been suggested and discussed in the literature (Kotchoubey, 2006; Luck, 2005; Otten & Rugg, 2005; Picton et al., 2000).

2.1.3. Artifacts in EEG recordings

According to Talsma and Woldorff artifacts can be defined as *"... occurrences of any given electrical activity that can be recorded by EEG equipment, which is not originating from cerebral sources, and either clearly distinguishable from the recorded background EEG or substantially large enough to modify the observed ERP waveform from its true waveform"* (Talsma & Woldorff, 2005, page 115).

For the sake of simplicity in this section EEG artifacts are classified in two main categories: biological and non-biological. The former can be eye blinks or other type of ocular activity, such as eye movements, muscle artifacts, electrocardiographic (ECG) activity, or pulse-wave artifacts, caused by the pulsation of an artery near a recording electrode. The latter can be caused by movement of the electrode wires, instrumentation artifacts or interference artifacts. Some non-biological artifacts can be minimized by adopting careful routines in the laboratory before recording EEG data. Sources of noise and interference for instance should be removed from the room or booth where the recordings are taking place. Examples are mobile phones, lights, or other unnecessary electronic equipment. The slow polarization of electrodes, due to perspiration of the participant, or detachment of the electrodes, can also cause instrumentation artifacts. Thus the electrodes and the wiring should be checked to confirm that there are no loose connections. Moreover the impedances of all electrodes should be evaluated before recording. It is important to make sure that the paste that establishes the connection between the scalp and the electrodes is not too dry. Furthermore participants should be instructed to sit still but relaxed during the recording session and not to pull or touch the electrodes and cables.

After the recording session some artifacts can also be attenuated by filtering and averaging the data. Filtering from 0.01 to 30 or 40 Hz is a typical approach, on the assumption that in many ERP experiments brain activity of interest is normally in this frequency range (Luck, 2005, cf. chapter 5). This procedure attenuates or excludes mainly non-biological artifacts and muscle artifacts. According to the ERP model, averaging across trials can also attenuate artifacts, as long as these are assumed to be random (see Figure 2.3). However artifacts are not always random, as is the case for instance with eye blinks associated with the presentation of visual stimuli. Another example is when a participant wears an electronic prosthesis such as a CI. The device causes an electrical artifact that is time-locked to auditory stimuli and cannot be attenuating by filtering or averaging.

The rejection of portions of EEG data where artifacts occur is also a common approach. This procedure can be effective in removing eye blinks or other ocular activity, as these artifacts are not expected to be present in every single trial. Nevertheless the reduction of the number of trials contributing to the average response reduces the SNR, as described previously (see Figure 2.4). It is then necessary to record long experiments to ensure that the number of trials after rejection is still large. This is sometimes not feasible, for instance when testing children or clinical populations.

In the case of the attenuation of ocular artifacts several regression methods have been proposed (cf. Croft & Barry, 2000). These approaches require the measurement of the activity of an extra electrode placed under the eye. This signal is then correlated to the EEG signal recorded at the scalp. This identifies the artifacts which can then be subtracted from the data. However it has been suggested that the regression procedures can cause distortions in the spatial distribution of EEG recordings (Berg & Scherg, 1991). Thus other techniques such as dipole source modeling, principal component analysis and independent component analysis (ICA) have been proposed (reviewed in Talsma & Woldorff, 2005). The next section explains the principles of ICA with a particular focus on using this method to attenuate artifacts from EEG recordings.

2.2. Independent component analysis

Independent component analysis (ICA) is a blind source separation technique that separates complex signals into maximal statistically independent sources (components). It had its origins in the 1980s and early 90s in France, and has been linked most frequently to the engineering field (Comon, 1994). Now it is also applied in in the field of human electro- or magnetographic signals, i.e. electrical and magnetic activity produced by the

cells of the human body. ICA has been used with the goal of separating the signal of interest, e.g. heart or brain activity, from artifact sources. Several studies using ECG (e.g. Chawla, Verma, & Kumar, 2008), magnetocardiography (MCG) (e.g. DiPietroPaolo, Muller, Nolte, & Erne, 2006; Muller, Nolte, Paolo, & Erne, 2006), EEG (e.g. Gwin, Gramann, Makeig, & Ferris, 2010; Jung et al., 2000a; Jung et al., 2000b; Makeig, Jung, Bell, Ghahremani, & Sejnowski, 1997) , EEG recorded inside a magnetic resonance imaging (MRI) scanner (e.g. Debener, Mullinger, Niazy, & Bowtell, 2008b; Debener et al., 2007), and magnetoencephalography (MEG) (e.g. Escudero, Hornero, Abasolo, Fernandez, & Lopez-Coronado, 2007; Mantini, Franciotti, Romani, & Pizzella, 2008) have reported that ICA could successfully disentangle different artifacts from brain sources.

In the case of EEG signals, ICA has been shown to be particularly successful in attenuating biological artifacts such as eye blinks (e.g. Hoffmann & Falkenstein, 2008; Jung, et al., 2000a; Jung, et al., 2000b; Mennes, Wouters, Vanrumste, Lagae, & Stiers, 2010), and even movement artifacts during walking and running (Gwin, et al., 2010). However the applications of ICA in the EEG field are not limited to the attenuation of artifacts. A number of studies have shown that ICA can also be used to provide insights about the dynamics of human cortical activity that go beyond the traditional ERP approach (Debener, Makeig, Delorme, & Engel, 2005a; Debener et al., 2005b; Gramann et al., 2010; Makeig, Debener, Onton, & Delorme, 2004a; Makeig et al., 2004b; Makeig et al., 2002; Onton, Westerfield, Townsend, & Makeig, 2006).

There are several ICA algorithms that have been applied to EEG data. Some examples are infomax (Bell & Sejnowski, 1995), extended-infomax (Lee, Girolami, & Sejnowski, 1999), JADE (Cardoso & Souloumiac, 1994), and fastICA (Hyvarinen & Oja, 2000). However in the last years the popularity of ICA has increased to the extent that nowadays there are many more different algorithms suited to different applications. In the online platform “ICA Central” (http://www.tsi.enst.fr/icacentral/), as of August 2011, there were 27 different ICA algorithms that could be freely downloaded. Some authors have proposed the implementation of ICA algorithms in the time domain (Makeig, et al., 1997; Makeig et al., 1999; Makeig, et al., 2002). Other authors have implemented ICA in the spatial domain, normally in applications to functional magnetic resonance imaging (fMRI) data, (e.g. Anemuller, Duann, Sejnowski, & Makeig, 2006; McKeown et al., 1998a; McKeown et al., 1998b). A combination of temporal and spatial ICA has also been suggested (James & Demanuele, 2010).

Comprehensive detailed explanations about ICA can be found in specialized text books (Comon & Jutten, 2010; Hyvärinen, Karhunen, & Oja, 2001; Stone, 2004). The goal here is to provide basic information about the mathematical assumptions behind ICA focused on its application to the processing of EEG signals (2.2.1). Section 2.2.2 describes the application of temporal ICA to the attenuation of artifacts from EEG data using the extended-infomax algorithm as implemented in the EEGLAB toolbox (Delorme & Makeig, 2004) running in the MATLAB (Mathworks, Natick, MA) environment. Lastly the practical problems associated with this attenuation procedure are described, and improvements are suggested (2.2.3).

2.2.1. Application to EEG data

In the late 90s ICA was applied with success for the first time to a set of EEG data (Makeig, et al., 1997). Nevertheless the application of ICA requires that various assumptions are considered. The implementation described here considers that the number of sensors and sources are the same, and is called a "complete" decomposition method. However it is not possible to know how many independent sources contribute to the EEG signal. Another *a priori* obvious pre-requisite is that the signal of interest needs to be a linear mixture of different sources that are assumed to be independent and summed linearly at the sensors. Additionally it is assumed that there are no differential delays involved in projecting the source signals to the different sensors. A further assumption is that the component source locations (and thereby their topographic projection patterns to the scalp sensors) are fixed throughout the data.

These assumptions are quite plausible for EEG data, as illustrated in Figure 2.6. Regarding the assumption of temporally independence of the sources, as long as two sources are not perfectly coupled during the recording, they may express some degree of temporal independence. This amount of partial independence (or partial connectivity) may be sufficient for ICA to achieve a good degree of unmixing (Debener, Thorne, Schneider, & Viola, 2010). The assumption that each signal is a linear mixture of source signals is quite plausible for electrical signals travelling through human tissue, as well as the assumption that any delay is negligible (Stone, 2004). Since most neural signals picked up by EEG are generated by PNs, it is also reasonable to assume that in the absence of movement of electrodes, the component source locations are fixed throughout the data (Debener, et al., 2010).

Another assumption that also needs to be met when applying ICA is that the probability distributions of the individual component source activity values are not precisely

Gaussian, which is important to ensure the independence of sources. This assumption is plausible for EEG sources generated by nonlinear cortical dynamics as well as for non-brain artifact sources including cardiac signals, line noise, muscle signals, eye blinks and eye movements (Makeig & Onton, 2011).

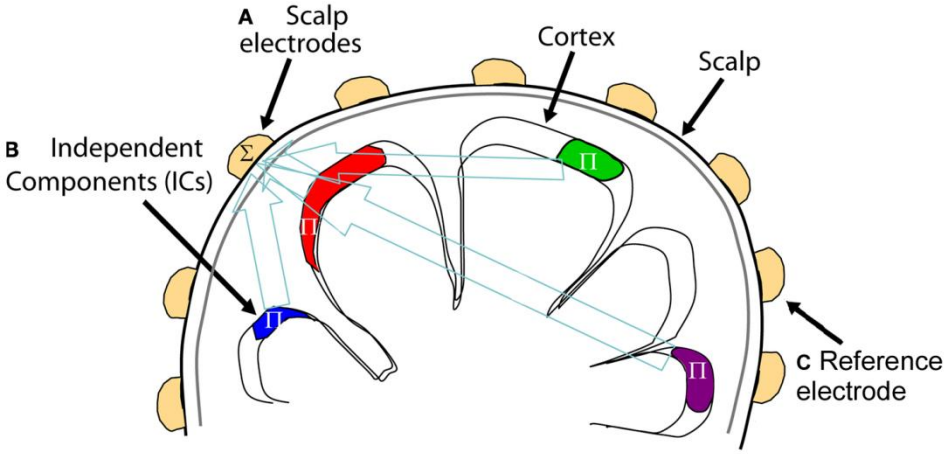

Figure 2.6 *ICA assumptions applied to EEG data. ICA identifies (A) temporally distinct (independent) signals generated by partial synchronization of local field potentials within cortical patches (B). The resulting far-field potentials summed (Σ), in differing linear combinations, at each electrode depending on the distance and orientation of each cortical patch generator relative to the (A) recording and (C) reference electrodes (adapted from Onton & Makeig, 2009).*

It seems that there is an approximate fit between ICA assumptions and the physiological nature of EEG sources. Nevertheless it is important to highlight that exact independence is such a strict requirement that it can never be established for EEG signals with finite length. ICA algorithms, therefore, may at best produce components with maximal independence by ensuring that components continually approach independence as the ICA algorithm is iteratively applied to the data. The degree of IC independence achieved may differ for different data sets and also for different ICA algorithms applied to the same dataset (Makeig & Onton, 2011).

The different ICA algorithms need to provide a measure of independence. However independence cannot be measured directly, and other quantities that are related to independence need to be considered. In the case of the infomax type algorithms, infomax (Bell & Sejnowski, 1995) and extended-infomax (Lee, et al., 1999), the measure adopted is entropy. Entropy is defined as a measure of the uniformity of a distribution of a bounded set of values, such that complete uniformity corresponds to maximum entropy. Variables with maximum entropy are statistically independent of each other (Stone,

2004). The infomax approach consists in finding an unmixing matrix that maximizes the entropy of the signals extracted by that matrix. This unmixing matrix will also maximize the amount of mutual information between the signals and the set of signal mixtures, hence the name infomax (Stone, 2004).

Figure 2.7 shows a schematic outline illustrating the application of ICA to EEG data. The EEG raw data (Scalp Data) can be defined as a matrix *X* (channels x time). The ICA decomposition finds an unmixing matrix *W* which, when multiplied by *X*, decomposes the data into a matrix of independent component signals, called the independent component (IC) activations matrix *A* (right). Please note that the number of ICs is determined by the number of EEG channels recorded ("complete" decomposition). Multiplying the IC activations matrix by the inverse of the unmixing matrix, also called mixing matrix W^{-1} (middle) reconstitutes or back-projects the original scalp data channels. The columns of the mixing matrix give the relative strengths and polarities of the projections of one IC to each of the scalp channels. This representation is normally called IC scalp maps or IC topographic maps. By setting a particular row from the activations matrix to zero it is possible to eliminate the contribution of that particular IC to the raw data when back-projecting, as discussed in the next section.

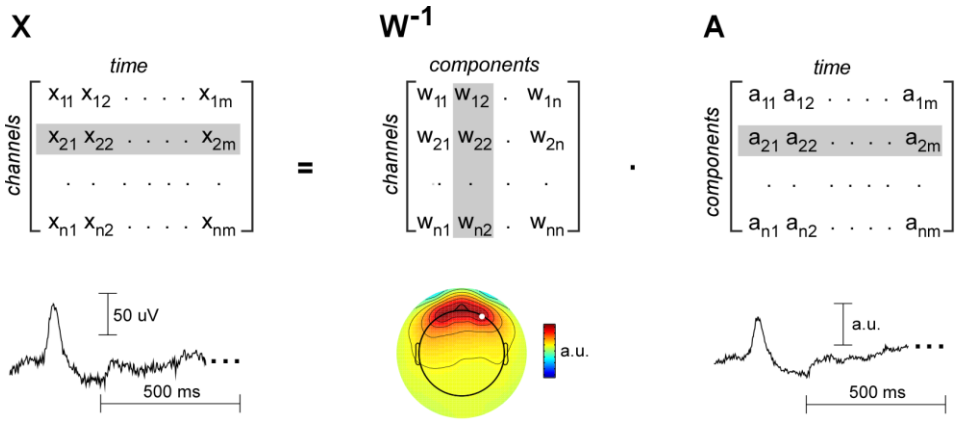

Figure 2.7 *Schematic outline illustrating the application of ICA to multi-channel EEG data (X).Inverse weights (W-1) represent the spatial pattern of each source time course. Matrix-multiplication of W-1 with the maximally temporally independent time courses (in A) gives the mixed channel data, a process called back-projection. For illustration purposes, one component/channel vector is highlighted in grey and shown below the corresponding matrices (from Debener, et al., 2010).*

When comparing IC activations and scalp maps it is also important to keep in mind that when evaluating both sets of information separately there will be an inherent ambiguity in terms of polarity and amplitude. This occurs because the sign and scaling of the back-

projected IC in the data is split arbitrarily between its activation and scalp map. Using a numeric example, since -1 × -1 = 1, inverting the signs of both an IC activation and its scalp map will not change their product, or the back-projection of the IC into the original data, which will retain its original polarity (Makeig & Onton, 2011). Moreover it is important to keep in mind that infomax based-ICA can produce different results from repeated application to identical data. This results from the unmixing weights (*W*) being learned over repeated iterations, which use randomly chosen samples from the training data submitted (*X*) (Debener, et al., 2010).

A major contribution that has made ICA popular among EEG/ERP laboratories all over the world was the development of a MATLAB (Mathworks, Natick, MA) open source toolbox called EEGLAB (Delorme & Makeig, 2004). The functions contained in the EEGLAB toolbox can be run from a graphical user interface or in scripts, making it a suitable tool both for novices and experienced researchers. In the last years ICA algorithms have also been implemented in many commercial software packages used for the recording and processing of EEG data. Details about applying ICA to attenuate artifacts from EEG recordings using EEGLAB are discussed in the next section.

2.2.2. EEG artifact attenuation

The quality of an ICA decomposition depends mainly on the quality of the EEG training data submitted to the ICA algorithm. Consequently the degree of artifact attenuation that can be achieved depends also on the quality of the decomposition, which can be substantially influenced by the pre-processing of the data, e.g. filtering. Practical guidelines for decomposing multi-channel EEG data and evaluating ICs have been covered by several authors (Debener, et al., 2010; Makeig & Onton, 2011; Onton, et al., 2006). An important aspect is that the ICA algorithm should be trained using sufficient data points from the *n*-channels recorded. It has been proposed that the number of points should be at least a *k* multiple of n^2, being recommend that *k* should not be smaller than 20 (Debener, et al., 2010; Onton, et al., 2006). However "quantity" and "quality" are both important in this respect. The "quality" of the data can be substantially improved by using appropriate filters (cf. Debener, et al., 2010) and also by removing from the data portions containing non-stereotyped artifacts, such as movements arising from the pulling of cables or electrodes. Sometimes it can be necessary to remove bad channels, i.e. those electrodes which have lost good contact to the scalp, from the raw data matrix before running ICA. In summary the pruning of the data is highly recommended, since these types of artifacts can introduce many different unique and independent scalp maps in the recorded data, i.e. fewer ICs will be available to represent other processes of interest

(Onton, et al., 2006). The EEGLAB toolbox contains implementations of several detection methods that can automatically identify trials containing non-stereotyped artifacts (Delorme, Sejnowski, & Makeig, 2007a).

Examples of ICs representing four common artifacts (ocular activity, muscle, and heartbeat related activity) are illustrated in Figure 2.8. The properties of each IC are described using different plots. The ERP image (Jung et al., 2001) is shown on the left. Note that the ERP image aids evaluation of whether the activity of a certain IC is time-locked to any particular event of interest. The 2D IC scalp map, also designated topographic map, and the power spectra are shown on the right. The ERP of the ICA activations is shown on the bottom.

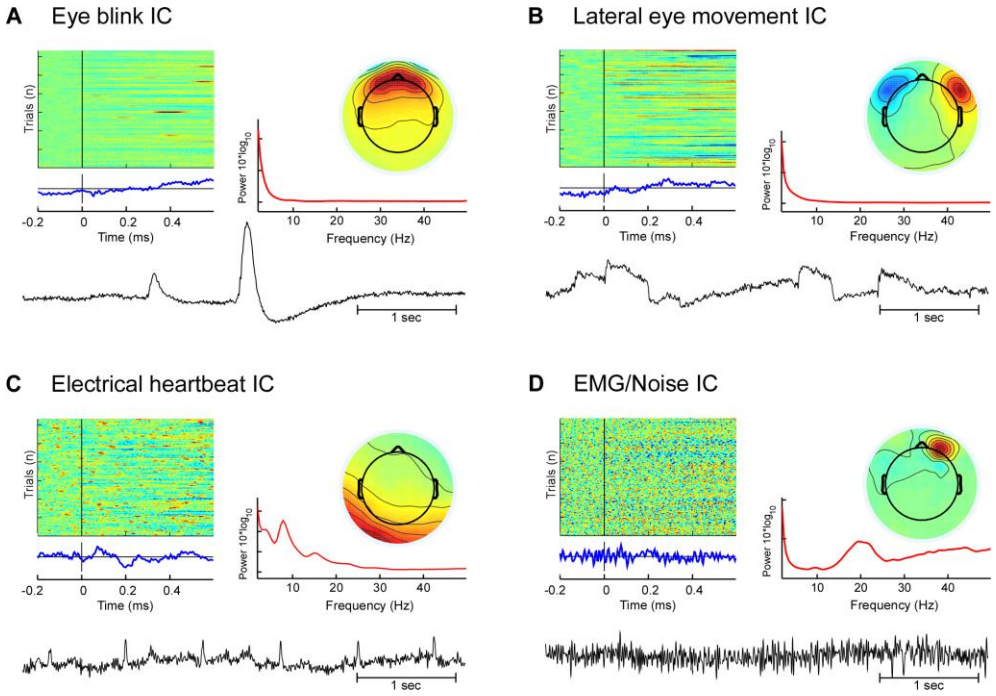

Figure 2.8 *Typical EEG artefacts as identified by ICA. A) Eye blink artefact components. Shown are the IC map, the single-trial activity as an image, the time-domain average, i.e., the ERP (blue) and the spectrum (red), along with a representative section of ongoing activity (below). B) Same for lateral eye movements. C) Same for electrical heartbeat artefact. D) Same for muscle/noise activity. All y-axis scales in arbitrary units (from Debener, et al., 2010).*

Another possible measure is the dipole modeling of the ICs (not shown in Figure 2.8). It is known from biophysics that coherent activity across a small patch of cortex will have a near-dipolar projection of pattern on the scalp (Onton, et al., 2006). Therefore an equivalent dipole model can be informative to categorize one particular IC as likely to represent brain related activity or artifact. The EEGLAB toolbox also contains a plugin

toolbox called DIPFIT that allows the dipole modeling of ICs (Oostenveld & Oostendorp, 2002). More details about how to interpret the results of dipole modeling of ICs can be found in the literature (Gramann, et al., 2010; Makeig & Onton, 2011; Onton, et al., 2006).

Figure 2.9 illustrates an example of the attenuation that can be achieved when correcting eye blinks and other noise from an EEG dataset. By back-projecting all but two ICs, representing eye blinks (IC 1) and noise (IC 2) respectively, the large deflections representing ocular activity across the different channels (amplitude range was -300 to 300 μV) are attenuated in the corrected data (amplitude range was reduced to -30 to 30 μV).

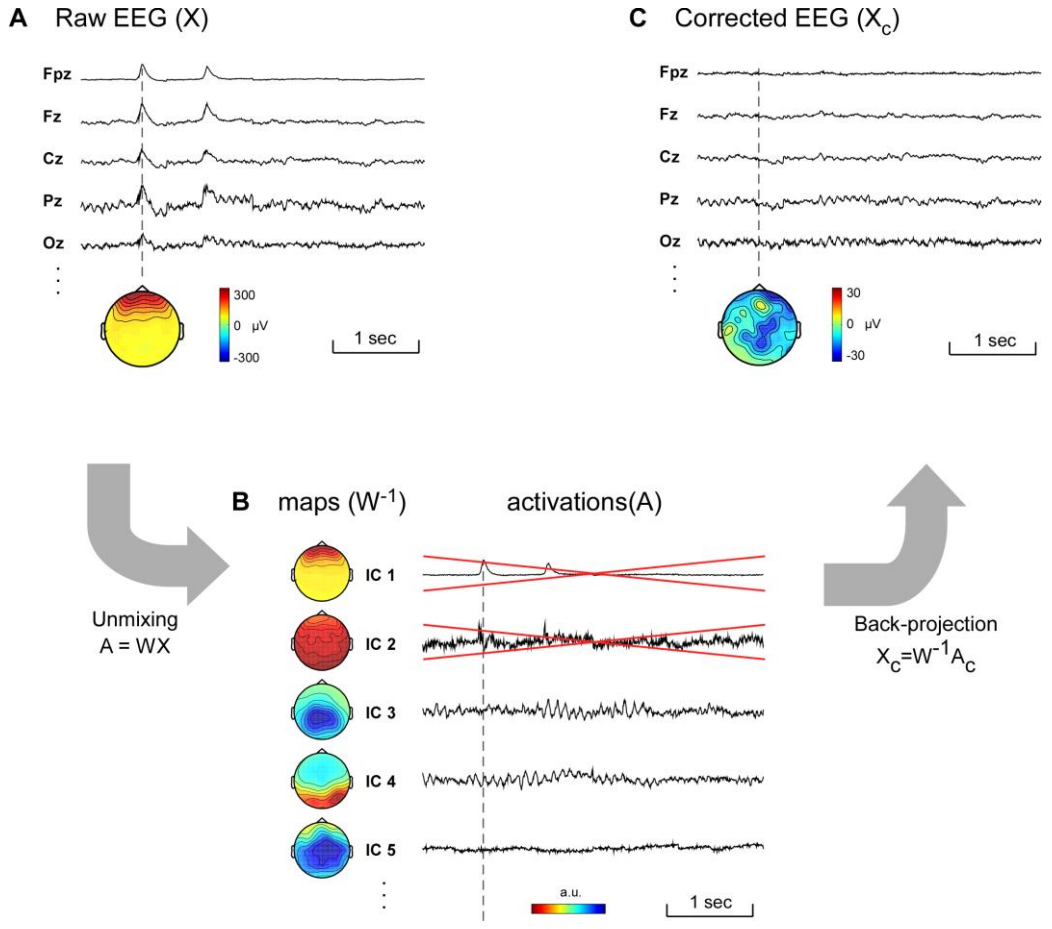

Figure 2.9 *Illustration of artifact removal by means of ICA. A: Section of selected channels from a multi-channel EEG recording is shown, with ongoing EEG oscillations in the alpha range evident at occipital electrodes and two eye blinks at fronto-polar channels. B: Unmixing of the EEG data into a set of independent components. Each component can be described on the basis of a spatial pattern (map) and a time course (activation). C: Back-projection of all but components 1 and 2 reveals artifact-corrected EEG data (from Debener, et al., 2010).*

Although the underlying mathematical formulations of ICA are complex, its application to EEG data is well described. Nevertheless the use of ICA requires dealing with some practical challenges. For instance, the larger the number of EEG channels available, the larger the number of ICs that need to be evaluated and the more likely that a particular type of artifact will be represented in more than one IC. In the next section the selection of ICs is described and possible improvements are suggested.

2.2.3. Practical problems

Several studies have shown that the attenuation of different types of artifacts can be successfully achieved using ICA (e.g. Debener, et al., 2007; Jung, et al., 2000a; Jung, et al., 2000b). It has been shown that even more complex artifacts such as stimulus-locked electrical artifacts from CIs can be attenuated (e.g. Debener, Hine, Bleeck, & Eyles, 2008a; Gilley et al., 2006). Details about this particular type of artifact will be discussed in a dedicated section (2.3.4.).

In practical terms, the procedure of screening and selecting ICs representing artifacts relies mainly on visual inspection of the properties of the ICs. This method is time consuming, since all ICs from all participants need to be evaluated. For example, in an experiment where 20 participants are measured with a 32 channels EEG system, a total of 640 (20x32) ICs would need to be screened. However the total number of ICs in an EEG study can be even larger because nowadays many laboratories use high-density EEG recordings with more than 60 channels. Moreover the screening procedure requires expert knowledge and training. Therefore questions about the subjectivity associated with the procedure of selecting ICs have been raised.

The EEGLAB toolbox contains special functions that allow the clustering of ICs across datasets from different participants, using clustering algorithms based on measures of the Mahalanobis distance or on a neural network approach. This clustering procedure relies on a multiple-measure approach where the user needs to set combinations of different parameters, i.e. weights for each measure. This approach has been used to cluster ICs related to distinct brain processes (e.g. Gramann, et al., 2010). On the other hand, due to the special properties of ICs related to some particular artifacts, it could be possible to implement procedures based on a single measure. One particular example is the eye blink artifact. It has been observed that ICs representing this artifact have very similar scalp maps across different participants, which can be assumed to be highly correlated. This results from the fact that the eyes, the source of the artifact, have a fixed position relative to the EEG electrodes. Due to the rising popularity of ICA, especially in attenuating

biological artifacts in EEG data, it would be of interest to develop user friendly approaches, targeted at identifying specific ICs.

Another important question concerns the evaluation of the stability and reliability of an ICA decomposition. As described previously, due to the iterative learning procedure of the unmixing matrix, ICA can produce different results from repeated applications to identical data (cf. Debener, et al., 2010). A method for ICA reliability analysis based on clustering and visualization has been proposed (ICASSO, described in Himberg, Hyvarinen, & Esposito, 2004). Recently other approaches have been suggested (Debener, et al., 2010; Groppe, Makeig, & Kutas, 2009). Some authors have proposed a method where ICA is applied separately to split-halves of a data, as well as for the whole data. Reliability is checked by evaluating IC triplets (Groppe, et al., 2009). Other authors have applied ICA twice to identical data, and correlated the weights from the first and second applications to identify maximum correlations for each IC. With this procedure it was possible to compare ICA decompositions obtained using different amounts of training data (Debener, et al., 2010).

2.3. Assessment of auditory evoked potentials in cochlear implant users

A cochlear implant (CI) is a neural prosthesis that uses electrical stimulation to enhance or restore auditory function in particular cases of hearing impairment. From conceptualization to the latest developments in CI technology it has been a journey of more than two centuries. Figure 2.10 shows a time line illustrating the main achievements in CI technology. An impressive single figure summarizes the success of these milestones: more than 220,000 individuals have been implanted with CIs worldwide (Cosetti & Waltzman, 2011).

This section is focused on the assessment of auditory cortical functions of CI users by means of AEPs, an objective measurement of auditory rehabilitation. First a brief introduction to the functioning of the healthy auditory system is presented (2.3.1), followed by the description of common causes of deafness, as well as available treatments with a particular focus on the CI technology (2.3.2). The components and working mode of a modern CI are described, as well as common clinical measurements used to evaluate auditory rehabilitation after the device is switched on (2.3.3). A particular emphasis is given to the use of EEG as a non-invasive technique to measure AEPs from CI users and investigate objectively auditory rehabilitation after implantation (2.3.4). Recent findings from studies that have used AEPs to study CI populations are briefly described. Lastly the challenges associated with the artifacts caused by the CI

device in the EEG recordings are presented and current solutions to overcome this problem are discussed (2.3.5).

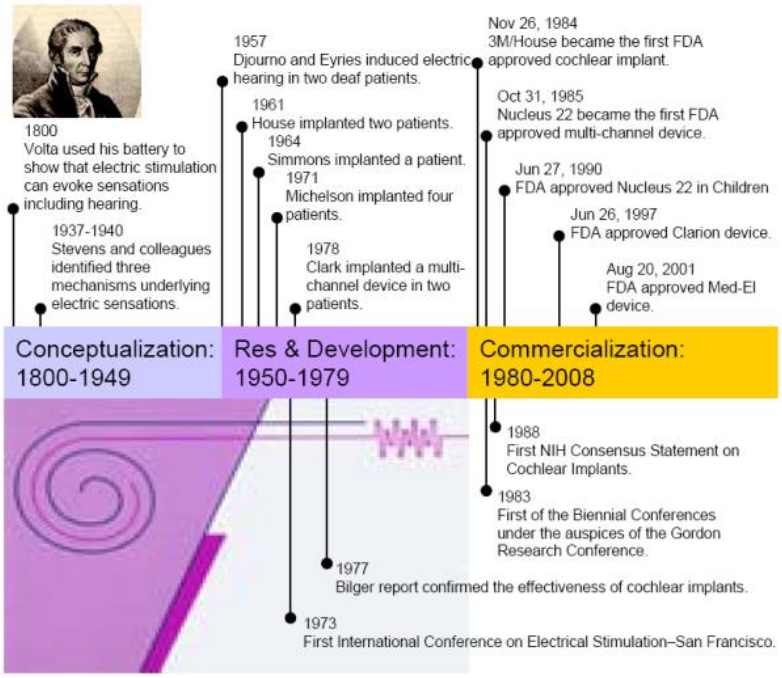

Figure 2.10 *Three phases defining the major events in the development of CIs. The conceptualization phase demonstrated the feasibility of electric stimulation. The research and development phase legitimized the utility and safety of electric stimulation. The commercialization phase saw a wide-spread use of electric stimulation in treating sensorineural hearing loss (from Zeng, Rebscher, Harrison, Sun, & Feng, 2008).*

2.3.1. The human auditory system

The human auditory system consists of the ear itself, which comprises three specialized regions, the outer, the middle, and the inner ear (Figure 2.11) plus the auditory pathways of the brain. Each region of the ear has a different function which allows sound waves travelling through the air to be converted to neural activity. The auditory pathways of the brain comprise different brain structures, in particular the brainstem, the pons, the midbrain, the thalamus, and the auditory cortex (Figure 2.12). A brief description of the mechanisms of hearing is provided here, with a special focus on the functioning of the cochlea. A detailed explanation of the auditory pathways is out of the scope of this work. This information can be found in specialized text books (Burkard, et al., 2007; Rosenzweig, Breedlove, Leiman, & Watson, 2005; Winer & Schreiner, 2010).

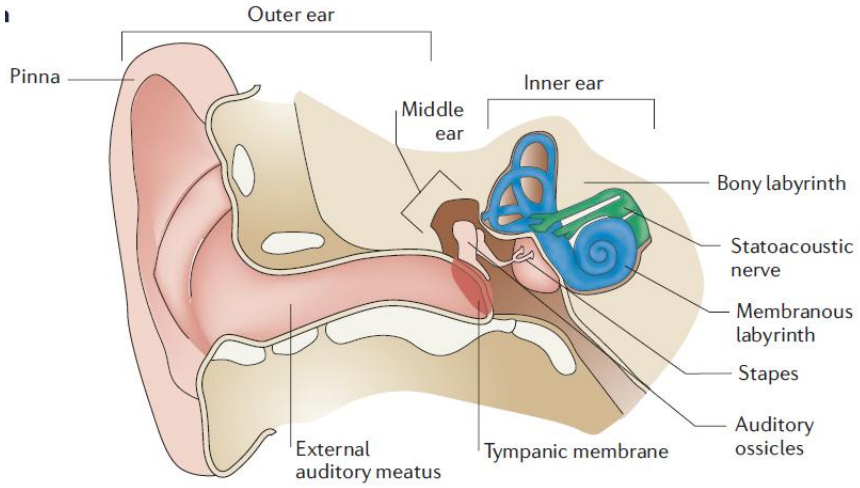

Figure 2.11 *Anatomy of the peripheral auditory system. Diagrammatic cross-section through the human head illustrating the three (outer, middle and inner) regions of the ear. The outer ear is comprised of the pinna and external auditory meatus, and is bounded on its medial side by the tympanic membrane. The middle ear is an air-filled space containing the three auditory ossicles bounded by the tympanic membrane as well as the round and oval windows. The inner ear is comprised of the cochlea, a membranous labyrinth (blue), which is surrounded by a bony labyrinth and innervated by the VIIIth (statoacoustic) cranial nerve (green) (adapted from Kelley, 2006).*

In a healthy hearing system the sound waves traveling through air are captured and filtered by the pinna in the outer ear. These waves reach the tympanic membrane via the ear canal, and cause vibrations that move a chain of ossicles in the middle ear. This action produces a piston–like movement and causes the tilting of the oval window that is a flexible membrane that separates the middle from the inner ear. The cochlea is part of the inner ear, and can be described as a membranous labyrinth. As the cochlea is filled with noncompressible fluid, the vibrational energy generated in the middle ear can be converted into waves of fluid. One of the complex structures of the cochlea is the basilar membrane. This structure divides the cochlea along its length, and vibrates producing the phenomenon of traveling waves. Furthermore it contains the organ of Corti that is the principal structure involved in converting these waves into neural activity. The organ of Corti contains specialized hair cells: the outer hair cells (OHC) and the inner hair cells (IHC). The OHC, the cells with active mechanical behavior, amplify sound by up to 60 decibels (dB) and provide superior frequency selectivity. This is of particular benefit for humans, because it enables sophisticated speech and music perception. The IHC, the sensory cells, sense the movement of the basilar membrane and deflect accordingly. This initiates a chain of electrochemical events that causes electrical spikes, or action

potentials. The electrical currents are in turn transmitted to the brain via the auditory nerve and the auditory pathways.

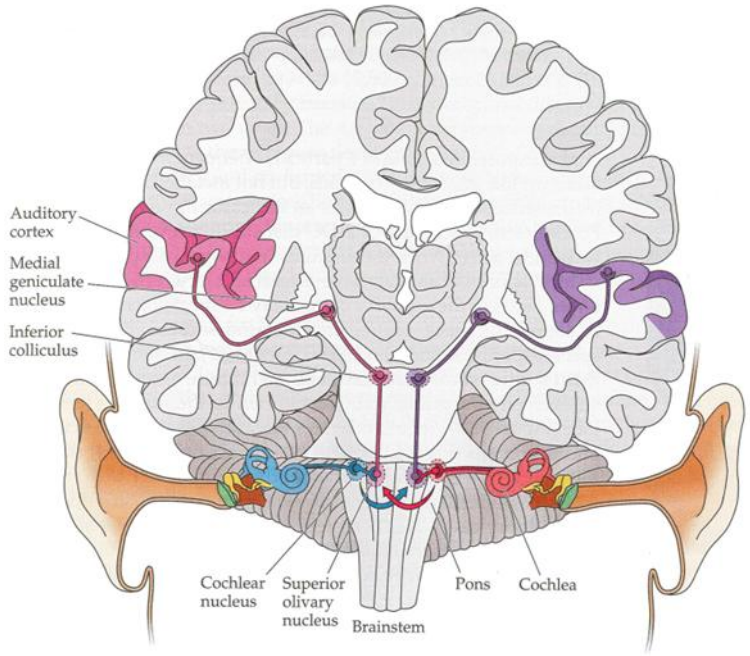

Figure 2.12 *Auditory pathways of the human brain. This view from the front of the head shows the first binaural afferent interactions in the brainstem. Most (but not all) of the information from each ear projects to the cortex on the opposite side of the brain, as illustrated here by the colors of the projections to the medial geniculate nucleus and cortex (from Rosenzweig, et al., 2005).*

Many events can disturb the normal functioning of the auditory system and even impair it permanently. One unavoidable example is age related hearing loss (ARHL) or presbyacusis which is related to functional loss of sensory and neural elements. It is known that hearing acuity declines with age. The high frequencies are affected first, followed by the frequencies of the speech spectrum (Roth, Hanebuth, & Probst, 2011). ARHL is the most widespread sensory impairment in aging people, and as it is a progressive condition, a formal diagnosis can sometimes only be provided at later stages. The next section describes types of hearing loss, etiologies and available treatments.

2.3.2. Deafness: etiologies and treatments

According to the World Health Organization (WHO), deafness and its causes can be defined as the following: "*Deafness is the complete loss of the ability to hear from one or both ears. Deafness may be inherited, or caused by complications at birth, certain infectious diseases, such as meningitis, use of ototoxic drugs, and exposure to excessive*

noise". The term hearing impairment is also commonly used and refers to partial or complete loss of the ability to hear. Deafness can be categorized in three types, according to which part of the hearing system is affected (Rosenzweig, et al., 2005).

The first type is conduction hearing loss and is related to disorders of the outer or middle ear. In this pathology the vibrations produced by the auditory stimuli are prevented from reaching the cochlea. The second type is sensorineural hearing loss (SNHL), which occurs when OHC and/or IHC are impaired, as illustrated in Figure 2.13. The OHC appear to be especially susceptible to noise trauma. Other causes for SNHL include genetic defects and treatments with ototoxic antibiotics. The third type of deafness is less common and is called central hearing loss. This pathology is caused by lesions in the auditory pathways or in the primary auditory cortex, hence sometimes also called "cortical deafness". This type of deafness has been investigated mainly in single case reports (Hood, Berlin, & Allen, 1994; Kaga, Nakamura, Takayama, & Momose, 2004).

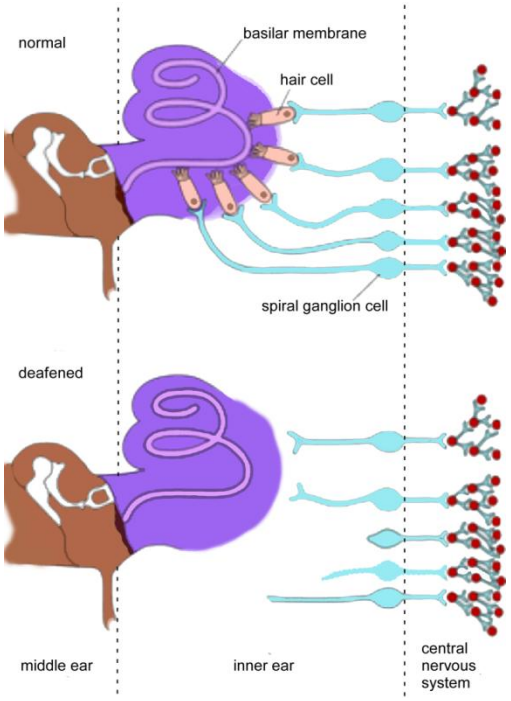

Figure 2.13 *Illustration of sensorineural hearing loss. This type of impairment is caused by damage to or destruction of hair cells and may also involve the deterioration of neural connections in the inner ear. In normal hearing, OHC along the basilar membrane detect sound vibrations. In response, IHC release chemical transmitters that trigger action potentials in neurons of the spiral ganglion. The patterns of evoked neural activity convey information to the central nervous system (top). In a profoundly deafened ear, IHC have died or no longer function, depriving the spiral ganglion cells of their normal input (bottom). Without regular use, the neural connections often wither and some cells of the spiral ganglion may die. For the sake of simplicity, this diagram does not reflect anatomical details or consistent scale (from Dorman & Wilson, 2004).*

According to WHO, solutions to hearing impairment should start with a focus on prevention and on early detection. It has been estimated that around half of all deafness and hearing impairment could be prevented (cf. WHO website: www.who.int). In the case of conduction hearing loss common treatments are the prescription of hearing aids or middle ear implants. The former provide sound amplification, increasing the movement of the eardrum and promoting indirectly the vibration in the middle ear. The latter enhance the signal that reaches the inner ear by directly vibrating the middle ear structures while leaving the ear canal open and the eardrum undisturbed. In the case of SNHL, when the only affected cells are the OHC, auditory function can be restored by means of hearing aids that provide powerful amplification. When the IHC are also damaged the prescribed treatment is a CI. These patients are clinically defined as profoundly deaf. These individuals can have a loss of more than 100 dB, so they cannot hear for instance the sound of an airplane flying close by. Treatment with a CI is only possible when the electrical excitability of the auditory nerve fibers remains intact. When the auditory nerve is damaged a solution is to use another device called a brainstem implant. In this case the electrical stimulation is delivered directly to the brainstem, more specifically to the cochlear nucleus. Figure 2.14 illustrates available treatments for conduction and SNHL in the form of medical devices such as hearing aids, middle ear implants, cochlear implants, and brainstem implants.

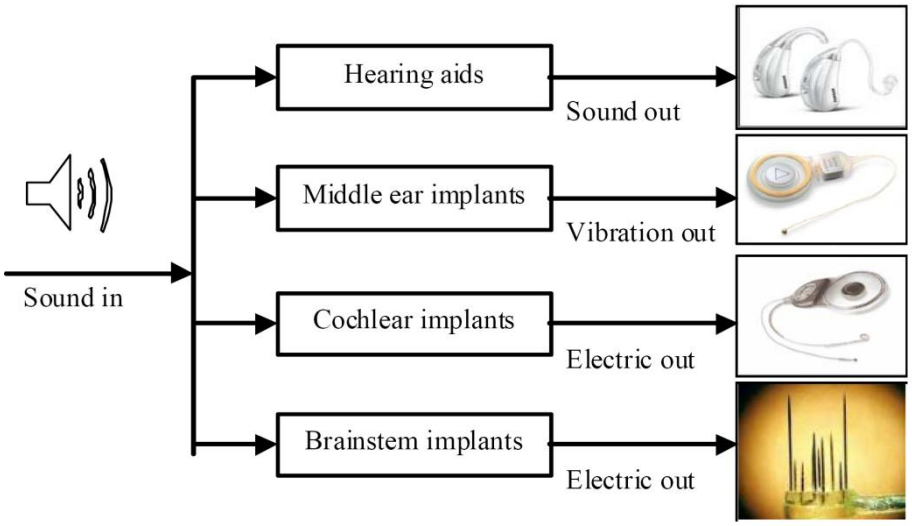

Figure 2.14 *Treatment of hearing impairment using hearing aids, middle ear implants, cochlear implants, and brainstem implants (from Zeng, et al., 2008).*

2.3.3. Restoration of auditory function with cochlear implants

In this section the general functioning of modern CIs, and the outcomes after cochlear implantation are described. Additionally typical clinical measurements of auditory rehabilitation are discussed. The first successful attempt to stimulate electrically totally deafened individuals dates to 1957, when a French physician and a French engineer, Djourno and Eyries, placed a coil of wire in the inner ear of two patients, who then reported some hearing (Moore & Shannon, 2009; Zeng, et al., 2008). This observation was replicated a few years later in the USA by William House in Los Angeles and by Blair Simmons in Stanford. In the following years fruitful research was conducted in multiple centers (for more details see Zeng, et al., 2008). But only in 1984 did the 3M/House device, a single electrode implant, gain Food and Drug Administration (FDA) approval in the USA. One year later the first FDA approved multi-channel device, the Nucleus 22, became available on the market. This device had 22 channels, being the precursor of the CI technology used nowadays. Currently there are devices on the market from four different manufacturers. The studies available in the literature do not show evidence of any specific device being superior to the others (Cosetti & Waltzman, 2011). A detailed comparison of CI technology among the different manufacturers is beyond the scope of this work but can be found in the literature (Cosetti & Waltzman, 2011; Wilson & Dorman, 2008b; Zeng, et al., 2008).

The general principle of a modern CI is to mimic the function of the healthy cochlea by delivering artificial electrical stimulation to the auditory nerve and thereby allowing the restoration of auditory function. These devices comprise external and internal components which are described briefly. As shown in Figure 2.15, the behind-the-ear external processor consists of four parts. There is a battery pack, a microphone, a speech processor, and an external transmitter, which includes an antenna. The microphone captures the sound in the environment and the speech processor transforms the microphone output into a digital signal. This digital signal is processed and encoded into a radio frequency (RF) signal, which is sent to the antenna. The external transmitter then provides a transcutaneous link for the transmission of power and stimulus information across the skin. (Wilson & Dorman, 2008a, 2008b; Zeng, et al., 2008).

Internally the CI consists of an implanted receiver/stimulator, and an array of electrodes (Figure 2.15). The receiver/stimulator decodes the information received from the RF signal and converts it into electrical currents. These currents are then sent along wires to the intra-cochlear electrodes, which at the end of the wire stimulate the auditory nerve directly. Several parameters need to be taken into account when providing the

stimulation, for instance the distance between electrodes and the depth of insertion. Since the goal is to mimic the tonotopic organization of the cochlea the stimulation needs to be provided to distinct sites. Nowadays the array comprises between eight and twenty two electrodes, but not all of them are active at the same time. The configuration of active electrodes is personalized for the user during the fitting session where the CI is switched-on.

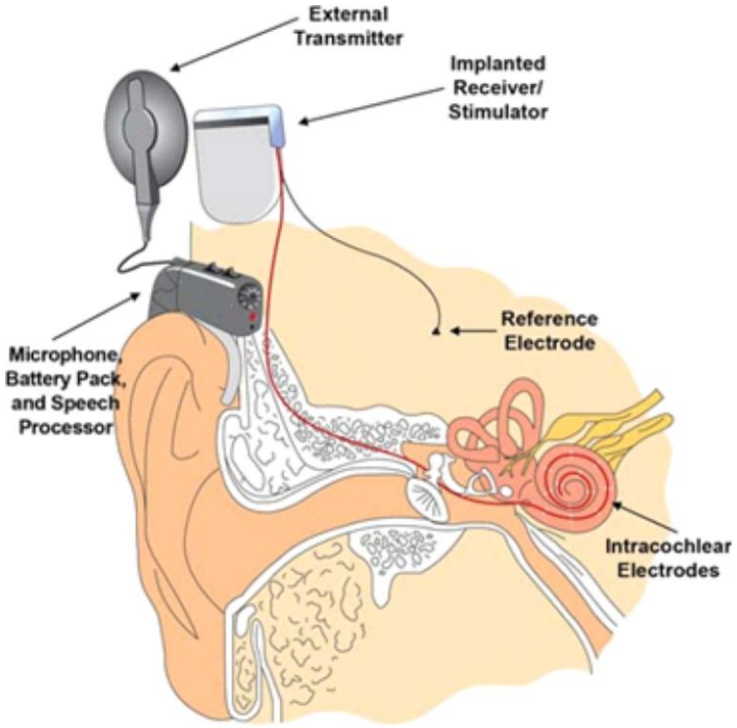

Figure 2.15 *Components of modern cochlear implant systems. A microphone, a battery pack, and a speech processor are incorporated into the behind-the-ear (BTE) housing in the illustrated system, much like BTEs of hearing aids. A thin cable connects the output of the speech processor (transmitting a radio frequency signal with encoded stimulus information) to the external transmitting coil that is positioned opposite the implanted receiver/stimulator. The transmitting coil is held in place with a pair of magnets, one in the center of the coil and another in the implanted receiver/stimulator. The receiver/stimulator is implanted in a flattened or recessed portion of the skull, posterior to and slightly above the pinna. The reference (or "ground") electrode is implanted at a location remote from the cochlea, usually in the temporalis muscle. For some implant systems, a metallic band around outside of the receiver/stimulator package serves as reference electrode. An array of active electrodes is inserted into the scala tympani through the round window membrane or through a larger drilled opening in the bony shell of cochlea (cochleostomy) near the round window (from Wilson & Dorman, 2008b).*

A significant achievement in CI technology has been the miniaturization of the external sound processor. The development of the coding strategies, also known as speech strategies, has also been crucial for the success of the CI technology. These strategies

consist of algorithms that are responsible for decomposing the input audio signal into different frequency bands or channels and delivering the most appropriate stimulation pattern to the electrodes. Current implementations use a filter bank or waveform approach (Rubinstein, 2004). Important aspects for this signal transformation are the implementation of temporal coding and the imitation of the tonotopic organization of the cochlea. The encoding of spectral and temporal fine structure cues has also received special attention (Zeng, et al., 2008). Advances in the encoding of these stimulus properties could contribute to the improvement of speech perception in noise, music appreciation, and recognition of emotions, which are still a challenge for many CI users (Cosetti & Waltzman, 2011). Details about the different strategies, their evolution, as well as advantages and disadvantages are out of the scope of this work and have been described in the literature (Wilson & Dorman, 2008b; Zeng, et al., 2008).

It is noteworthy that successful encoding of sounds requires not only developments in the encoding strategies, but also in the intra-cochlear electrode array arrangement and mode of operation. Other challenges include providing longer lasting batteries and improving the microphone technology. For instance the use of directional microphones could contribute to improvements (Cosetti & Waltzman, 2011). Recent developments and future improvements in CI technology, as well as safety concerns, have been discussed in the literature (Cosetti & Waltzman, 2011; Wilson & Dorman, 2008a, 2008b; Zeng, et al., 2008).

Although CI technology has dramatically improved in the last 30 years, the outcome after implantation is still variable across CI users. Several authors have suggested that the auditory cortex and its capacity for cortical plasticity should be regarded as an "extra CI component". This "biological component" may have a crucial role, since it needs to adapt to the artificial electrical stimulation in order to allow the restoration of the hearing function (Moore & Shannon, 2009; Wilson & Dorman, 2008a).

In the last years the implantation candidacy criteria have been broadened to such an extent that the age of CI users nowadays ranges from children under one year old (Cosetti & Roland, 2010) to elderly patients implanted after their 70th birthday or later (e.g. Carlson et al., 2010; Chatelin et al., 2004; Williamson, Pytynia, Oghalai, & Vrabec, 2009). Prelingually deafened adolescents and adults were once considered poor candidates for cochlear implantation. However nowadays these patients use CIs, and several assessment studies have been performed after implantation (Most, Shrem, & Duvdevani, 2010; Santarelli, De Filippi, Genovese, & Arslan, 2008).

The main goal in CI technology is to develop devices that allow users to be able to understand speech and communicate with other people. Therefore the assessment of outcome after implantation has been based on tests that evaluate speech recognition, and on questionnaires such as the Abbreviated Profile of Hearing Aid Benefit (Cox & Alexander, 1995). There are multiple versions of speech recognition tests. These tests can comprise recognition of phonemes, words or sentences. Results from different speech recognition tests are summarized in Figure 2.16 (Gifford, Shallop, & Peterson, 2008). The stimulation can be delivered in silence or in noisy conditions, with or without visual cues, and with or without the use of hearing aids. The scores are normally calculated as the percent (%) of correct phonemes or words repeated by the CI user. For tests performed in noise, the score is typically a speech recognition threshold measured in dB that corresponds to the SNR at which 50% of the speech material is recognized correctly. In Figure 2.16 it can be observed that for test A, the Hearing in Noise Test (HINT) with sentences in quiet, a large number of CI users scored above 90%. On the other hand, for test D, the Bamford-Kowal-Bench Speech-in-Noise (BKB-SIN), a large variability in performance was observed across CI users.

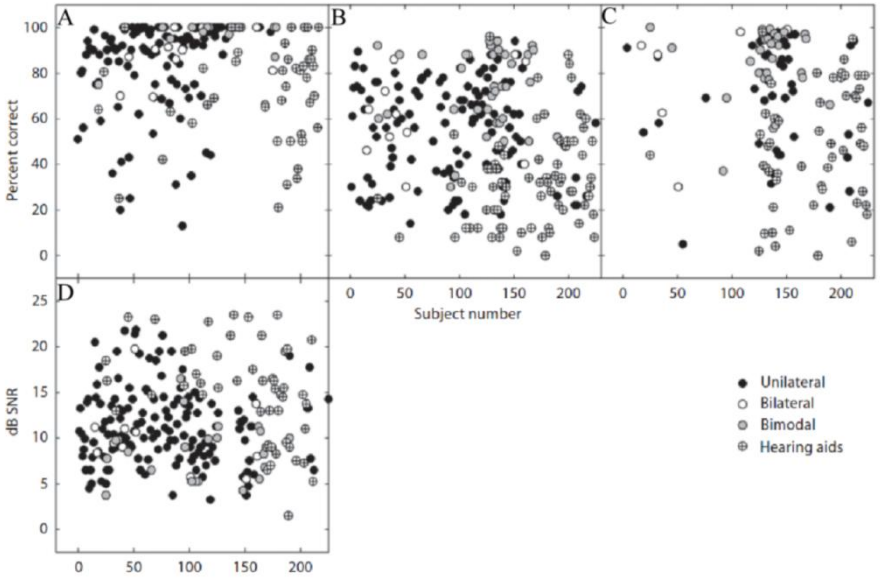

Figure 2.16 *Individual subject performance for the Hearing in Noise Test (HINT) with sentences in quiet (A; n = 188), the Consonant-nucleus-consonant (CNC) monosyllables test (B; n =287), AzBio sentences in quiet (C; n = 137), and Bamford-Kowal-Bench Speech-in-Noise (BKB-SIN) test (D; n = 231) (from Gifford, et al., 2008).*

Other authors have also shown that speech recognition tests in quiet can be prone to ceiling effects, i.e. many adult CI users can achieve scores of 100% (Gifford, et al.,

2008). This reflects that with current CI technology for the majority of CI users it is not difficult to communicate in quiet environments. However, when CI users are assessed with speech-in-noise tests, the scores tend to be lower, and the large variability of outcomes across subjects becomes evident (Donaldson et al., 2009; Gifford, et al., 2008; Wilson & Dorman, 2008a). It is also noteworthy that speech scores are frequently used to categorize CI users in terms of their performance with the CI.

It seems that parameters such as age at implantation, duration of deafness, exposure to oral communication and pre-operative hearing thresholds condition the outcome (Cosetti & Waltzman, 2011). In the case of children, age of implantation seems to be crucial, since an earlier implantation favors the normal development of auditory functions (Sharma, Dorman, & Kral, 2005; Sharma, Dorman, & Spahr, 2002) and acquisition of language (Peterson, Pisoni, & Miyamoto, 2010; Uhler, Yoshinaga-Itano, Gabbard, Rothpletz, & Jenkins, 2011). In the case of post-lingually adults, the duration of deafness seems to be a key parameter. It is likely that these deafened individuals can associate the new artificial stimulation patterns provided by the implant to their memories of what speech should sound like (Dorman & Wilson, 2004). In the case of pre-lingually deafened not only does the duration of deafness seems to be important, but also the exposure to oral communication (Cosetti & Waltzman, 2011). However it is not always easy to establish the onset of deafness for each patient. As mentioned previously, deafness is frequently a progressive condition and formal diagnosis can sometimes only be provided at later stages.

In order to better investigate outcomes after implantation, it has been suggested that CI users should be assessed with a battery of tests, instead of a single test (Gifford, et al., 2008). Moreover it is also important to establish recommendations and guidelines for the use of the different speech recognition tests. This may ensure that the interpretation of the results across clinics would provide unbiased, objective measurement of auditory rehabilitation (Theunissen, Swanepoel de, & Hanekom, 2009). On the other hand a number of authors have argued that AEPs can be a valuable measurement to objectively evaluate auditory rehabilitation (e.g. Brix & Gedlicka, 1991; Cone-Wesson & Wunderlich, 2003; Kraus et al., 1993; Shallop, 1993), especially when dealing with prelingually deafened CI users (McNeill, Sharma, & Purdy, 2009) or pediatric populations (Kileny, 2007; Singh, Liasis, Rajput, Towell, & Luxon, 2004).

2.3.4. Auditory evoked potentials as an objective assessment of auditory rehabilitation

Evidence of plasticity in the auditory cortex of adult post-lingually deafened CI users has been reported in a longitudinal MEG study, where it was shown that the auditory cortex of CI users could adapt to the artificial stimulation within just the first six months (Pantev, Dinnesen, Ross, Wollbrink, & Knief, 2006). However it is still not yet well understood how either the adaptation process itself or any deficits of adaptation could relate to the large variability of outcomes observed after implantation. Furthermore only a few studies have investigated which parameters can be used as best predictors of outcome after implantation (van Dijk et al., 1999) and it is still not yet clear which rehabilitation strategies can contribute to improved performance with the CI (Champoux, Lepore, Gagne, & Theoret, 2009; Rouger et al., 2007). In the last years, due to its objectivity and feasibility, AEPs have become a popular technique to investigate how the auditory cortex from patients adapts to the artificial input delivered by the implant. Evidence has been provided that electrophysiological responses could be related to clinical parameters, such as duration of deafness (Kelly, Purdy, & Thorne, 2005; Sandmann et al., 2010), experience with the implant (Kelly, et al., 2005), or performance in speech recognition tests (Kelly, et al., 2005; Zhang et al., 2011).

Tables 2.1 and 2.2 list a summary of representative AEP studies with adult CI users, and implanted children, respectively. The selected studies comprise different research settings, including different experimental paradigms, EEG montages, and signal processing tools to attenuate CI artifacts. Studies published before 2002 are not included in the tables due to space limitations (e.g. Brix & Gedlicka, 1991; Hoth, 1998; Kileny, Boerst, & Zwolan, 1997; Kraus, et al., 1993; Kubo et al., 2001; Shallop, 1993). Furthermore, note that AEP studies where the auditory stimulation was delivered directly to the CI electrodes are also not listed in the tables. (e.g. Guiraud et al., 2007; Makhdoum, Groenen, Snik, & van den Broek, 1998).

Among the studies with adults, several have investigated the relationship of AEPs to speech perception (Henkin et al., 2009; Kelly et al., 2005; Lonka et al., 2004; Zhang et al., 2010; Zhang et al., 2011) or to music perception (Koelsch, Wittfoth, Wolf, Muller, & Hahne, 2004; Sandmann, et al., 2010). Other authors have investigated brain asymmetries in the auditory cortex of adult CI users (Debener, et al., 2008a; Sandmann et al., 2009). Outcomes of these studies have revealed relationships between AEPs and clinical profiles. For instance shorter P2 latencies were associated with higher speech recognition scores and shorter durations of deafness (Kelly, et al., 2005). In a study investigating the

adaptive pattern of the N1-P2 complex, it was found that poor performers with the CI had a smaller adaptation index than good performers, whereas the adaptation index was similar for good performers and NH listeners (Zhang, Anderson, Samy, & Houston, 2010). It has been also reported that moderate-to-poor CI users have smaller MMN responses than good performers (Zhang, et al., 2011). Moreover an inverse relationship between MMN amplitudes and duration of profound deafness has been shown (Sandmann, et al., 2010). It has also been found that CI users have altered hemispheric asymmetries compared to NH listeners (Sandmann, et al., 2009). In a single case study it was reported that a CI user had a faster ipsilateral N1 response (Debener, et al., 2008a). According to the authors this result could be evidence of adaptation of the auditory cortex to the artificial monaural stimulation provided by the device (Debener, et al., 2008a).

In children the functional development of the auditory cortex has been investigated by measuring the P1 (Bauer, Sharma, Martin, & Dorman, 2006; Gilley, Sharma, & Dorman, 2008; Sharma, et al., 2005; Sharma, et al., 2002), the P3 (Beynon, Snik, & van den Broek, 2002; Henkin, Kileny, Hildesheimer, & Kishon-Rabin, 2008; Henkin et al., 2004) and the MMN response (Watson, Titterington, Henry, & Toner, 2007). The studies investigating the P1 response, a typical marker of cortical maturation, have shown evidence of sensitive periods in the development of the central auditory system (Gilley, et al., 2008; Sharma, et al., 2005; Sharma, et al., 2002). These results favor the implantation of congenitally deaf children in their first two or three years of life, since these children tend to develop normal P1 responses after the first months of artificial auditory stimulation (Sharma, et al., 2005).

In the studies described above the authors used different approaches to attenuate the CI artifact. In the studies using a small number of recording electrodes, it was possible to identify AEPs free from artifacts (Kelly, et al., 2005; Lonka et al., 2004; Watson, et al., 2007). In other studies the authors have focused the analysis on the P3 response, because the P1-N1-P2 complex was contaminated by CI artifacts (Henkin, et al., 2008; Henkin, et al., 2004; Henkin, Tetin-Schneider, Hildesheimer, & Kishon-Rabin, 2009). Other authors have used an optimized differential reference (ORD) technique (Bauer, et al., 2006; Sharma, et al., 2005), while studies using high-density EEG recordings, have used ICA (Debener, et al., 2008a; Gilley, et al., 2008; Sandmann, et al., 2009; Sandmann, et al., 2010; Sharma, et al., 2005; Zhang, et al., 2010; Zhang, et al., 2011). The application of the ORD technique and ICA in the context of the CI artifact is described in section 2.3.5.

Tabel 2.1 *Examples of AEP studies with adult CI users published between 2004 and 2011*

1st author, year	CI users[◊]	CI type	Control group	Nr. EEG channels	Stimuli type[†]	Stimuli duration (ms)	Task	CI artifact attenuation	Research question investigated	Target AEP response
Debener, 2008	1	n.a.	n.a.	68	tones, white noise	220	passive listening	ICA	auditory cortex asymmetries	P1-N1 complex
Henkin, 2009	15	diff.	unmatched	19	consonant-vowel syllables	250	odd-ball	none	relationship between P3 and behavioral measures	P3
Kelly, 2005	12	same	matched	7	tones	60	passive listening, odd-ball	reference: contralateral earlobe	neural correlates of speech perception	P1, N1, P2, MMN, P3
Koelsch, 2004	12	same*	matched	19	5 chords	600 or 1200	odd-ball	none	neural correlates of musical perception	ERAN, N5
Lonka, 2004	5	same	n.a.	5	speech vowels	400	passive listening	none	auditory discrimination (longitudinal design)	MMN
Sandman, 2009	12	same	matched	63	dyadic tones	150	odd-ball	ICA	auditory cortex asymmetries	P1, N1, P2
Sandman, 2010	12	same	matched	63	musical tones	150	passive odd-ball	ICA	neural correlates of musical perception	MMN
Zhang, 2010	9	same	n.a.	40	tones	60	passive listening	ICA	AEPs adaptive pattern	N1, P2
Zhang, 2011	10	same	unmatched	40	speech syllables, tones	40	passive listening	ICA	AEPs adaptive pattern	MMN

Notes. CI = Cochlear implant; n.a. = not applicable; ICA = Independent component analysis; diff. = different; ERAN = Early right anterior negativity.
[◊]In all studies the CI users tested were post-lingually deafened adults. [†]In all studies auditory stimulation was delivered using loudspeakers, except in Sandmann et al, 2009, 2010, where the stimulation was delivered via an audio cable connected to the CI speech processor. [*]One out of the twelve CI users had a device from a different manufacturer with a different speech coding strategy.

Table 2.2 *Examples of AEP studies with children using CIs published between 2002 and 2011.*

1st author, year	CI users◊	CI type	Control group	Nr. EEG channels	Stimuli type†	Stimuli duration (ms)	Task	CI artifact attenuation	Research question investigated	Target AEP response
Bauer, 2006	4	n.avail	n.a.	3	speech syllables	90	passive listening	ODR	maturation of auditory cortex of children with bilateral CIs (longitudinal	P1
Beynon, 2002	10	same	matched	3	Tones and speech syllables	n. avail.	odd-ball	reference: contralateral earlobe	relationship between AEPs and speech recognition scores	N1, P2, P3
Gilley, 2008	16	n. avail.	matched	66	speech syllables	97	passive listening	ICA	P1 response generators	P1
Henkin, 2004	4	same	unmatched	21	tones, speech syllables	100	odd-ball	none	P3 response generators	P3
Henkin, 2008	10	same	n.a.	19	consonant-vowel syllables	250	odd-ball	none	relationship between P3 and behavioral measures	P3
Sharma, 2002	121	n. avail.	matched	3	speech syllables	90	passive listening	none	maturation of auditory cortex	P1
Sharma, 2005	23	n. avail.	n.a.	3	speech syllables	90	passive listening	ODR	maturation of auditory cortex (longitudinal design)	P1
Watson, 2007	15	n. avail	matched	5	tones	50	passive listening	none	auditory sensory (echoic) memory	MMN

Notes. CI = Cochlear implant; n. avail = not available; n.a. = not applicable; ODR = Optimized differential reference; ICA = Independent component analysis. †In all studies stimulation was delivered using loudspeakers. ◊In all studies the CI users tested were congenitally deaf children, except in Sharma et al, 2002, where 3 congenitally deaf adults were also tested.

2.3.5. EEG recordings from cochlear implant users

This section describes several techniques that have been used to measure neuronal activity in CI users. A particular emphasis is given to the use of EEG, due to its advantages. The challenges associated with EEG are also discussed, such as the characteristics of the CI artifact. Furthermore the techniques that have been implemented to attenuate the CI artifact are also discussed briefly.

In the past years a few studies have used MEG to study the cortical functions of CI users (Hari et al., 1988; Hoke, Pantev, Lutkenhoner, Lehnertz, & Surth, 1989; Pantev, et al., 2006). This technique is similar to EEG in that it is non-invasive and has high temporal resolution. MEG measures the magnetic fields produced by the electrical currents occurring in the brain. In contrast to EEG, MEG requires a RF shield to protect the sensors from the RF interference generated by the CI-processor. Unfortunately the whole-head helmets that are part of the modern MEG systems (Figure 2.17) do not allow the implementation of shielding. Therefore the use of MEG to study CI users has been discontinued.

Figure 2.17 *Example of a participant undergoing a MEG recording. Note that the sensor arrays are set in a helmet-shaped that covers most of the head. Courtesy of National Institute of Mental Health, USA.*

A larger number of studies have used the positron emission tomography (PET) technique to investigate patterns of cortical activation in CI users (Coez et al., 2008; Giraud & Lee, 2007; Giraud, Price, Graham, Truy, & Frackowiak, 2001a; Giraud & Truy, 2002; Giraud, Truy, & Frackowiak, 2001b; Green, Julyan, Hastings, & Ramsden, 2005, 2008; Ito et al., 2004; Lee et al., 2001; Lee et al., 2007; Rouger et al., 2011; Strelnikov et al., 2010). This technique is a high resolution imaging method that uses radioactive markers to quantitatively evaluate the blood flow that results from local synaptic activity in the brain (Phelps, 2006). One of the limitations of PET is the fact that it is an invasive technique which therefore limits the number of sessions that can be done with the same participant. Additionally the associated costs are high.

Other imaging methods are MRI or fMRI. Both rely on the indirect measurement of the blood-oxygenation-level-dependent (BOLD) response to localize brain regions engaged during cognitive processes (Jezzard, Matthews, & Smith, 2001). The first generation of CI devices were not compatible with the magnetic fields generated by the MRI scanners (Majdani et al., 2009), thus ruling out this technique for clinical and experimental studies with CI users. However MRI is an important diagnostic tool in clinical settings. Furthermore obtaining brain scans from CI users before implantation could also be informative in research studies (Lazard, Giraud, Truy, & Lee, 2011). Recent advances in CI technology have led to devices with and without removable magnets which are reported to be safe in MRI scanners up to 1.5 T (Crane, Gottschalk, Kraut, Aygun, & Niparko, 2010; Heller, Brackmann, Tucci, Nyenhuis, & Chou, 1996; Hochmair, 2001). Nevertheless it is not well understood if the image quality could be substantially compromised due to artifacts (Majdani, et al., 2009). It is also noteworthy that the CI speech processor would not work inside the scanner. Therefore fMRI studies to investigate the function of the auditory cortex are only feasible when the stimulation is provided directly to the CI electrodes (Lazeyras et al., 2002).

Near-infrared spectroscopy (NIRS) is another non-invasive technique. This involves measuring the transmission of near-infrared light through the tissue in order to detect changes in blood oxy- and deoxy-hemoglobin concentrations, which in turn reflect neuronal activity (Siesler, 2002). NIRS has been used recently in a single study with a pediatric CI sample. This study has reported that speech-evoked cortical activity was observed in 78% of deaf children who have used a CI for longer than four months, as well as in 78% of deaf children who completed NIRS testing on the day of CI initial activation (Sevy et al., 2010). These preliminary results have revealed that NIRS can measure cortical responses in pediatric CI users but await replication.

EEG is a well-established technique with several advantages, since it is also non-invasive, cost-effective, and can be used to test different types of CI users, including pediatric samples. Figure 2.18 shows a CI user before and after preparation for the EEG recording session. The preparation and the recording session were performed exactly as they would have been for a NH participant, the only difference being that a few electrodes coinciding with the location of the external parts of the CI device had to be disconnected (Figure 2.18, right).

Figure 2.18 *EEG recording from a CI user. On the left side is a CI user before starting the preparation for the recording session. On the right side is the same participant after applying the EEG cap. The only change in the recording consisted of disconnecting the electrodes, in this case three, located in the same region as the external parts of the CI device.*

However EEG recordings are contaminated by an electrical artifact. The magnitude of the artifact can be much larger than the brain responses. Thus in some cases the AEPs cannot be evaluated since the responses are completely corrupted by the CI artifact. The origin of the artifact is not well described. It has been suggested that the artifact may be caused by RF transmission of the signal from the implant transmitter to the receiver (Debener, et al., 2008a; Henkin, et al., 2008; Martin, 2007), but other parts of the device could also contribute.

Common ways of dealing with artifacts consist of either ignoring contaminated portions of the EEG recording or averaging the data over trials, as described in section 2.1.3. The CI artifact however is ubiquitous since it is time-locked to the auditory stimulus and has the same duration as the stimulation. The two solutions described above are therefore not suitable. Figure 2.19 shows the typical signature of a CI artifact. The onset of the artifact occurs slightly after the onset of the sound (0 ms) and is followed by a "pedestal" where the amplitude of the artifact achieves its maximum value, then a plateau is reached, and lastly the offset of the artifact is observed slightly after the offset of the sound (220 ms).

The artifact problem could be overcome by conditioning the type of auditory stimuli used. One option is the use of very short auditory stimuli, hoping that the responses of interest would be free of artifact. However it was found that even with speech stimuli as short as 23 ms the AEP time window of interest (P1 response) was still contaminated by the CI artifact. This was due to the filter characteristics of the recording amplifiers (Gilley, et al., 2006). Furthermore experimental paradigms using natural speech or environmental sounds require stimuli with longer durations, meaning that the CI artifact

would likely overlap with the entire AEP. Other authors have suggested that the artifact could be attenuated by implementing a subtraction technique. This requires the manipulation of the auditory stimuli in order to create experimental conditions where the AEP response varies but the CI artifact remains constant (Friesen & Picton, 2010). One significant disadvantage is that this type of manipulation limits the experimental paradigms that can be used.

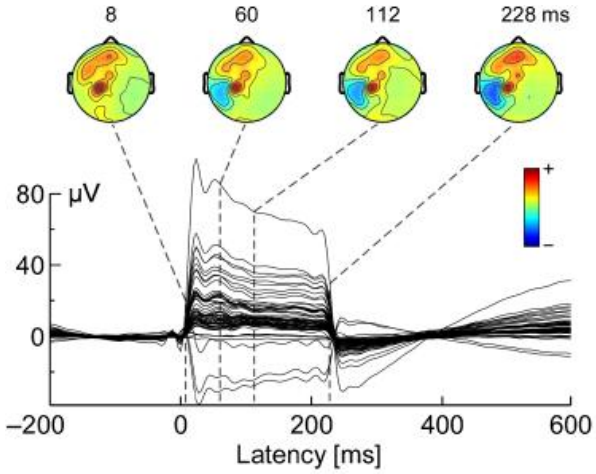

Figure 2.19 *AEPs before ICA-based artifact reduction, together with voltage maps at selected latencies, scaled to the absolute maximum (adapted from Debener, et al., 2008b).*

Another approach would be to focus the research questions in later AEP responses, such as the P3 (Henkin, et al., 2008; Henkin, et al., 2004; Henkin, et al., 2009) or the N5 (Koelsch, et al., 2004). However these solutions are very limited, as it can also be of major interest to investigate the P1-N1-P2 complex, since these responses reveal early sensory processes (reviewed in Cone-Wesson & Wunderlich, 2003; Hyde, 1997; Martin, et al., 2008). Moreover the P1 response is a reliable indicator of cortical maturation in children (Sharma, et al., 2005; Sharma, et al., 2002).

Due to the limitations of the approaches described previously, the implementation of other methods has received special attention. One approach has been using the ODR technique, which consists in placing the reference of the EEG montage in a location that allows recording a particular electrode of interest free of artifact (Bauer, et al., 2006; Gilley, et al., 2006; Sharma, et al., 2005). A shortcoming of the ODR technique is finding and validating the best location for the reference for each CI user, which can be time consuming. This technique then seems to be feasible only when a few channels are recorded (Bauer, et al., 2006; Sharma, et al., 2005). Other authors used linearly constrained minimum variance beamformers to reconstruct cortical activity with minimal

artifact interference (Wong & Gordon, 2009). However the feasibility and validity of this approach is still discussable, since it was validated using a single CI user dataset.

Another option is the use of ICA. Several studies have reported that AEPs from CI users could be reconstructed after ICA-based CI artifact attenuation (Debener, et al., 2008a; Gilley, et al., 2006; Gilley, et al., 2008; Sandmann, et al., 2009; Sandmann, et al., 2010; Zhang, et al., 2010; Zhang, et al., 2011). However less successful outcomes have also been reported (Martin, 2007). It is also not clear how sensitive and specific the ICA correction for this type of artifact is. In most of the studies that have used ICA results have been obtained using small samples of CI users with similar CI devices (Gilley, et al., 2008; Sandmann, et al., 2009; Sandmann, et al., 2010; Zhang, et al., 2010), or even single cases (Debener, et al., 2008a), raising concerns about the generality of the results. Moreover the attenuation of CI artifacts requires the visual inspection of all ICs in order to select the ones representing the artifact. This process is subjective, time consuming and requires expertise, as discussed in section 2.2.3.

Since AEPs allow the objective study of auditory functions in CI users, the improvement of methods to overcome the CI artifact problem would be of great value. Assuming that the ICA-based attenuation is the most promising approach, it would be important to develop more objective tools to screen and select the ICs related to the CI artifact. This improvement would likely facilitate the reconstruction of AEPs and extend its potential to complement results from other clinical tests. It is expected that in the long run AEP studies could shed some light into possible rehabilitation strategies or even be used as a predictor of outcome after implantation.

3. Objectives

It is impossible to record multi-channel EEG free of artifacts. A number of approaches have been used to substantially attenuate different types of artifacts. Some examples are filtering, averaging, applying regression-based or blind source separation methods. The technique adopted in this project was ICA. There is strong evidence that ICA can successfully be used to attenuate a variety of different artifacts ranging from common biological artifacts such as eye blinks (e.g. Hoffmann & Falkenstein, 2008; Jung, et al., 2000a; Jung, et al., 2000b) to specific non-biological artifacts such as CI artifacts (e.g. Debener, et al., 2008a; Gilley, et al., 2006).

In order to attenuate the artifacts from the EEG signal, it is necessary to identify artifact-related ICs. These components are then removed in the back-projection step, allowing the recovery of a corrected version of the original EEG signal. The standard method for selecting and categorizing ICs has been the visual inspection of the component properties in both the time and frequency domain. This procedure is time consuming, requires expertise and can be influenced by subjective decisions. Therefore it seems desirable to develop new tools, which could allow a more objective selection of ICs and facilitate the process of attenuating artifacts. The benefit would be not only in making the ICA approach easier and quicker but also in standardizing results from different laboratories.

The goal of the first study was to develop and validate an ICA-based tool that identifies ICs related to biological artifacts across individuals. This tool is based on the correlation of ICA scalp maps (i.e. inverse weights) with a user-defined template, hence the name CORRMAP. The template should be an IC representing one of the following three biological artifacts: eye blinks, lateral eye movements, or heartbeat related artifacts. Each of these artifact-related ICs is known to have similar scalp maps across individuals. This similarity is predictable because the sources of the artifact, i.e. eyes and heart, have approximately the same location relative to the EEG electrodes. This study is described in Chapter 4.

Study 1 showed that ICs representing common biological artifacts can be semi-automatically identified, facilitating the investigation of ERPs. AEPs in particular are an objective measure of auditory cortical function and can be used to evaluate auditory rehabilitation after cochlear implantation. The auditory cortex can adapt to the electrical stimulation provided by the CI within a few months (Pantev, et al., 2006). However the outcomes after implantation vary substantially between CI users. By using objective

measurements of auditory cortex function, researchers expect to complement other clinical measurements that characterize the profile of a CI user.

However EEG recordings from CI users are corrupted by an electrical artifact caused by the CI device, the amplitude of which is much larger than the auditory neural responses. This artifact has special characteristics, one being the fact that it is time-locked to an auditory stimulus. Therefore AEPs tend to be completely masked by the artifact. It has been proposed that ICA can disentangle the electrical artifact from brain activity and other artifacts, making it possible to reconstruct AEPs from CI users (Debener, et al., 2008a; Gilley, et al., 2006; Gilley, et al., 2008; Sandmann, et al., 2009; Sandmann, et al., 2010; Zhang, et al., 2010; Zhang, et al., 2011). However these results are still preliminary and the effects of artifact attenuation on AEP quality have not been yet investigated.

The goal of the second study was to investigate the effects of electrical artifact attenuation on the quality of AEPs from 18 adult post-lingually deafened CI users. The sensitivity of ICA, i.e. the ability to reduce the CI artifact, was investigated. The specificity of ICA, here defined as the ability to attenuate the CI artifact while preserving the AEPs, was also assessed. Lastly, the quality of the AEPs was evaluated with an SNR measure. This study is described in Chapter 5.

Study 2 showed evidence that ICA is successful in attenuating CI artifacts from EEG data. However since researchers have only recently started to use multi-channel EEG recordings to test CI users, the guidelines in the literature explaining how to identify ICs representing CI artifacts are still limited (Gilley, et al., 2006; Sandmann, et al., 2009). Moreover none of the "automatic" tools developed seems to be able to identify CI artifacts across CI users (Mognon, Jovicich, Bruzzone, & Buiatti, 2010; Nolan, Whelan, & Reilly, 2010; Viola et al., 2009).

The goal of the third study was to develop and validate a new ICA-based tool to evaluate temporal and topographical properties of ICs and to automatically select these components representing CI artifacts. The Cochlear Implant Artifact Correction (CIAC) tool identifies ICs across CI users stimulated with the same type of auditory stimuli. This study is described in Chapter 6.

4. Study 1: Semi-automatic identification of independent components representing EEG artifact

The study described in this chapter was published in volume 120 of the journal "Clinical Neurophysiology" in January 2009 (Viola, et al., 2009). FCV designed and developed the tool code, run the validation study and prepared the manuscript, JT contributed to the design of the validation study and to the preparation of the manuscript, BE, TS and TE were raters in the validation study and helped with the preparation of the manuscript. SD supervised all parts of the work, and also contributed to the preparation of the manuscript.

4.1. Abstract

Objective: Independent component analysis (ICA) can disentangle multi-channel electroencephalogram (EEG) signals into a number of artifacts and brain-related signals. However, the identification and interpretation of independent components is time-consuming and involves subjective decision making. We developed and evaluated a semi-automatic tool designed for clustering independent components from different subjects and/or EEG recordings.

Methods: CORRMAP is an open-source EEGLAB plug-in, based on the correlation of ICA inverse weights, and finds independent components that are similar to a user-defined template. Component similarity is measured using a correlation procedure that selects components that pass a threshold. The threshold can be either user-defined or determined automatically. CORRMAP clustering performance was evaluated by comparing it with the performance of 11 users from different laboratories familiar with ICA.

Results: For eye-related artifacts, a very high degree of overlap between users (*phi* > 0.80), and between users and CORRMAP (*phi* > 0.80) was observed. Lower degrees of association were found for heartbeat artifact components, between users (*phi* < 0.70), and between users and CORRMAP (*phi* < 0.65).

Conclusions: These results demonstrate that CORRMAP provides an efficient, convenient and objective way of clustering independent components.

Significance: CORRMAP helps to efficiently use ICA for the removal EEG artifacts.

4.2. Introduction

For many years, electroencephalogram (EEG) recordings have been successfully used in clinical diagnosis and cognitive brain research. However, a key characteristic of scalp recorded EEG signals is that they consist of a mixture of an unknown number of brain and non-brain contributions. In other words, the EEG signals suffer from the presence of various artifacts, which renders the identification and analysis of brain-related EEG activity difficult (Makeig, et al., 2004a). Here we present a new approach to the identification of prominent EEG artifacts. In combination with independent component analysis (ICA), this approach provides an efficient, accurate and less subjective correction procedure for multi-channel EEG recordings.

Over the past few years, ICA has gained considerable popularity for the processing of EEG signals (e.g., Debener, Ullsperger, Siegel, & Engel, 2006; Makeig, et al., 2004a). ICA performs a linear un-mixing of multi-channel EEG recordings into maximally temporally independent statistical source signals, which are further referred to as independent components (ICs). ICA belongs to a larger family of blind source separation algorithms that separate mixed signals without the aid of detailed a priori information about the nature of these signals (Hyvärinen, et al., 2001). Given the lack of knowledge about the exact nature, number, and configuration of neural and non-neural sources contributing to the scalp-recorded EEG, blind source separation algorithms are particularly well suited to the decomposition of EEG data. Indeed, several laboratories have successfully demonstrated that ICA can separate multi-channel EEG recordings into meaningful brain and non-brain processes. Typical examples include the removal of artifacts, in particular eye blinks and lateral eye movements (Jung, et al., 2000a; Jung, et al., 2000b); the removal of stimulus-locked electrical artifacts from cochlear implants (Debener, et al., 2008a; Gilley, et al., 2006); or the removal of residual ballistocardiogram and magnetic resonance imaging (MRI) gradient artifact from EEG data recorded inside the MRI (Debener, et al., 2008b; Debener, et al., 2007; Eichele et al., 2005; Feige et al., 2005; Onton, et al., 2006). Moreover, ICA has been used for the identification of neuronal event-related oscillations (Makeig, et al., 2002; Onton, Delorme, & Makeig, 2005) and event-related potentials (Debener, et al., 2005a; Debener, et al., 2005b). A thorough discussion of the concepts related to the application of ICA to EEG data is provided by Onton et al. (2006).

From a practical point of view, the efficient removal of EEG artifacts is very desirable, as a proper correction substantially improves the number of trials that can be retained for event-related EEG analysis. Some studies have suggested (Debener, et al., 2007; Joyce,

Gorodnitsky, & Kutas, 2004) that the removal of some EEG artifacts by means of ICA could be implemented as a fully automatic procedure if a well-defined criterion or template were provided. However, it is still necessary and often mandatory to visually inspect and evaluate the quality of ICA decompositions before artifact processing.

Regarding eye blink artifacts, ICA-based correction compares favorably to more frequently used linear regression procedures (Joyce et al., 2004). The eye blink correction quality that can be achieved by means of ICA is illustrated in Figure 4.1. As can be seen, ICA finds components that closely resemble the topography and time course of single, representative eye blinks, and thus can separate this artifact from other EEG activity. However, the user is left with the problem of component selection, interpretation and clustering, because ICA is usually applied to single subject datasets (for review see Onton, et al., 2006). For example, if 64-channel EEG were recorded from 20 subjects, 1280 components would require evaluation. A number of different methods can be used to guide the IC identification and selection process, such as visual inspection of IC properties (Debener, et al., 2005a), a selection based on IC topographies and experimental condition effects (Debener, et al., 2005b) or more formal cluster analysis procedures (e.g., Makeig, et al., 2004b).

Formal cluster approaches based on the modified Mahalanobis distance are part of the EEGLAB open source environment (Delorme & Makeig, 2004). Types of IC information or features that can jointly be used for clustering comprise IC topographies (i.e., inverse ICA weights), event-related potentials (ERPs, i.e., component activation time-domain averages), spectra, time–frequency results, and source localization information. However, this approach leaves the user with a large number of parameters to determine by trial and error, as the dimensionality and relative weight for each of these features requires specification. Accordingly, clustering based on a joint consideration of multiple features is a time consuming and difficult task, regardless of the actual cluster algorithm used. Even if an optimal configuration were to be found, an inevitable problem would still be the need to re-cluster or re-group the first level results, which would also be guided by subjective decision making rather than objective, data-driven criteria.

We developed a new, simple way of clustering, named CORRMAP, designed to identify certain prominent artifact ICs across subjects in a semi-automatic way with full user control but using a statistically guided cluster definition. We validated the performance of our template-correlation based cluster approach by comparing the results with the identification and classification of ICs representing various EEG artifacts from 11

different EEGLAB users who were familiar with ICA. This test data comprised 4256 ICs from three different studies recorded in three different laboratories

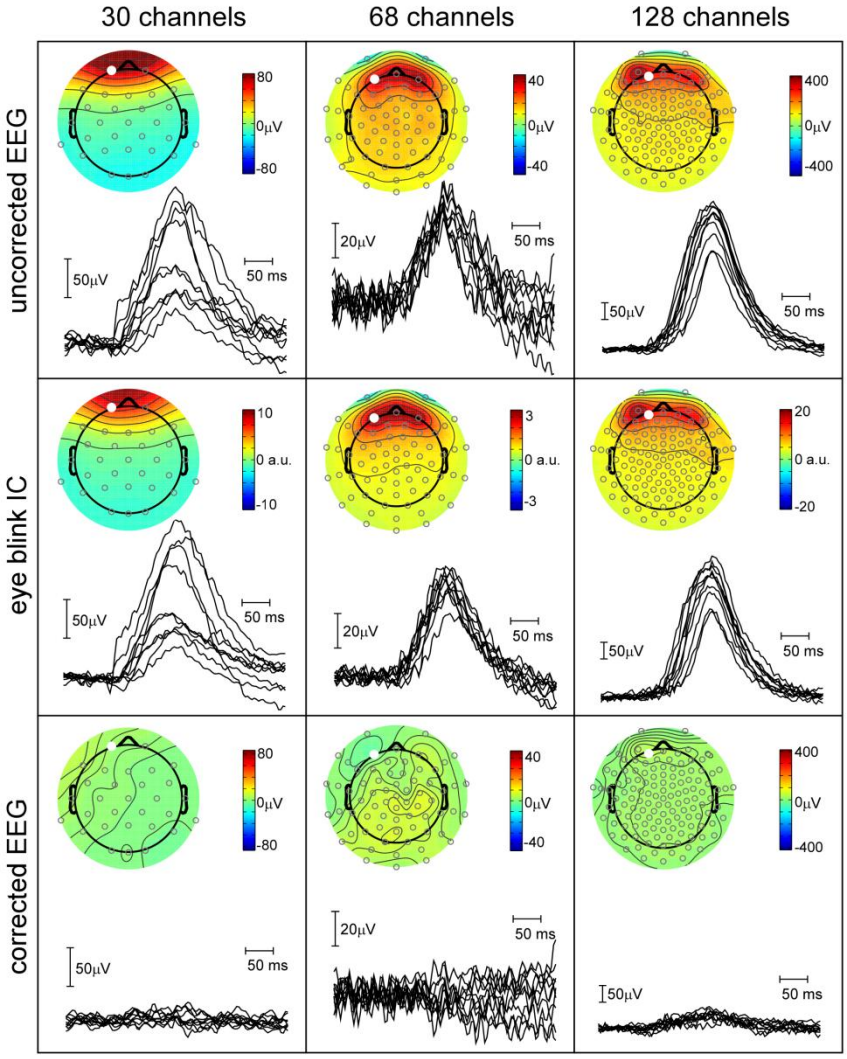

Figure 4.1 *ICA-based eye blink artifact correction, illustrated for three different datasets recorded in different laboratories and based on 30 (left), 68 (middle) and 128 (right) EEG channels, respectively. Top row shows 10 representative eye blinks at a channel in close proximity (68 and 128 channel datasets), or corresponding to (30 channel dataset) Fp1 of the international 10–20 system, and the mean voltage map for these eye blinks. Middle row shows the identified ICA eye blink component map (inverse weights, in arbitrary units) together with the 10 back-projected eye blinks at ~Fp1. Bottom row shows the result of the back-projection of all components except for the one shown in the middle row. Inspection of maps and voltage traces in the bottom row indicates near perfect eye blink correction for the 30 and the 68 channel datasets. Residual eye blink activity can be seen in the 128 channel dataset, illustrating our common observation that eye blinks can be represented by more than one ICA component in high-density EEG recordings.*

4.3. Methods

4.3.1. CORRMAP description

CORRMAP is a semi-automatic ICA clustering tool. It requires as its main input a template map (inverse IC weights) and it operates in two different modes. In the automatic mode, CORRMAP identifies all ICs correlating with the template above an automatically determined threshold (see below). In the manual mode, CORRMAP identifies all ICs correlating with the template above a user specified threshold. A schematic illustration of all processing steps involved is shown in Figure 4.2.

The core of the algorithm is a two-step loop. In the first step (Figure 4.2., left) the inverse weights (i.e., IC maps) from a selected template IC are correlated with all ICs from all datasets. For each dataset, CORRMAP selects up to three ICs with the largest suprathreshold correlation with the template. The maximum number of ICs selected can be changed by the user. This approach was chosen because in high-density EEG recordings, the same process (e.g., eye blinks) can be represented by more than one IC (e.g., Onton, et al., 2006). Across all datasets, the selected ICs are then sorted in descending order of correlation. Here, absolute correlations are used to take into account the sign ambiguity problem (Onton, et al., 2006). The mean correlation of a resulting cluster is then computed via Fisher's z transform, to account for the non-normal distribution of correlation values. Next, an average cluster map is calculated, after inversion of those ICs showing a negative correlation (sign ambiguity problem) and root mean square (RMS) normalization of each individual IC.

In the second step, the average cluster map obtained in the first step is then used as a new template and the same process is repeated (Figure 4.2.). This step evaluates the dependence of a cluster on the template IC initially selected. A similarity index (SI) was defined as one minus the absolute difference between the mean correlation values obtained from steps 1 and 2. A value close to 1 indicates that the resulting cluster is robust against the selection of the initial map, whereas a small value indicates that the initial template is not very representative of the cluster. For each of the two processing steps, a summary plot showing the template, the selected ICs, their correlations with the template and further cluster information, is produced.

The correlation threshold initially used can either be given as an input parameter (manual mode) or can be determined automatically using an iterative process (automatic mode). In automatic mode, this process consists of repeating the two core steps described above using a range of correlations from 0.95 to 0.80 in steps of 0.01. This range and step size

(determined in pilot tests) results in 16 iterations returning 16 similarity indices. In cases where correlations below 0.80 are considered, CORRMAP calculates additional iterations ranging from 0.79 to 0.55 in steps of 0.01. The final correlation threshold is then determined by choosing the iteration that returned the maximum SI. This procedure is based on the rationale that, with a low correlation threshold, qualitatively different maps would be included in the clusters, resulting in a smaller SI.

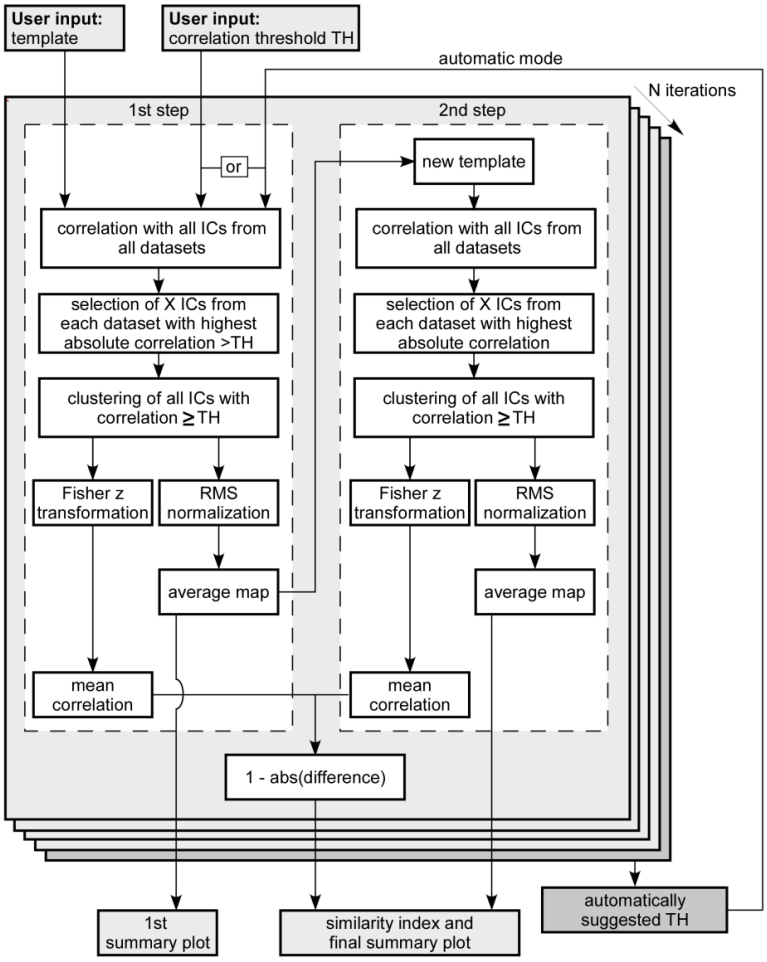

Figure 4.2 *Schematic flow chart of the CORRMAP tool. The main inputs are a template ICA component map selected by the user and a correlation threshold (TH) that can be selected or calculated by the tool (automatic mode). The template is compared with all component maps from all datasets by calculating a correlation value. All components with an absolute correlation equal to or greater than TH are selected to be part of the cluster and the mean correlation is calculated after Fisher z transformation. Up to X (usually 1–3) components per dataset are considered. This parameter can be changed by the user. An average map is calculated for the clustered components. The same procedure is repeated in a second step using this new map as the template (right column). A similarity index informs about the dependency of the result on the originally selected template. In automatic mode the procedure is repeated for N iterations utilizing different TH values and the TH which shows the maximum similarity index is suggested as the automatic correlation threshold.*

The default ICA algorithm used by EEGLAB (Delorme & Makeig, 2004) is Infomax ICA, where the number of ICs is usually equal to the number of EEG channels, normally corresponding to the rank of the data. However, CORRMAP also accepts a different number of ICs per dataset (in case of rank-deficiency or prior dimensionality reduction), thus providing greater flexibility. CORRMAP can also deal with variations in EEG channel numbers within a dataset, such as happens in the case of defective channels. In this case, CORRMAP requests a channel configuration file, and the inverse weights for missing electrodes are then automatically replaced using a modified version of the EEGLAB function eeg_interp(). All CORRMAP functions are written in Matlab (The MathWorks, Inc., MA, USA) and designed as a plugin for the EEGLAB toolbox (Delorme & Makeig, 2004). CORRMAP is available under the General Public Licence (GPL-Free Software Foundation, Inc., Boston, MA) and can be downloaded from http://www.debener.de.

4.3.2. Validation study

In order to evaluate CORRMAP, we compared its performance in the automatic mode with the visual identification and selection of artifactual ICs from EEGLAB users familiar with ICA (further referred to as 'users'). For that purpose, we used IC maps from three different EEG studies recorded in three different EEG laboratories and spanning 30–128 channels.

Study 1 is based on 16 resting EEG datasets from 4 different subjects, recorded inside (1.5, 3 and 7 T) and outside (~0 T) the MRI environment in Nottingham, UK, and published by Debener et al. (2008b). Briefly, the EEG data were recorded using a 30-channel MR-compatible EEG system (Brainamp MR, Brain Products GmbH, Munich, Germany) and an electrode cap with an extended 10–20 layout (Easycap, Herrsching, Germany). Extended Infomax ICA was performed on the continuous 30-channel EEG data. This study consisted of a total of 480 ICs.

Study 2 comprised auditory evoked potential recordings from 16 subjects, recorded in Southampton, UK (Hine & Debener, 2007). Continuous EEG data were recorded using a 68-channel infracerebral electrode cap (Easycap) connected to a Synamps2 amplifier (Compumedics, Charlotte, NC), and extended Infomax ICA was performed on the concatenated single-trial EEG data. This study consisted of a total of 1088 ICs.

Study 3 comprised 128-channel EEG data recorded in a cross-modal semantic priming paradigm from 21 subjects using a Brainamps MR plus amplifier system and an equidistant electrode cap provided by Easycap (Schneider, Debener, Oostenveld, &

Engel, 2008a). Data for this study were recorded in Hamburg, Germany, and consisted of a total of 2688 ICs. Further information on experimental and data processing details of the datasets used here are given in the respective publications of the three studies.

The inverse ICA weights (IC maps) from these three studies were sent to 16 users from 16 different EEG laboratories experienced with using ICA. Eleven users responded to our request and returned the classification information. The IC maps were provided as part of a Matlab program that displayed all maps in 2-D and required the user to input IC indices. For each dataset from each study, the IC indices representing three different types of artifacts, if present, had to be specified: eye blink ICs, lateral eye movement ICs and heartbeat artifact ICs. Note that users were provided only with the IC maps and did not have access to further information such as raw data or component activations. This was done to control for the information type that had to be used by the users for the classification. They received no further information except for the number of EEG channels used on each study. The maximum number of components they could select for each dataset and each artifact type was set to 3 (see above for rationale). A single example for each artifact type was provided. The selected indices were saved in a file for further analysis. Manual clustering was performed independently by the 11 users without time constraints. None of the users had access to the clusters selected by the others users. The users also indicated their experience with using ICA for removing artifacts on a Likert rating scale (from 1 = novice/beginner to 8 = expert).

4.3.3. Statistical analysis

CORRMAP was run in automatic mode, using as its input templates IC maps selected by visual inspection from the first dataset in each study. The output of CORRMAP was compared to the ICs selected by our users in three ways. First, we calculated the number of users that identified ICs also selected by CORRMAP for a given artifact type. Second, in order to evaluate whether users were significantly more liberal or conservative than CORRMAP, we calculated a paired *t*-test (i.e., the mean difference between the number of ICs identified by CORRMAP and each user) for each dataset, study and artifact type. Note that this measure does not inform about the degree of overlap between the ICs identified. Thus, in a third step, we calculated the degree of overlap or association (*phi*) between the users, and between the users and CORRMAP. Phi represents the degree of association between two binary variables with values close to 1 representing a high degree of association, and values close to 0 representing a low association. The significance calculation of phi scores corresponds to the significance calculation used for parametric correlations.

We also calculated the proportion of ICs that were missed by the users. This is defined in respect of only those ICs picked by CORRMAP and is the ratio of the total number of ICs picked by the 11 users to the total possible (i.e., 11 multiplied by the number of ICs selected by CORRMAP). As a 'true' classification cannot be defined in real data, we used CORRMAP selection as the reference.

4.4. Results

In automatic mode on a typical PC (2.13 GHz CPU), it took CORRMAP between 11 s (Study 1, 480 ICs) and 44 s (Study 3, 2688 ICs) to compute the cluster and generate output figures for further inspection. We are not aware of another clustering tool capable of producing the same output within similar time parameters. Furthermore informal feedback provided by the users revealed that they required substantially more than 30 min for performing the same classification task.

The descriptive statistics and results for the significance tests for all three studies and the three artifact types analyzed are summarized in Table 4.1. The first three rows show the total number of ICs identified by CORRMAP for each type of artifact for each study, respectively.

In Study 1, the eye blink cluster consisted of 15 ICs from a total of 16 datasets (four subjects in four separate experimental conditions). For the eye blinks in the other two studies, the number of ICs selected by CORRMAP was greater than the total number of datasets (Study 2 = 16 datasets, Study 3 = 21 datasets), indicating that in some cases more than one IC per dataset contributed to the eye blink artifact. Figure 4.3 shows a typical CORRMAP summary plot for the eye blink cluster in Study 1. Each IC map is depicted along with the absolute correlation with the template and information about the dataset to which it belongs. In this output, the mean map is shown enlarged, together with the correlation with the average map after the first iteration (below), and summary cluster information (above). The line plot in the upper right hand corner shows the sorted correlation values with the selected threshold indicated by a dashed line. A threshold value of r = 0.94 was automatically found by analyzing the similarity indices over a number of iterations. The similarity indices from all iterations are shown in the second line plot. A dashed line indicates the threshold used for the cluster depicted; it points towards the highest similarity index across all iterations performed.

Table 4.1 *Number of Independent Components (ICs) Identified by CORRMAP and by Users for Three Artifact Types for Three Studies*

	Artifact type					
	Blink		Lateral eye movements		Heartbeat	
Study						
	Number of ICs identified by CORRMAP					
1) 30 channels	15		13		4	
2) 68 channels	24		15		7	
3) 128 channels	47		22		7	
	Number of ICs identified by users					
	Mean	SD	Mean	SD	Mean	SD
1) 30 channels	15.27	0.47	16.45	3.45	12.55	10.11
2) 68 channels	23.73	3.52	17.55	2.77	9.00	3.22
3) 128 channels	38.63	3.98	22.45	3.96	8.82	5.55
	t-Test between users and CORRMAP (two-tailed)					
	$t(10)$	p Value	$t(10)$	p Value	$t(10)$	p Value
1) 30 channels	1.94	0.08	3.33	<0.01	2.80	0.02
2) 68 channels	-0.26	0.80	3.05	0.01	2.06	0.07
3) 128 channels	-6.97	<0.001	0.38	0.71	1.09	0.30

Note. p values < 0.05 were considered significant

For the other two artifact types analyzed, the total number of ICs selected per cluster by CORRMAP was smaller than the total number of datasets, except for the lateral eye movement cluster in Study 3. For this study there was one dataset that contributed more than one IC (not shown). In four out of the nine cases studied (3 types of artifact, 3 studies), a significant ($p < 0.05$, see Table 4.1.) difference between the number of ICs selected by CORRMAP and the number of ICs selected by the users was observed. Differences were largest for heartbeat artifacts in Study 1 and eye blink artifacts in Study 3.

For the eye blink and eye movement artifacts in Studies 1 and 2 (30 and 68 channels, respectively), only a few ICs that were identified by CORRMAP were not selected by users (range between 1.2% and 11.7%, not shown) and vice versa. For Study 3 (128 channels) on the other hand, the ratio of missed ICs was 17.4% (lateral eye movements)

and 25% (blinks). For the heartbeat artifact cluster this ratio ranged between 27.3% and 90.9%. This result reveals that only a few heartbeat ICs identified by CORRMAP were selected by some users, and the cluster of Study 1 includes a single IC that was not selected by any of the 11 users.

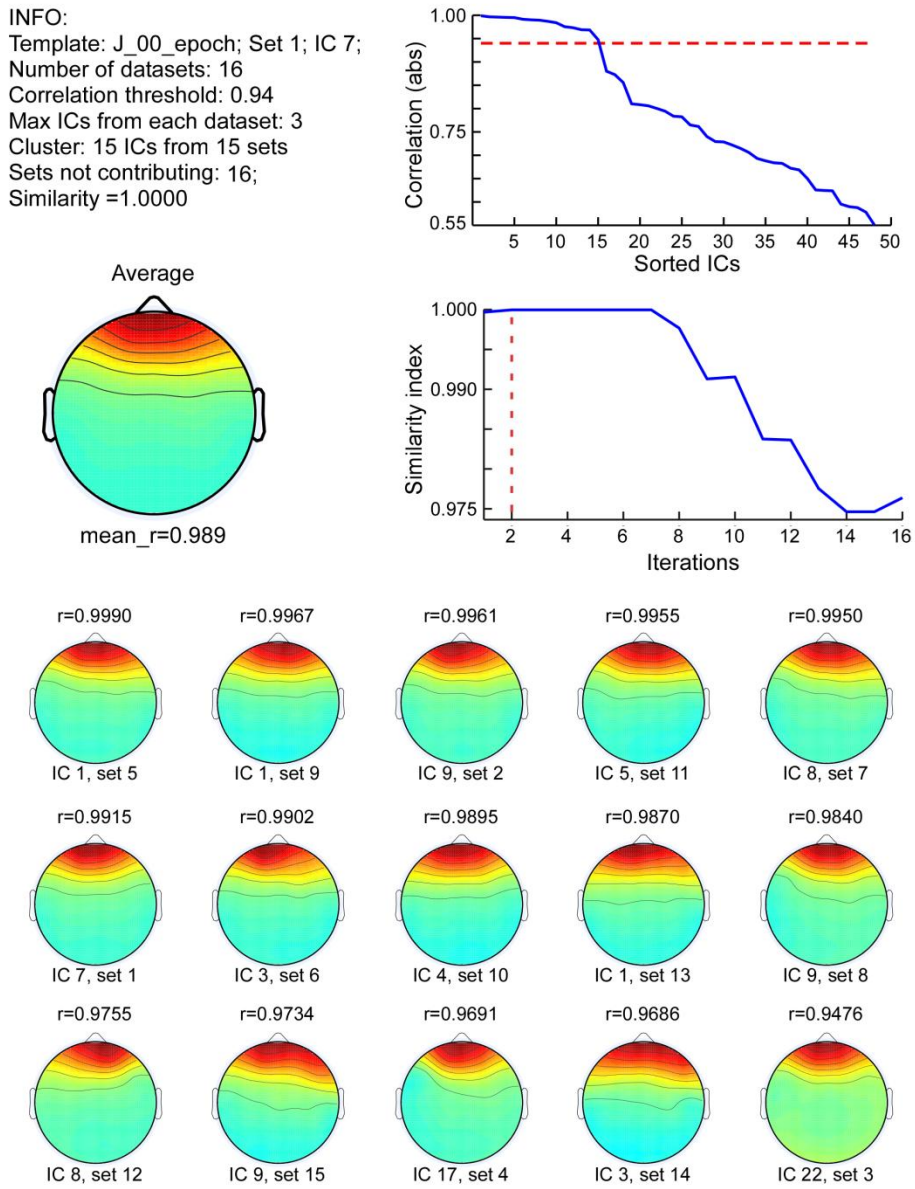

Figure 4.3 *Example CORRMAP output figure showing the eye blink artifact component cluster from 16 datasets recorded with 30 EEG channels. The plot displays information about the cluster (top left) and, in the top right corner, the correlations sorted in descending order and with the correlation threshold used indicated in red. Below, the similarity indices are plotted, illustrating the result of the automatic mode threshold detection. The iteration picked by the automatic mode is indicated in red. Below, all component maps (inverse weights, in arbitrary units) identified as belonging to this cluster are shown, together with their correlation with the template and information about the original dataset and component index therein.*

Table 4.2 summarizes the evaluation of the overlap between users and CORRMAP (first three rows) and across users (last three rows). High degrees of association between users and CORRMAP were found for ICs representing eye blinks (phi scores ranged between 0.83 and 0.99) and for ICs representing lateral eye movements (phi scores ranged between 0.85 and 0.91). Evaluation of the consistency across users also resulted in high phi scores for these artifact types, suggesting that independent users were similarly consistent in their classification between themselves as they were with CORRMAP. However, for ICs representing heartbeat artifacts phi score calculations revealed only low to moderate degrees of association both within users (range 0.19–0.65) and between CORRMAP and users (range 0.07–0.71). This suggests that the identification of heartbeat artifacts by ICs is more difficult than the identification of eye blinks or lateral eye movements.

Table 4.2 *Degree of Association Between CORRMAP Clusters and Users' Identification of Three Artifact Types in Three Studies*

	Artifact type					
	Blink		Lateral eye movements		Heartbeat	
Study						
	Association between CORRMAP and users					
	Mean	Range	Mean	Range	Mean	Range
1) 30 channels	0.99	[0.93 1.00]	0.91	[0.71 0.96]	0.07♦	[-0.02 0.56]
2) 68 channels	0.89	[0.85 0.94]	0.89	[0.75 0.94]	0.62	[-0.01 0.84]
3) 128 channels	0.83	[0.76 0.87]	0.85	[0.61 0.95]	0.71♦	[-0.01 0.85]
	Association between users					
	Mean	Range	Mean	Range	Mean	Range
1) 30 channels	0.99	[0.92 1.00]	0.93	[0.73 0.99]	0.19♦	[0.02 0.33]
2) 68 channels	0.89	[0.82 0.93]	0.90	[0.71 0.97]	0.65	[0.07 0.76]
3) 128 channels	0.91	[0.83 0.98]	0.75	[0.55 0.82]	0.58♦	[0.21 0.73]

Note. ♦One user was excluded from the analysis

The high degree of overlap between users and CORRMAP is illustrated for the eye blink cluster of Study 2 in Figure 4.4. The number of users that indicated each IC is displayed on the top of each map. The ICs are sorted in descending order of correlation with the cluster average (not shown). In 19 out of the 24 ICs, a perfect match between users and CORRMAP was evident; that is, all 11 users identified these 19 maps as representing eye blink artifacts. Of the other five ICs selected by CORRMAP, only four were identified by fewer than five users, indicating a moderate discrepancy.

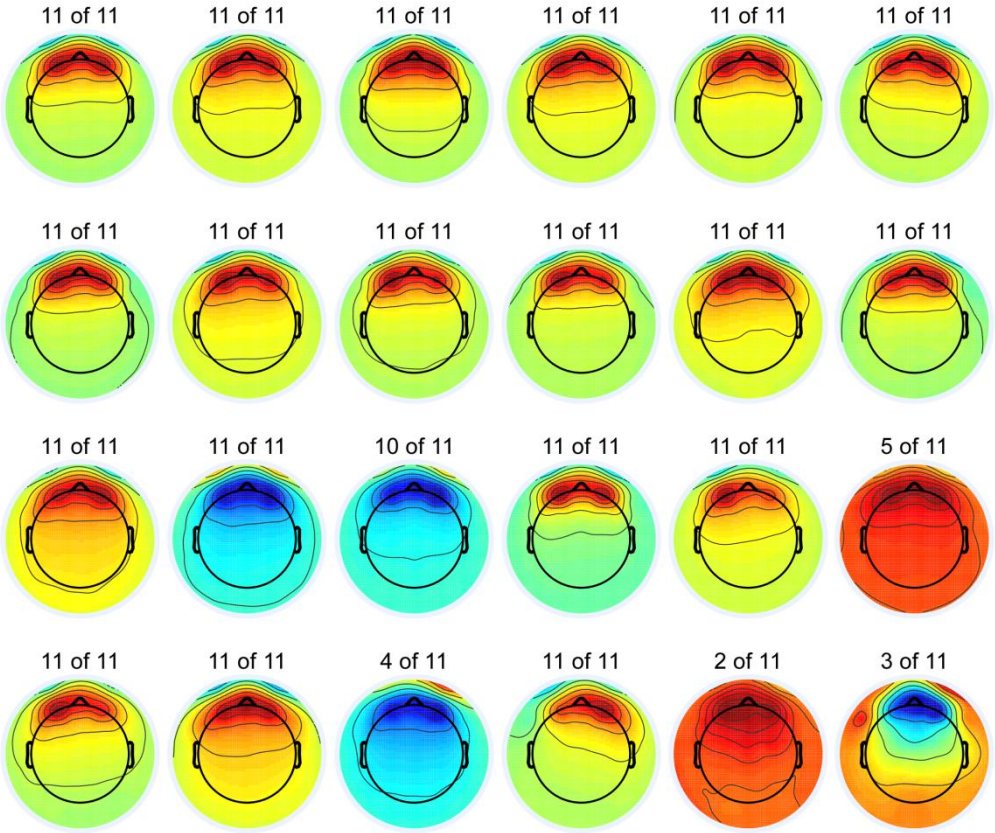

Figure 4.4 *CORRMAP validation result for eye blink ICA components based on 16 subjects and 68 EEG channel recordings. The cluster was obtained by running CORRMAP in automatic mode, which selected 24 components with a correlation value equal to or greater than 0.87. The number of users that labelled these components as representing an eye blink artifact is represented at the top of each component map. Maps represent inverse weights in arbitrary units.*

Figure 4.5 illustrates two types of discrepancy between CORRMAP and users. Figure 4.5-A shows an example of two ICs selected by CORRMAP and both contributing to an eye blink artifact, but with only one being consistently identified by all users. Figure 4.5-B, on the other hand, shows one IC that was not selected by CORRMAP but was labeled

as an eye blink by some of the users. In this case 4 out of 11 users mis-interpreted a possible brain event-related IC (cf. Delorme, Westerfield, & Makeig, 2007b) as an eye blink. Topographically, this IC indeed resembled a typical eye blink, but did not actually contribute to eye blinks, as revealed by a comparison of the raw data with the respective IC time course.

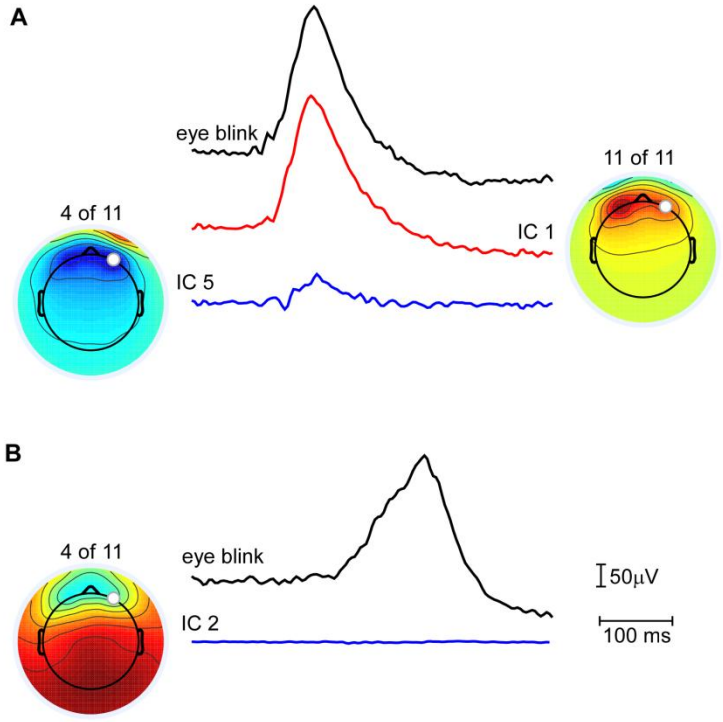

Figure 4.5 *Two examples showing inconsistencies between CORRMAP results and user selection. (A) Illustration of a representative eye blink artifact for a frontal channel (black), and back-projected activities at this channel for the two ICA component maps displayed (blue and red). Note that the left component was identified by only 4 out of 11 users, but shows a contribution to the eye blink. (B) An example where 4 out of 11 users have indicated an eye blink component not selected by CORRMAP. Inspection of the component activity (in blue) in comparison to a representative channel eye blink (black) does not support the interpretation of this component as representing eye blinks.*

The high degree of association found for lateral eye movements is illustrated by the cluster of Study 2 in Figure 4.6-A. Out of the 16 subjects, 15 contributed one IC each to the CORRMAP cluster. In 10 out of the 15, a perfect match between users and CORRMAP was evident, and only a single IC was selected by fewer than 10 users. Here, as in the cluster shown in Figure 4.4, a very high similarity between the resulting IC maps was found, irrespective of the polarity reversal across ICs that can cause confusion. Figure 4.6-B, on the other hand, illustrates the lower level of agreement found for the

heartbeat cluster of Study 2. In this case, CORRMAP found only seven ICs from seven different datasets out of the 16 datasets in this study. Note that none of these ICs was identified by all users.

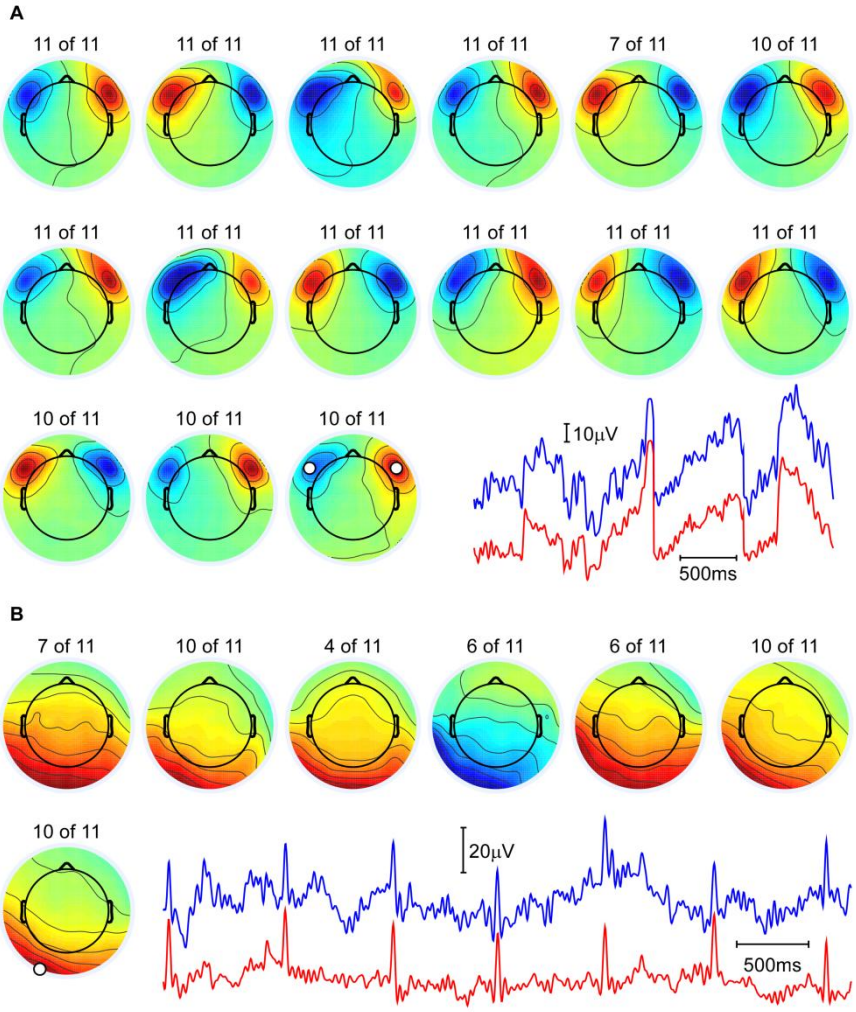

Figure 4.6 *CORRMAP validation result for lateral eye movement (A) and heartbeat artifact (B) ICA components based on 16 subjects and 68 EEG channel recordings. (A) The cluster was obtained in automatic mode, which selected 15 components with a correlation value equal to or greater than 0.91. An example of lateral eye movements is shown for the raw data (blue, linear derivation of left and right fronto-lateral channels) and the back-projected component (red, for the component with indicated electrode locations). (B) Similar plot for the heartbeat artifact IC cluster. CORRMAP automatic mode identified 7 components with a correlation value equal to or greater than 0.91. In A and B, the number of users that labeled the components as representing the respective artifacts is displayed on the top of each component map.*

4.5. Discussion

The aim of the present study was to evaluate a simple and efficient procedure for the clustering of ICs representing EEG artifacts. ICA has become a popular and powerful choice for removing EEG artifacts (e.g., Jung, et al., 2000a), but it requires the correct interpretation of ICs by the user. This interpretational step is required for brain-related as well as artifactual ICs, which, ideally, should be robust across independent observations (i.e., subjects). Component identification and evaluation is a time-consuming and potentially error-prone process, as a large number of ICs needs to be considered. Typically, the number of ICs in a study is given by the product of the number of EEG channels and the number of subjects. The EEGLAB plug-in CORRMAP developed here can help to screen large numbers of components quickly and objectively, and thus provides guidance for the identification and efficient removal of EEG artifacts such as eye blinks and lateral eye movements.

In contrast to other available clustering approaches (Delorme & Makeig, 2004), CORRMAP introduces a strategy that is focused on just a single feature (inverse ICA weights). This allowed us to code CORRMAP capabilities in a simple, quick, easy to revise and user friendly way, while keeping the number of subjective decisions to be performed by the user to a minimum: Users only need to choose one template IC map to initiate clustering. In the current version of CORRMAP, we have focused on the inverse IC weights as the single clustering parameter. It should be noted, however, that other features may be more useful for clustering other types of processes identified by ICA. ICA for example has been shown to disentangle mu rhythms from EEG alpha activity (e.g., Makeig, et al., 2002), but this classification probably requires the consideration of spectral information in addition to, or instead of, topographical information (Makeig, et al., 2004b).

It is our experience that a careful visual inspection of EEG raw data, and the ICA decomposition, helps to substantially improve the quality of the decomposition and ultimately the quality of the artifact correction and thus the signal quality that can be achieved. However, if the focus is on ICA-based artifact correction, CORRMAP quickly guides the visual inspection of ICA decompositions and reduces the time necessary for data evaluation to a minimum. It may be argued that, in order to maximize the performance of CORRMAP, the template selected should be representative of the type of artifact to be removed. This selection in itself requires some experience with ICA and the consistency of ICA decompositions across different recordings. The CORRMAP output facilitates the identification of representative ICs, and in the fully automatic mode, the

resulting cluster is to a substantial extent independent of the exact template chosen, as long as the template belongs to the same group of ICs. It is possible to quickly and easily compare the effects of different templates on the clustering output of CORRMAP. This approach not only helps to select representative cluster templates, but also helps to build up experience in using and understanding the benefits and limitations of ICA in the processing of EEG data. Accordingly, CORRMAP also provides some potential for the teaching of lab members about the identification, consistency and interpretation of ICs.

In many situations it should be sufficient for the user to choose the automatic mode feature, allowing the tool to suggest the best correlation threshold. This approach would be particularly useful for less experienced ICA users, or for situations where CORRMAP is being used to evaluate the robustness of ICA by evaluating the presence of specific components. In our experience the automatic mode reveals reasonable results, in particular for eye blink and lateral eye movement IC clusters, but it is important to regard the automatic threshold as a first guiding value only. In some situations it may be necessary to adjust the threshold after inspection of the cluster initially obtained.

Importantly, by comparing the classification of 11 users with CORRMAP, we observed that there was a large overlap in the selection of ICs representing eye blinks and lateral eye movements, probably because all users are very experienced with these types of common EEG artifacts. The main benefit of artifact removal with CORRMAP is that it provides an objective, repeatable and quick method for identifying artifact-related ICs.

On a descriptive level, the overlap between users and CORRMAP was larger for studies comprising fewer channels and therefore fewer ICs. We attribute the low consistency observed for high-density data to the ICA ‘over-fitting’ problem that is more evident in high-density than low-density EEG recordings. With high-density recordings it is commonly observed that the same physiological process can be represented in a number of ICs (typically less than 4), making its identification more complicated and thus error-prone. As a result, several ICs that account for the same process can be included in the same decomposition, and the number of ICs to be attributed to the same process may thus vary across datasets and laboratories, causing some confusion. CORRMAP addresses this issue by allowing the selection of up to three ICs per dataset for any one artifact. On the other hand, users with less experience in analyzing high-density data may have expected only one IC, or very few ICs, as representative of a physiological process such as eye blinks. In this case, we would conclude that using CORRMAP can result in a cluster of ICs more representative of the artifact in question than might be possible for an

inexperienced user.

Much less prominent, and therefore less well known by EEG researchers (including many users that participated in the validation study), are heartbeat artifacts. The prominence of heartbeat artifacts in EEG data depends on the recording reference, with the nose-tip reference usually allowing for a better identification than linked earlobes or vertex. The other factor is the spatial sampling of the head sphere, and thus the recording montage used. The recording montage used in Study 2 (Hine & Debener, 2007) included infracerebral electrode sites, similar to the layout of the geodesic sensor net as provided by Electrical Geodesics Inc. (Eugene, OR), to improve the spatial sampling of the EEG. However, electrodes placed at the lower half of the head sphere are closer to the heart, and thus prone to pick up more electrical heartbeat activity by means of volume conduction. As a result, ICA decompositions of Study 2 included ICs reflecting a heartbeat artifact in most data sets, which was not the case for Studies 1 and 3. In Study 1 (Debener, et al., 2008b), a scalp reference (Fcz) was used in combination with a 10–20 electrode layout, whereas in Study 3 (Schneider, et al., 2008a), although a nose-tip reference was used, electrode layout was similar to the 10–10 system only. Moreover, in Study 1, most ICs classified by users as heartbeat ICs in fact probably reflected residual ballistocardiogram activity, which is typical of EEG data recorded inside an MRI scanner (Debener, et al., 2008b). The topographies of these ICs resemble those that can be attributed to electrical heartbeat activity, but, as only two users were familiar with analyzing EEG data recorded inside an MRI scanner, a mis-attribution may have contributed to the rather poor overlap between CORRMAP and users. Furthermore, heartbeat artifact, and the related topography, is less well known among EEG researchers than, say, eye blinks, probably because it less frequently affects EEG recordings. Accordingly, the results also represent, to some extent, the familiarity of users with the different artifact topographies investigated, among which the heartbeat artifact topography is probably the least common.

While a ‘true’ best classification cannot be easily determined in real data, the examples discussed above highlight possible reasons for poor classification outcomes and poor inter-rater reliability. It should be noted, however, that a detailed investigation of the sensitivity of CORRMAP was beyond the scope of this study. Such a validation approach would require the use of artificial data, where the ground truth (i.e., the number and type of artifact ICs per dataset) is known. A study based on simulated data could be performed to examine, and further compare, the performance of users and software (such as CORRMAP), and would complement the current approach.

In conclusion, CORRMAP has proved to be efficient, quick, and at least as consistent as a group of 11 ICA users from different laboratories in the classification of eye blink and lateral eye movement ICs. This was made possible by focusing solely on topographic information as a single clustering parameter. Other types of information should of course be considered for the detailed examination of ICs, in particular those representing brain-related activity (e.g., Debener, et al., 2005a; Debener, et al., 2005b; Makeig, et al., 2004a; Makeig, et al., 2002; Onton, et al., 2005) or more complex artifacts such as those caused by cochlear implants (Debener, et al., 2008a). CORRMAP could be further optimized to take into account such parameters, making it potentially useful for clinical applications. However, if the focus is on EEG artifact removal, in particular eye blinks and lateral eye movements, then CORRMAP in combination with ICA provides a powerful, user-friendly approach.

5. Study 2: Uncovering auditory evoked potentials from cochlear implant users with independent component analysis

The study described in this chapter was accepted for publication in the journal "Psychophsysiology" in April 2011 (Viola, Thorne, Bleeck, Eyles, & Debener, 2011). FCV designed the experimental paradigm, collected and analyzed the EEG data, run all sensitivity and specificity validation tests and prepared the manuscript. JT contributed to the analysis and to the preparation of the manuscript. SB and JE provided the clinical information about the cochlear implant users and helped with the preparation of the manuscript. SD supervised all parts of the work, and also contributed to the preparation of the manuscript.

5.1. Abstract

Auditory evoked potentials (AEPs) provide an objective measure of auditory cortical function, but AEPs from cochlear implant (CI) users are contaminated by an electrical artifact. Here, we investigated the effects of electrical artifact attenuation on AEP quality. The ability of independent component analysis (ICA) in attenuating the CI artifact while preserving the AEPs was evaluated. AEPs recovered from CI users were systematically correlated with age, demonstrating that individual differences were well preserved. CI users with high-quality AEPs were characterized by a significantly shorter duration of deafness. Finally, a simulation study revealed very high spatial correlations between original and recovered normal hearing AEPs ($r > .95$) that were previously contaminated with CI artifacts. The results confirm that after ICA, good quality AEPs can be recovered, facilitating the objective, noninvasive study of auditory cortex function in CI users.

5.2. Introduction

In the last decades, technological developments have made it possible for sensorineural deafness to be reversed by bionic auditory stimulation with a cochlear implant (CI). The CI device mimics the function of the healthy cochlea and delivers electrical stimulation to the auditory nerve, bypassing the damaged inner hair cells, and subsequently to the auditory cortex, allowing the processing of auditory stimuli. Although CIs can bring large benefits to the quality of life of many deafened individuals, the outcome after implantation is variable. Clinical outcome depends on a number of parameters such as duration of deafness, age at implantation, and experience with the implant (Fallon, Irvine, & Shepherd, 2008). It is likely that the degree of auditory cortical rehabilitation also plays an important role (Moore & Shannon, 2009), although this is somehow neglected probably because CIs are unsuitable for functional magnetic resonance imaging. In a few cases, auditory cortical function in CI users has been investigated with magnetoencephalography (e.g., Pantev, et al., 2006), but, more frequently, multichannel electroencephalography (EEG) has been used to assess auditory evoked potentials (AEPs) (Debener, et al., 2008a; Gilley, et al., 2008; Henkin, et al., 2009; Sandmann, et al., 2009; Sandmann, et al., 2010; Sharma, et al., 2002; Zhang, et al., 2010). However, the recording of AEPs from CI users presents some challenges. During EEG recordings a large electrical artifact is evoked each time an auditory stimulus is presented, and this artifact obscures the AEPs, as shown in previous studies (Debener, et al., 2008a; Gilley, et al., 2006; Sandmann, et al., 2009; Zhang, et al., 2010). Accordingly, the time-locked artifact cannot be attenuated by averaging across trials, the conventional procedure for improving the signal-to-noise ratio (SNR) of event-related potentials.

Independent component analysis (ICA) is a linear decomposition method that is typically applied to continuous or concatenated single-trial, multi-channel EEG data (Makeig, et al., 2004a; Onton, et al., 2006). ICA can be used for the reduction of conventional EEG artifacts (Mennes, et al., 2010), and has recently been shown to outperform other correction approaches with regard to eye blink correction (Hoffmann & Falkenstein, 2008), although for other conventional EEG artifacts, such as the myogenic artifact, a much less complete separation between artifact and brain-related activity has been found (McMenamin, Shackman, Greischar, & Davidson, 2010).

In principle it should be possible to recover AEPs free from the electrical CI artifact by correction of the artifact independent components (ICs). Indeed, several studies support this conclusion by reporting that, after ICA-based CI artifact attenuation, typical AEPs could be evaluated in detail (Debener, et al., 2008a; Gilley, et al., 2008; Sandmann, et al.,

2009; Sandmann, et al., 2010; Zhang, et al., 2010, although others have been less successful). Nevertheless, it is still not clear how the ICA approach affects the quality of the resulting AEPs, that is, how sensitive and specific ICA correction for this type of artifact is (Sandmann, et al., 2009). Moreover, previous results have been obtained using small samples with similar CI devices, or even single cases (Debener, et al., 2008a), raising concerns about the generality of the results. Indeed, it is known that CI artifact properties vary across devices and individuals, and also depend on the type of stimulation used (Gilley, et al., 2006). This problem is illustrated in Figure 5.1, which shows electrical artifacts from four different CI users presented with two different environmental sounds. As can be seen, different sounds produce somewhat different artifacts for the four CI users. It is also evident that the same sound can produce different artifacts across individuals even when the same CI devices are used.

The present study sought to investigate the quality of late AEPs recovered from a relatively large sample of CI users (N=18) using a variety of CI devices stimulated with a variety of environmental sounds and pictures of natural scenes. To explore the ability of ICA to reduce the CI artifact, the degree of CI artifact attenuation was computed. Henceforth, we refer to this procedure as evaluating ICA ‘‘sensitivity’’. AEPs were also evaluated with an SNR measure. SNR was compared between CI users and age-matched normal hearing (NH) controls and, for the CI users, SNR was then related to clinical parameters. For both CI users and NH controls, we also evaluated the correlations of AEP amplitude with age. Although exact predictions could not be made, we speculated that, if data quality were sufficient, age-related effects evident in AEPs of NH listeners (Kerr, Rennie, & Robinson, 2011; Schiff et al., 2008) should also be preserved in CI users. In order to evaluate the ability of ICA to preserve the cortical evoked responses in the data, two procedures were applied. First, a hybrid simulation was performed. Here, the CI artifact extracted from CI user datasets using ICA was added to the single-trial EEG data from NH participants. The resulting simulated datasets were then submitted to ICA. The AEPs obtained after ICA-based CI artifact attenuation were then compared with the original NH AEPs. Second, visual evoked potentials (VEPs) from CI users collected in the same task were compared before and after ICA-based CI artifact attenuation. These procedures are henceforth referred to as evaluating ICA ‘‘specificity’’. Taken together, we expected that this set of analyses would allow us to systematically evaluate the quality of ICA-recovered cortical AEPs from deaf individuals using a CI.

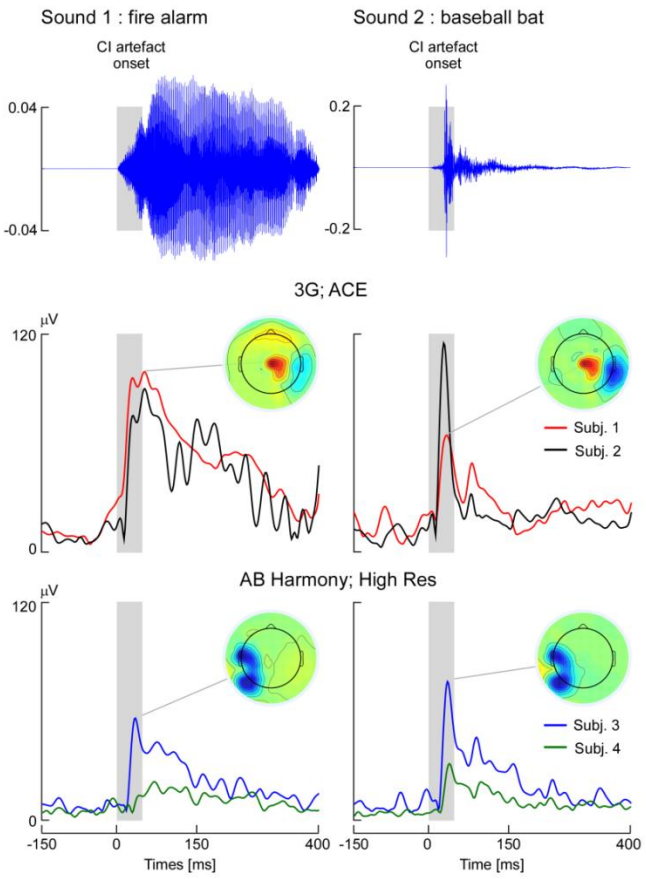

Figure 5.1 *Cochlear implant (CI) artifact evoked by different environmental sounds. Panels in the top row show the sound profile of two stimuli used in the experiment, on the left side a ''fire alarm'' sound, on the right side a ''hitting baseball bat'' sound. The panels in the middle row show the root mean square (RMS) of the EEG activity of two CI users when stimulated with the two sounds during the first 400 ms of presentation, respectively. Both implantees used a Nucleus CI system on the right side with the ESPrit G processor and the ACE speech processing strategy. The topography at the latency of maximum amplitude is illustrated for the same subject in both panels. The panels in the bottom row show RMS activity for another two CI users and the respective topography at the latency of maximum amplitude for one of them. Both implantees used the Advanced Bionics CI system on the left side with the AB Harmony processor and the HiRes-S with Fidelity 120 speech processing strategy. Gray shadow represents the average time window of CI artifact onset.*

5.3. Methods

5.3.1. Participants

Eighteen post-lingually deafened cochlear implant (CI) users (10 females, *M* = 59.89, *SD* = 13.06 years) and 18 age and gender matched NH participants (10 females, *M* = 55.17, *SD* = 12.31 years) took part in the study after giving written informed consent. NH participants in the control group were screened for normal hearing, defined as pure-tone thresholds better than 20 dB hearing level (HL) at 0.5, 1, 2, and 4 kHz. Eight NH

participants were aged between 30 and 50 years and had pure-tone thresholds ≤ 20 dB HL for all frequencies tested. For the ten older NH participants, higher thresholds for the higher frequencies (2 kHz, left ear [LE]: *M* = 19.50, *SD* = 10.66 dB, right ear [RE]: *M* = 18.50, *SD* = 16.33 dB; 4 kHz, LE: *M* = 41.00, *SD* = 20.39 dB, RE: *M* = 35.50, *SD* = 30.86 dB) were accepted, reflecting natural age related hearing loss (Humes, Kewley-Port, Fogerty, & Kinney, 2010). All CI users were implanted unilaterally except one. During the task, only the first implanted CI was switched on for this user (Table 5.1). The CI users were recruited from the South of England Cochlear Implant Centre in Southampton, UK. The clinical profile of each CI user is presented in Table 5.1. All 36 participants were right handed and had no history of neurological or psychiatric disorders and had normal or corrected-to-normal vision. Procedures were approved by the local ethics committee and conformed to the Declaration of Helsinki.

Table 5.1 *Cochlear Implant Users' Clinical Profile*

CI user	Age (years)	Gender	CI side	Duration deafness (months)	Age Implantation (months)	Device	Processor	Sound coding strategy	CI use (months)	Score (% correct)	Sound level (dB SPL)
01	55	Male	Right	150	622	Nucleus	ESPrit 3G	ACE	45	93	65
02	63	Male	Right	568	704	Nucleus	ESPrit 3G	ACE	54	90	65
03	77	Male	Left	265	899	Nuclues	Freedom	ACE	33	42	80
04	54	Male	Left	614	627	Nucleus	Freedom	ACE	22	93	75
05	70	Female	Left	531	771	Nucleus	ESPrit 3G	ACE	78	91	75
06	73	Male	Right	693	837	Nucleus	ESPrit 3G	ACE	46	91	65
07	61	Female	Left	478	718	Nucleus	Freedom	ACE	21	62	65
08	60	Male	Left	416	572	Nucleus	ESPrit 3G	SPEAK	156	83	70
09	79	Male	Left	30	896	Nucleus	ESPrit 3G	ACE	51	66	70
10	43	Female	Left *	251	491	ABS	AB Auria	HiRes-S	35	99	75
11	80	Female	Left	631	883	Nucleus	CI24M	ACE	80	53	70
12	39	Female	Left	447	447	Nucleus	Freedom	ACE	28	51	60
13	57	Female	Left	403	679	ABS	AB Harmony	HiRes-S	12	99	65
14	58	Male	Right	452	692	ABS	AB Harmony	HiRes-S	6	97	75
15	58	Female	Right	41	682	Nucleus	Freedom	ACE	18	88	70
16	33	Female	Left	378	390	ABS	AB Harmony	HiRes-S	8	48	70
18	38	Female	Left	230	446	Med El	Medel Opus2	FSP	18	93	75
19	62	Female	Right	417	741	Med El	Medel Opus2	FSP	10	97	70

Notes. Device names and processor names according to manufacturers' labeling. Score corresponds to the percentage correct on the BKB speech recognition test in quiet. Sound level in dB SPL chosen by each participant for the presentation of auditory stimuli.*Subject was implanted bilaterally, but during the recording session only the implant on the left side was switched on.

5.3.2. Stimuli

Auditory stimuli were taken from a pool of 270 environmental sounds of natural objects previously rated in a normative study (Schneider, Engel, & Debener, 2008b). Sounds (sampling rate=22 kHz, 16-bit) had a duration of 400 ms and were played twice (800 ms), in order to increase recognition, via two loudspeakers (Quad L12) positioned at an

azimuth of 45°/135° in front of the participant. Sounds were presented at a comfortable level adjusted individually for each participant using a five-level loudness comfort rating scale varying from 60 to 80 dB sound pressure level (SPL) in steps of 5 dB SPL. There were no systematic differences for the preferred level between CI users and NH participants. CI users were effectively stimulated monaurally and NH participants were stimulated binaurally. Visual stimuli were taken from a pool of 320 degraded pictures of natural objects from the same normative study. The stimuli were presented centrally for 800 ms, with the visual stimuli covering an angle of 8.6° vertically and horizontally. In visual blocks (see Experimental Design and Task), trials included a gray square, which was presented centrally for 800 ms subtending a visual angle of 1.9°. Stimuli were presented using a 23-in. monitor (1280 X 1024 X 32-bit color, 60 Hz refresh rate). Screen background was black at all times. All stimuli were presented using Presentation 10.0 software (Neurobehavioral Systems).

5.3.3. Experimental Design and Task

An adapted audiovisual semantic priming paradigm (Schneider, et al., 2008a; Schneider, et al., 2008b) was used. Eighty environmental (auditory primes) and 160 degraded pictures of natural objects (visual targets) were included (taken from www.multimost.com). Each visual target was paired with either a congruent or an incongruent sound, constituting the audiovisual (AV) block, or with a gray square (temporal cue) in a visual only (V) block. The order of the pairs was pseudo randomized to ensure that response type and object category were distributed equally over the course of stimulus presentation. Each trial started with a fixation cross (500 ms), followed by the audio prime (800 ms) or by the square (800 ms). The fixation cross remained on screen until the visual target was presented (800 ms). After the target offset, the participants had a maximum of 2900 ms to indicate a response using a keypad. The next trial started 1000 ms after the response. Each participant was presented with a total of four blocks (two V and two AV) and a break of 1 min was included between blocks. The order of presentation was counterbalanced across participants. The task consisted of judging whether the objects shown in the degraded pictures (visual targets) would fit (‘‘Yes’’) or not (‘‘No’’) into a box (dimensions 33.5 X 24.0 X 12.5 cm) shown in the lab. Participants were comfortably seated at a distance of 150 cm from the screen, and all responses were made using a keypad with two keys, marked with ‘‘Yes’’ and ‘‘No,’’ respectively (Cedrus RB series, San Pedro, CA, USA). The assignment of the keys was counterbalanced across participants. Note that the behavioral results and the relationship

between hearing loss, semantic priming, and event-related EEG are not reported here and will be presented elsewhere.

5.3.4. EEG Recording

Participants were seated in an electrically shielded, sound attenuated, and dimly lit booth (Industrial Acoustics, Winchester, UK). EEG data were recorded from 68 channels using a high input impedance amplifier system (Compumedics Neuroscan, Charlotte, NC, USA) and a customized electrode cap (Easycap, Herrsching, Germany) specifically designed to improve spatial sampling and facilitate AEP source localization (Hine & Debener, 2007; Hine, Thornton, Davis, & Debener, 2008). The cap was fitted with 66 Ag/AgCl electrodes in an equidistant layout that spans a larger part of the head sphere than standard 10–20 montages. Two additional electrodes were placed below the eyes. For the CI users, EEGs from some electrodes (*M*=3.94, *SD*=0.94 electrodes, range 2–6 electrodes) could not be recorded due to the location of the CI device (i.e., transmitter-receiver coil, cable to processor, processor). Data were recorded with a sampling rate of 1000 Hz using the nose-tip as reference, and were analogue filtered between 0.1 and 200 Hz. Electrode impedances were maintained below 20 kΩ prior to data acquisition.

5.3.5. Data Processing

EEG data were processed using custom scripts and EEGLAB (Delorme & Makeig, 2004) running in the MATLAB (Mathworks, Natick, MA) environment. Data were offline filtered from 1 to 40 Hz using windowed sinc FIR filters with a Hann window (taken from the FIRfilt plugin for EEGLAB developed by A. Widmann: www.uni-leipzig.de/~biocog/content/widmann/eeglab-plugins/). Data were then down-sampled to 500 Hz and pruned of unique, non-stereotyped artifacts using the EEGLAB function *jointprob.m* (Delorme, et al., 2007a). Extended infomax ICA as implemented in EEGLAB was then applied to the remaining data in order to achieve a reliable decomposition (Debener, et al., 2010). Independent components (ICs) representing eye-blinks and electrocardiograph (ECG) artifacts were semi-automatically identified using CORRMAP (Viola, et al., 2009) and then corrected from all datasets. These ICs are labeled as conventional artifacts. For the CI users a second, additional step was included. Here, the properties of the remaining ICs were visually inspected to identify those representing the CI artifact. The same features (IC maps showing a centroid on the side of the implanted device; IC activations matching the onset/offset of acoustic stimulation) were used as reported previously (Debener, et al., 2008a; Gilley, et al., 2006; Sandmann, et al., 2009). After component identification, CI artifact ICs were corrected from the CI users' datasets. Afterwards all datasets were segmented into epochs from -200 to 600 ms

relative to sound onset. AEPs were then obtained by time-domain averaging. A baseline correction was performed using the pre stimulus interval (i.e, -200 to 0 ms) and AEPs at missing electrodes were interpolated with the EEGLAB function *eeg_interp.m*, which implements a smoothed inverse distance approach. AEP amplitude and latency analyses were performed for the frontocentral electrode with the largest grand average amplitude for both groups (approximately FCz). AEP peak amplitudes and latencies were determined using a semi-automatic procedure as implemented in *peakdet.m* (www.billauer.co.il/peakdet.html).

5.3.6. ICA sensitivity

Previous reports differ regarding the incidence and magnitude of the CI artifact (Zhang, et al., 2010). The sensitivity of the ICA approach was evaluated by calculating the individual CI artifact attenuation rate. This rate was calculated as the difference between the mean root mean square (RMS) for the original data and the mean RMS for the corrected data for bins of 50 ms (-200 to 400 ms). This procedure allowed evaluation of the attenuation rate at critical latencies, such as the onset (0–50 ms) of the artifact and at latencies of the N1 and P2 components (100–250 ms).

5.3.7. AEP quality

An SNR measure was calculated to assess the quality of the AEPs. Traditionally the SNR is defined as the power of the signal at a peak latency of interest divided by the mean power of the activity in the baseline period. Here, a more conservative approach was chosen that allowed signal and noise to be estimated at the same, post-stimulus onset latency range (Schimmel, 1967). The plus-minus procedure consists of averaging all trials after polarity reversal of every other trial. The remaining average is an estimation of noise, since all time-locked features, including both AEPs and the CI artifact, can be assumed to sum to zero due to the artificial polarity reversal. In this study, the focus was on theN1 component of the AEP, since it is typically the largest response and is easily identified in single subjects. The N1 SNR was calculated by dividing the RMS of the N1 component at peak latency ± 10 ms by the RMS of the estimated noise in the same time window, scaled to dB (20log10(signal/noise)).

In addition, AEPs were further evaluated by comparing peak amplitudes with demographic and clinical scores. It is well known that AEPs change due to aging (Kerr, et al., 2011; Schiff, et al., 2008). There is a considerable range in age at implantation, and thus a wide age range in the sample of CI users studied. We therefore reasoned that, if individual differences in AEPs are retained, N1-P2 amplitudes should show a systematic

correlation with age. A positive outcome would clearly suggest that individual differences in AEPs are not erased by ICA-based CI-artifact attenuation.

5.3.8. ICA specificity

In order to evaluate the effect of ICA-based artifact attenuation on the reconstruction of the AEPs, a hybrid simulation was performed. Here, a CI artifact template was added to an original NH subject dataset with a known AEP response, and the modified dataset was then processed using the same procedure as for the CI dataset. This procedure provided a comparison between the ‘‘true’’ AEP and the post-ICA recovered AEP, and was therefore informative about the specificity of the ICA approach. In the semantic priming paradigm employed here, 80 different environmental sounds were presented using two different sequences. The examples in Figure 5.1 show that different sounds produce different artifacts. Taking this into account, two CI artifact templates matching each presentation sequence were created. In order to produce the two templates, data from two CI users (one for each sequence) were randomly chosen. For each CI user, all ICs except those labeled as CI artifact related were removed from the original data. In one case, six CI artifact ICs were kept in the original data and in the other, three. This procedure resulted in two CI template datasets where only the CI artifact related activity was kept and all other sources of activity were removed. We preserved the single-trial artifact responses in the simulation by adding the respective single-trial template dataset to the single-trial NH datasets. In order to evaluate ICA specificity, spatial correlations between the ‘‘true’’ and the recovered AEPs were computed (Sandmann, et al., 2009), thus providing information about the amount of variance in the data that was unaffected.

A further, less direct approach for the assessment of ICA specificity was performed by the evaluation of portions of EEG data that were not primarily related to auditory processing. Here, the reasoning is that these portions of the data should not be substantially altered by the removal of ICs supposedly reflecting the CI artifact. Following this line of reasoning, we analyzed the VEPs from the CI users, of considerable interest in the context of crossmodal compensatory plasticity (Doucet, Bergeron, Lassonde, Ferron, & Lepore, 2006). VEPs were computed for all blocks after the removal of both conventional and CI artifacts with ICA. The similarities between the original VEPs and the CI-corrected VEPs were assessed as described for the simulation study.

5.3.9. Statistical Analysis

All variables were tested for normality using Shapiro-Wilk tests. Comparisons between CI users and NH controls in terms of number of ICs corrected, number of trials included in AEP analysis, AEP N1-P2 peak to peak amplitude, and N1 and P2 peak latencies were evaluated using two-tailed independent *t* tests or, when normality criteria were not met, Mann-Whitney *U* tests. For four out of the eighteen CI users, it was not possible to identify a P2 component in the AEPs. For these participants, P2 amplitude was taken by 0 μV and P2 latency as the mean value of the other CI users (245 ms). For the hybrid simulation, comparisons between NH original and post-ICA simulated datasets in terms of number of ICs corrected, number of trials included in AEP analysis, N1-P2 peak to peak amplitude, and N1 and P2 latencies were evaluated using two-tailed paired *t* tests or, for the variables where the normality test failed, Wilcoxon signed-rank tests. The spatial correlation between original and recovered AEPs was computed for all time frames, in order to investigate topographical similarities. The mean correlation across NH participants was calculated, after first applying Fisher's *Z* transformation. VEP differences for P1, N1, and P2 amplitudes were also assessed using either two-tailed paired *t* tests or Wilcoxon signed rank tests, and spatial correlations between original and CI-corrected datasets were calculated as described above. For all tests, differences were considered significant when $p<.05$. For all parametric tests, the effect size was calculated using Cohen's *d* estimate (Cohen, 1988). For all non-parametric tests, the effect size estimate *r* was computed (Rosenthal, 1991). Parametric Pearson correlation coefficients are indicated with r_P and Spearman rank correlations with r_S, to avoid confusion.

5.4. Results

5.4.1. ICA Sensitivity

AEPs from all CI users were buried in large electrical CI artifacts. This was evident from evaluation of CI-uncorrected AEPs, which showed large, not biologically plausible deflections in the AEP response interval. Figure 5.2 shows box plots for the median attenuation rate across the 18 CI users for 50 ms bins from -200 to 400 ms. As can be seen, substantial individual differences were observed in the amount of attenuation, largely reflecting large individual differences in the magnitude of the artifact (range 12 to 760 μV). The attenuation was largest for the 50–100 ms bin where the median RMS difference was > 15 μV. This is the typical morphology, characterized by a sharp onset followed by a ''pedestal'' (Debener, et al., 2008a; Gilley, et al., 2006; Sandmann, et al., 2009). Only after CI artifact attenuation was it possible to recover AEPs for CI users that resembled in morphology and topography those that can be observed in NH subjects.

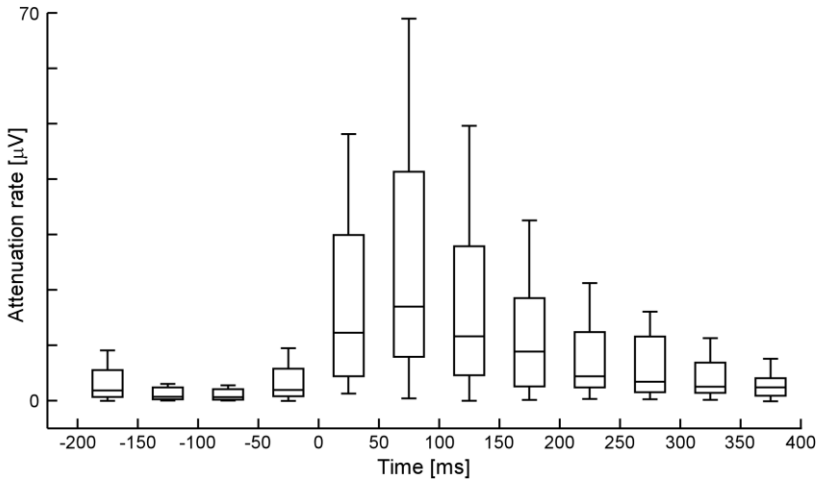

Figure 5.2 *Box plots showing median cochlear artifact (CI) attenuation rate (horizontal line in the middle) across 18 CI users for bins of 50 ms (range: -200–400 ms). Bottom and top of each ''box'' are the 25th and 75th percentiles of the samples, respectively. Whiskers are drawn from the end of the interquartile range to the furthest observation (cf. Matlab function boxplot.m). Attenuation rate was calculated as the difference between mean RMS for original data and mean RMS for corrected data for each bin.*

5.4.2. AEP quality

No differences were found between CI users and NH participants in terms of the number of trials included in the AEP calculation (Mann-Whitney, U = 204.00, n.s.). The number of rejected ICs representing conventional artifacts was not significantly different between NH participants and CI users (Mann-Whitney, U = 154.5, n.s.). When both conventional and CI artifacts were accounted for, the total number of rejected ICs was significantly larger for CI users compared with NH participants (Mann- Whitney, U = 293.00, p < .001, r = .12). Table 5.2 presents a summary of these comparisons.

Table 5.2 *AEP Parameterization, Number of Rejected ICs, and Number of Averaged Trials for Both Groups and Simulation Study*

		Latency [ms]		Nr. rejected ICs		
Group	N1-P2 peak-to-peak amplitude [μV]	N1	P2	Conv.	Total	Nr. trials
CI	8.9 ± 4.1	132.3 ±13.7	237.2 ± 32.5	6.6 ± 2.0	11.7 ± 2.5	153.8 ± 2.7
NH	15.5 ± 3.6	114.2 ± 12.3	215.8 ± 26.7	7.2 ± 2.5	7.2 ± 2.5	152.0 ± 3.6
NH simul	15.3 ± 3.7	114.4 ± 12.3	216.4 ± 28.1	6.9 ± 2.3	10.0 ± 2.5	152.3 ± 3.8

Notes. CI = cochlear implant users; Conv. = conventional; ICs = independent components; NH = normal hearing listeners; NH simul = normal hearing listener post-ICA simulated datasets. All results are presented as M ± SD.

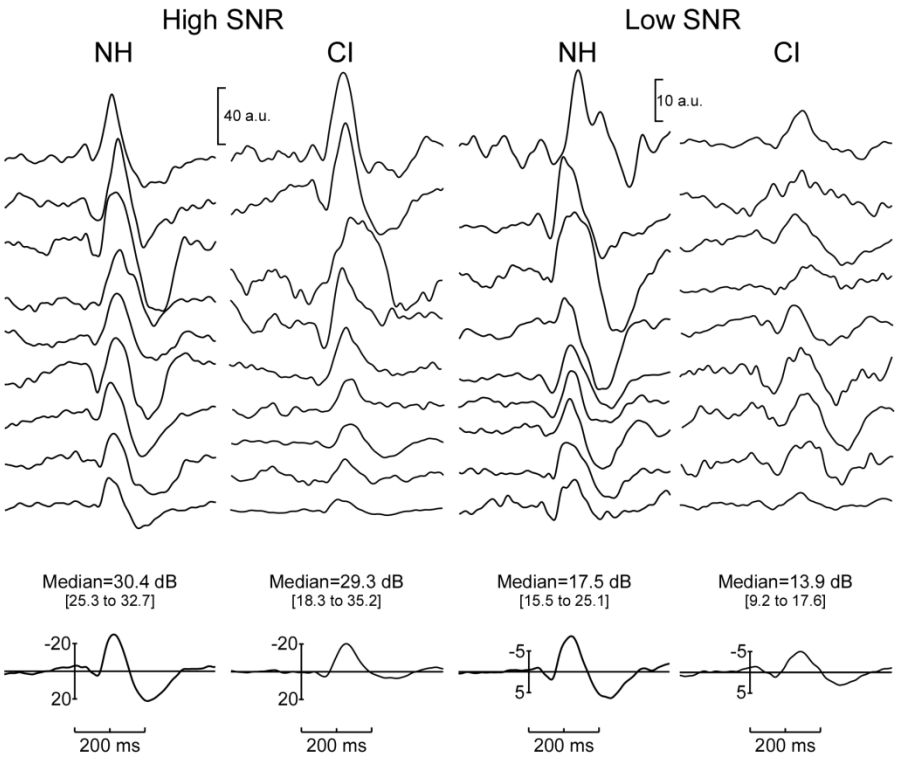

Figure 5.3 *Auditory evoked potentials (AEPs) at a frontal-central electrode for all 36 participants. Each column shows the AEPs sorted by N1 signal to noise (SNR), for both normal hearing (NH) participants (left) and cochlear implant (CI) users (right). On the bottom of each column the grand average AEP, the median SNR, and the range in dB are shown. For illustrative purposes, all AEPs were normalized by the single subject RMS of the noise in the latency range of the N1 component. Hence values are expressed in arbitrary units (a.u.).*

No significant differences were found when comparing SNR values in the N1 interval in NH participants (*Mdn* = 25.19 dB) and in CI users (*Mdn* = 17.93 dB) (Mann-Whitney, *U* = 120.00, n.s.). Figure 5.3 shows the single-subject AEPs for all NH participants and CI users, sorted by SNR in descending order and divided into high and low groups using a median split. AEPs were first divided by the mean noise RMS for better visualization and comparison. Although the SNR did not significantly differ between groups, the range was larger for the CI users (SNR range, NH: 15.51 to 32.71 dB; CI: 9.18 to 35.23 dB). It is worth noting that, for the large SNR groups, the largest CI SNR was 35.23 dB, while the largest NH SNR was slightly smaller (32.71 dB), which indicates that for some CI users the recovered AEPs had very robust N1 responses. For all NH datasets, the N1 and P2 components could be easily identified, even for the participant with the smallest SNR (15.51 dB). For all CI users the N1 AEP response was identified, but for four CI users the

P2 response was difficult to discern, if not completely absent. CI users showed a significantly reduced N1-P2 peak-to-peak amplitude (t[34] = -5.13, p < .001, d = -1.76). The N1 peak latency was significantly delayed for CI users (t[34] = 4.18, p < .001, d =1.43), as was P2 peak latency (t[34] = 2.16, p = .038, d = .74). Table 5.2 presents a summary of these comparisons.

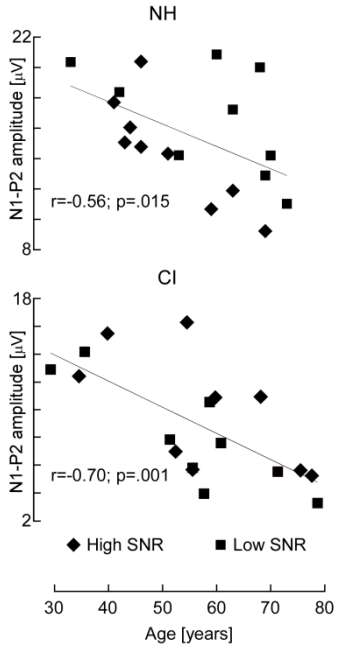

Figure 5.4 *Correlation between N1-P2 peak-to-peak latency at electrode of maximum amplitude and subject age. Top: normal hearing (NH) participants; bottom: cochlear implant (CI) users. Diamonds represent participants with high N1 SNR and squares participants with low N1 SNR.*

The correlation between age and N1-P2 peak-to-peak amplitude is shown in Figure 5.4. As expected, a significant negative correlation between age and peak-to-peak amplitude was found for the NH participants (r_S = -0.56, p = .015). For the CI users a similar pattern was found (r_S = -0.70, p = .001), indicating that individual differences were preserved after CI artifact attenuation. In order to further evaluate the quality of the recovered AEPs, the CI group was split into high and low SNR subgroups based on the SNR median (17.93 dB). Note that the age for CI users in the two subgroups was not significantly different (HIGH: M = 59.89, SD = 13.99 years, LOW: M = 57.89, SD = 14.79 years; t[16] = .30, n.s.). CI users with low SNR values had been deaf for a significantly longer period (HIGH: M = 257.56, SD = 170.46 months, LOW: M = 519.67, SD = 109.59 months; t[16] = -3.88, p < .001, d = -1.94), but no significant differences were found when comparing age at implantation (HIGH: M = 690.89, SD = 157.79

months, LOW: *M* = 650.78, *SD* = 163.33 months; *t*[16] = .53, n.s.), as shown in Figure 5.5 . The period of CI experience was not significantly different for the two subgroups (HIGH: Mdn533.00 months, LOW: *Mdn* = 28.00 months; *U* = 43.50, n.s.). The score in the speech recognition test was not significantly different among CI users with low and high SNR (HIGH: *Mdn* = 93.00% correct, LOW: *Mdn* = 83.00% correct, *U* = 24.00, n.s.).

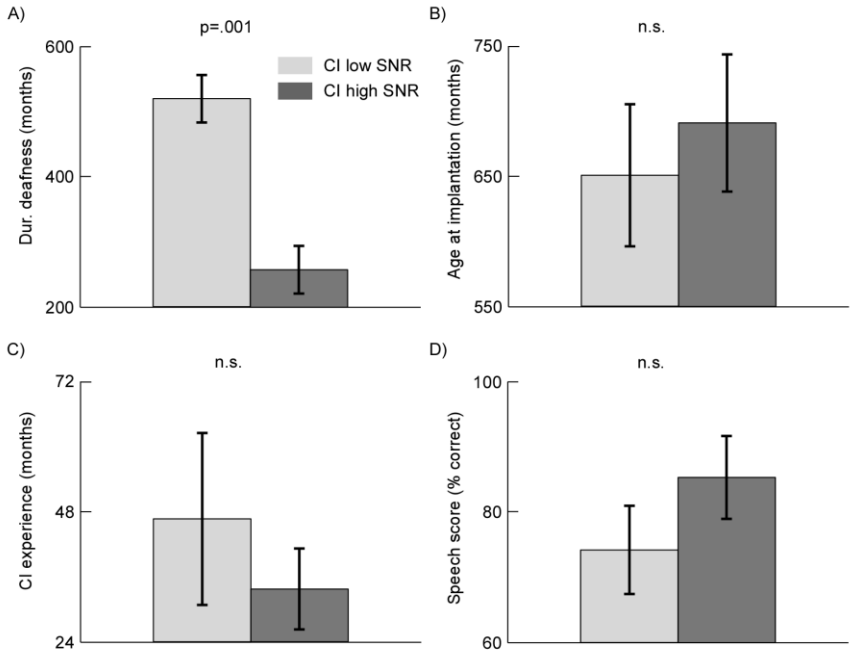

Figure 5.5 *Comparison of clinical profiles from cochlear implant (CI) users with low (light gray) and high (dark gray) N1 SNR AEPs. All panels show mean ± SEM values. (A) Self-reported duration of deafness in months. (B) Age at implantation in months, i.e., age when the CI device was switched on. (C) Experience with the CI device in months. (D) Speech scores: percentage correct on the Bamford-Kowal-Bench (BKB) speech recognition test in quiet.*

5.4.3. ICA Specificity

After ICA-based artifact attenuation, no differences were found between post-ICA simulated and original NH datasets in terms of the number of trials included in the AEP calculation (Wilcoxon, *T* = 34.50, n.s.). Fewer conventional artifact ICs were rejected for the post-ICA simulated data (Wilcoxon *T* = 0.00, *p* = .02, *r* = -.55). No significant differences were found for the N1 peak latency (*t*[17] = -.70, n.s.) and P2 peak latency (*t*[17] = -.62, n.s.). The N1-P2 peak-to-peak amplitude was smaller for simulated data (*t*[17] = 3.23, *p* =.005, *d* = 1.57). Although the amplitude was slightly altered, the correlations between original and post-ICA simulated amplitudes were very high (r_P = .99, *p* < .001). Table 5.2 presents a summary of these comparisons. Moreover, the spatial correlation was generally high for all time frames (range .82 to .99), indicating that

topographies were not substantially altered by CI attenuation. Figure 5.6 shows the grand average results across the 18 pre-ICA corrected simulated NH datasets. As shown, the artifact completely obscured the AEP response. The comparison between original and post-ICA simulated grand average AEPs is also shown, as well as the grand average spatial correlation for all time frames. Only for latencies between 0 and 50 ms were the correlations below r_P < .90. This interval corresponds to the onset of the artifact and visual inspection of single-subject data revealed that for some datasets this interval was still contaminated with residual CI artifact. In contrast, between the latencies of the N1 and the P2 components (100 to 300 ms), the correlation was above r_P = .95, indicating that over 90% of the variance was left unaltered by the CI artifact attenuation.

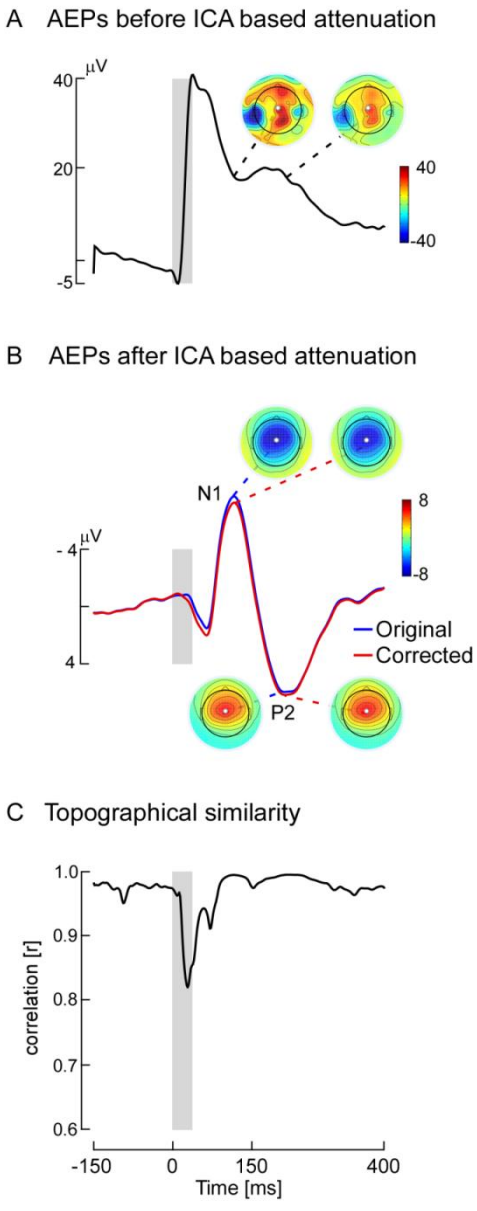

Figure 5.6 *Evaluation of ICA specificity by simulating cochlear implant (CI) artifacts in normal hearing (NH) participant datasets. (A) Grand average CI artifact for 18 NH datasets after addition of CI artifact templates for the electrode highlighted. Topographies at mean N1 and P2 peak latencies are shown.*
(B) Original grand average auditory evoked potentials (AEPs) (blue) and reconstructed grand average AEPs after ICA-based CI artifact attenuation (red) for the highlighted electrode.
Topographies at N1 and P2 peak latencies are shown for the original and the reconstructed data, respectively.
(C) Topographical similarity assessed using the mean spatial correlation between original and reconstructed datasets at all time frames. Gray shadow represents the average time window of CI artifact onset.

When a similar comparison was performed for original (ORIG) and CI-corrected (CORR) CI users' VEPs, no differences were found between peak latencies for the P1 (t[17] = -1.08, n.s.), the N1 (t[17] = -.49, n.s.) or the P2 responses (t[17] = .46, n.s.). Similarly, no differences were found between the P1 (t[17] = 1.52 n.s.), the N1 (t[17] = 1.04, n.s.) or the P2 peaks (t[17] = 1.44, n.s.). Table 5.3 presents a summary of these comparisons. When assessing the topographical similarity, a high spatial correlation (range .91 to .99) was also found for all time frames. Figure 5.7 shows a summary of the main VEP results. The RMS amplitude across channels of 18 CI users for original (blue) and CI-corrected (red) datasets is shown, as well as the topographies at P1, N1, and P2 peak latencies. It is clear that the differences between original and CI-corrected VEPs were minimal.

Table 5.3 Mean RMS Across Channels for P1, N1, and P2 Peak Latencies and Amplitudes (± SD)

	RMS VEP Latency [ms]			RMS VEP Amplitude [μV]		
Group	P1	N1	P2	P1	N1	P2
CI	117.6 ± 12.2	167.9 ± 14.0	251.7 ± 34.2	2.6 ± 0.9	4.2 ± 1.4	3.4 ± 1.1
CI corr	119.7 ± 10.5	168.1 ± 13.7	249.7 ± 31.1	2.6 ± 1.0	4.2 ± 1.4	3.3 ± 1.1

Notes. CI = cochlear implant users' original datasets; CI corr = ICA-based corrected datasets; RMS = root mean square; VEP = visual evoked potential.

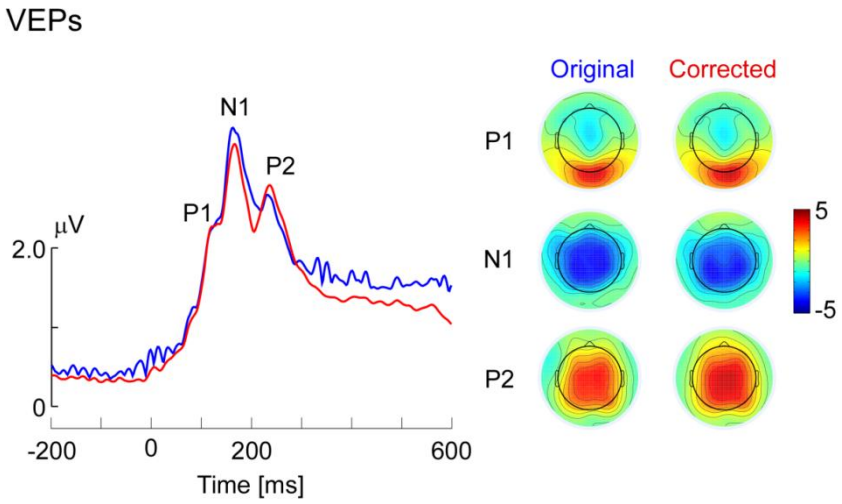

Figure 5.7 *Evaluation of ICA specificity by comparing visual evoked potentials (VEPs) from cochlear implant (CI) users with and without ICA-based CI artifact attenuation. Left, root mean square (RMS) amplitudes across all channels for original (blue) and for corrected (red) VEPs after ICA-based CI artifact attenuation. Right, topographies at mean P1, N1, and P2 peak latencies are shown for the original and corrected data, respectively.*

5.5. Discussion

This study evaluated the quality of AEPs from a large and heterogeneous population of post-lingually deafened CI users. The ICA-based CI artifact attenuation was evaluated in terms of both its sensitivity and specificity. Several previous studies have used ICA to attenuate the CI artifact (Debener, et al., 2008a; Gilley, et al., 2006; Gilley, et al., 2008; Sandmann, et al., 2009; Sandmann, et al., 2010; Zhang, et al., 2010), but negative findings exist (Martin, 2007). Overall, our results confirm the value of ICA in the context of AEPs from CI users, which could become an important tool for guiding further implant technology (Moore & Shannon, 2009).

After a careful manual screening of all independent components (ICs), a group of ICs with the characteristics associated with the CI artifact could be found, similar to previous reports from our group and others (Debener, et al., 2008a; Gilley, et al., 2006; Sandmann, et al., 2009). However, the identification of ICs reflecting the CI artifact is difficult for several reasons. First, in contrast to the ICA representation of other more conventional artifacts, which are normally represented by one or very few ICs, electrical artifacts from the implant device were represented by up to 11 ICs in this study. In only two out of 18 datasets was the CI artifact represented by a single IC. This raises issues about the subjectivity of the component selection procedure. Second, ICs representing conventional artifacts can be efficiently and semi-automatically identified using topographical information (Viola, et al., 2009). Unfortunately, the automatic identification of ICs reflecting the CI artifact does not seem possible based on topographical information alone and currently requires laborious visual inspection of additional features in the component activation patterns. This manual visual screening process can be seen as a major drawback of the ICA procedure, since it is subjective, time consuming, and error prone and also requires expert knowledge. To overcome this limitation, an important goal for the future is to develop software solutions that automatically identify and select components representing the CI artifact. This is a worthwhile goal, since AEPs can objectively inform about auditory cortex function and thus help to guide further improvements in implant technology (Moore & Shannon, 2009).

The sensitivity of ICA in attenuating the CI artifact was high in our study, since the majority of recovered AEPs showed little CI artifact, and were comparable with NH AEPs in terms of SNR and individual differences, such as aging effects. Another advantage of the ICA procedure is the potential for using almost the entire recorded data for the AEP calculations. For instance, in this experiment on average 95% of the original epochs were retained. Previous studies rejected trials contaminated both with ocular and

with CI artifacts (Henkin, et al., 2009; Sharma, et al., 2002), thereby reducing the potential for obtaining good AEP SNR. More importantly, ICA solves the problem discussed in other studies of having to use very short auditory stimulation to avoid overlap of the CI artifact with longer latency AEP components (Gilley, et al., 2006; Henkin, et al., 2009). Our study shows that good quality AEPs can be acquired using complex sounds with long durations (800 ms). This opens up the possibility of using stimuli with high frequency resolution, complexity, and ecological validity, such as speech or musical sounds.

Previous studies have already reported the high ICA sensitivity shown here, but an evaluation of ICA specificity has not been performed. One possible reason is that specificity issues can be examined only with a rather indirect approach. Since AEPs cannot be obtained from CI users without the CI artifact, it is necessary to use a simulation approach in which the true degree of mixing of signal and artifact is known. One simple yet realistic hybrid simulation approach consists of adding an averaged CI artifact template to the AEPs from NH participants and then correcting the data with ICA. The comparison of original and recovered AEPs then provides information about ICA specificity. In this study, an improvement was made to this simulation approach by matching artifact templates to the individual auditory stimuli. A high spatial correlation between original and post-ICA simulated AEPs was found, indicating a high similarity in topography between the two, as previously reported for single subject cases (Sandmann, et al., 2009). In our study, we observed in some datasets a small residual CI artifact at onset latencies. However, this residual artifact, which demonstrates that the ICA approach is not perfect, was restricted to latencies before the early P1 AEP component. The P1 component has been used as the main marker in the investigation of auditory cortical maturation in implanted children (Gilley, et al., 2008; Sharma, et al., 2002), but has a longer latency in this population. Our results also showed that N1 and P2 latencies were not affected by the correction procedure, while the amplitudes were slightly reduced. However, the correlation between original and corrected amplitudes was very high, confirming that individual differences in amplitudes were preserved and ICA over attenuation affected all datasets similarly. Moreover, similar results were obtained when comparing original and CI-corrected VEPs. The VEP P1, N1, and P2 peak amplitudes and latencies were similar for original and CI-corrected data, and the topographical similarity at peak latencies of these components was also high. Thus, the combination of simulated NH AEPs results and the analysis of VEPs from CI users provides strong

evidence of high specificity. We conclude that high-quality AEPs can be recovered from CI users.

When evaluating the quality of the AEPs from CI users, a large variability in terms of component morphology, amplitude, and latency was found. Since the sample tested had a considerable age variance and also varied in clinical parameters, these differences were to be expected. Nevertheless, more than half of the sample of CI users was characterized by AEPs with an SNR generally similar to that of age-matched NH individuals. Although the CI users had significantly smaller N1 and P2 amplitudes, individual features of the population such as aging effects that are evident in NH participants were preserved in the recovered AEPs. This result strongly suggests that the ICA-based CI artifact attenuation procedure did not eliminate individual differences. The subgroup analysis based on SNR values revealed an interesting clinical result. It was found that the CI users with larger SNR, that is, more robust N1 responses, had been deaf for significantly shorter periods. Similar findings have been previously reported, where duration of deafness has been linked to both auditory cortical activations as revealed by functional neuroimaging (Green, et al., 2005) and mismatched negativity amplitudes (Sandmann, et al., 2010). Taken together, these findings imply that the longer the auditory cortex was deprived of sensory input, the more difficult auditory rehabilitation with a CI becomes.

The duration of deafness, therefore, seems to be a key clinical parameter. However, onset of deafness is not always easy to determine, as hearing loss can be progressive with a formal diagnosis only at later stages. In this study, the duration of deafness was established using the information provided by CI users at interviews done prior to EEG recording. One neuroimaging study (Green, et al., 2005) and another EEG study (Kelly, et al., 2005) found a correlation between duration of deafness and scores in speech recognition. Speech scores have been used as the main evaluation measurement of rehabilitation in clinical settings. However, previous studies reported that an isolated speech recognition score can be misleading and therefore recommended that the rehabilitation assessment should be done using a combination of tests (Donaldson, et al., 2009; Gifford, et al., 2008). Other authors have supported the use of AEPs as a complementary assessment tool (Kileny, 2007; McNeill, et al., 2009). In some cases, AEPs may even replace such tests, for instance, when dealing with pre-lingually deafened CI users (McNeill, et al., 2009) or paediatric populations (Kileny, 2007). In any case, making the evaluation of CI users' AEPs easy and reliable seems to be a key factor for a better monitoring of implantation outcome in the future. The available evidence from

longitudinal AEP studies is based on a few single cases (Pantev, et al., 2006) but clearly demonstrates that AEPs can provide important insights into auditory rehabilitation.

In conclusion, the results presented here complement previous studies showing that ICA can successfully attenuate the electrical CI artifact in EEG data from CI users, thus allowing the recovery of AEPs. ICA is an adequate tool for this task, demonstrating good sensitivity and specificity. In addition, the recovered AEPs from CI users reflected the expected correlations with aging and clinical parameters. Overcoming practical limitations of component selection would help to establish multi-channel AEPs in response to speech and musical sounds as a useful research tool. Speech-evoked AEPs could provide an important tool for the objective monitoring of auditory cortical rehabilitation after implantation, and appear particularly promising in cases where conventional measures of speech perception and auditory performance cannot be used. A complementary use of objective measurements of auditory cortex function may help to shape rehabilitation programs and thus improve the quality of life for CI users.

6. Study 3: Automatic attenuation of cochlear implant artifacts for the evaluation of late auditory evoked potentials

The study described in this chapter was submitted on 29th, June 2011 to the journal "Hearing Research". The manuscript is under revision. FCV designed and developed the algorithm, run the validation studies and prepared the manuscript. MDV contributed to the design of the validation studies and to the preparation of the manuscript. JH collected the EEG datasets contained in the Tones and Noise Study (TNS) and helped with the preparation of the manuscript. PS classified the ICs in the TNS and helped with the preparation of the manuscript. SB and JE provided the clinical information about the cochlear implant users and helped with the preparation of the manuscript. SD supervised all parts of the work, and also contributed to the preparation of the manuscript.

6.1. Abstract

Electrical artifacts caused by the cochlear implant (CI) contaminate electroencephalographic (EEG) recordings from implanted individuals and corrupt auditory evoked potential (AEPs). Independent component analysis (ICA) is efficient in attenuating the electrical CI artifact and AEPs can be successfully reconstructed. However the manual selection of CI artifact related independent components (ICs) obtained with ICA is unsatisfactory, since it contains expert-choices and is time consuming.

We developed a new procedure to evaluate temporal and topographical properties of ICs and automatically select those components representing electrical CI artifact. The CI Artifact Correction (CIAC) algorithm was tested on EEG data from two different studies. The first consists of published datasets from 18 CI users listening to environmental sounds. Compared to the manual IC selection performed by an expert the sensitivity of CIAC was 91.7% and the specificity 92.3%. After CIAC-based attenuation of CI artifacts, a high correlation between age and N1-P2 peak-to-peak amplitude was observed in the AEPs, replicating previously reported findings and further confirming the algorithm's validity.

In a further study AEPs in response to pure tone and white noise stimuli from 12 CI users that had also participated in the other study were evaluated. CI artifacts were attenuated based on the IC selection performed automatically by CIAC and manually by one expert. Again, a correlation between N1 amplitude and age was found. Moreover, a high test-

retest reliability for AEP N1 amplitudes and latencies suggested that CIAC based attenuation reliably preserves plausible individual response characteristics.

We conclude that CIAC enables the objective and efficient attenuation of the CI artifact in EEG recordings, as it provided a reasonable reconstruction of individual AEPs. The systematic pattern of individual differences in N1 amplitudes and latencies observed with different stimuli at different time points after implantation, strongly suggests that CIAC can overcome the electrical artifact problem. Thus CIAC facilitates the use of cortical AEPs as an objective measurement of auditory rehabilitation.

6.2. Introduction

Auditory evoked potentials (AEPs) are important for the evaluation of auditory cortex functions in normal hearing and hearing impaired humans. Several studies have used AEPs to investigate how the auditory cortex adapts to the artificial input provided by a cochlear implant (CI). Examples are the measurement of the P1 response to investigate the functional development of the auditory cortex in children fitted with CIs (Gilley, et al., 2008; Sharma, et al., 2005) the study of brain asymmetries in the auditory cortex (Debener, et al., 2008a; Sandmann, et al., 2009), the investigation of neural correlates of musical sound perception (Koelsch, et al., 2004; Sandmann, et al., 2010), and the relationship of AEPs to speech perception (Henkin, et al., 2009; Kelly, et al., 2005; Lonka, et al., 2004; Zhang, et al., 2010; Zhang, et al., 2011). Based on those and other studies it has been suggested that the functional integrity of the auditory system from CI users, which varies widely across patients, as well as the capacity for cortical plasticity, deserves more attention when investigating implantation outcome (Moore & Shannon, 2009; Wilson & Dorman, 2008a).

One of the limitations of using AEPs as a routine research or clinical tool is the fact that the EEG recordings taken from CI users are contaminated by electrical artifacts which coincide in time with auditory stimulation. Other authors have already described in detail the characteristics of the CI artifact (Gilley, et al., 2006). The CI artifact properties vary widely across devices, individuals, and types of stimulation (Gilley, et al., 2006; Viola, et al., 2011) and the literature is inconsistent concerning the prevalence of the artifact. In some CI users the absence of artifacts in EEG recordings has been reported (Zhang, et al., 2010). Moreover, at least one study suggested electrical artifacts only at response latencies different from cortical AEPs and thus did not report difficulties in the measurement of AEPs (Koelsch, et al., 2004). It has also been speculated that the CI artifact may be present until one year after CI activation (Lonka, et al., 2004). Despite these reports, most studies presenting multi-channel EEG data have found that AEPs from CI users are strongly corrupted by a large electrical artifact generated by the CI device, thus impairing any type of analysis unless tailored, sophisticated and often time-consuming artifact processing techniques are applied. Accordingly, adequate artifact attenuation seems crucial for the AEP-based study of auditory cortex rehabilitation in CI users.

A traditional approach to attenuate the CI artifact is the subtraction technique, where the presentation of the auditory stimuli is manipulated to create experimental conditions where the AEP response varies but the CI artifact remains constant (Friesen & Picton,

2010). Unfortunately this approach limits the type of experimental paradigms that can be used and it has only been tested for a small population. Other authors used linearly constrained minimum variance beamformers to reconstruct cortical activity with minimal artifact interference (Wong & Gordon, 2009). This approach has been reported to work in a single case study. It is also possible to minimize the CI artifact by using an optimized differential reference (ODR) technique. Here the reference of the EEG montage is placed in a location that allows recording a particular electrode of interest free of artifact (Gilley, et al., 2006). A shortcoming of the ODR technique is finding and validating the best location for the reference for each CI user, which is time consuming. The ODR approach makes it also difficult to analyze AEPs on the cortical source level. A more generic and promising approach is the use of independent component analysis (ICA) to separate the EEG signals into statistically maximally independent components (Makeig, et al., 2004a; Onton, et al., 2006). These independent components (ICs) need to be evaluated by an expert in order to select those representing the CI artifact. It has been shown in various CI users using different types of devices that the ICA method allows good attenuation of the CI artifact and the reconstruction of individual AEPs (Debener, et al., 2008a; Gilley, et al., 2006; Gilley, et al., 2008; Sandmann, et al., 2009; Sandmann, et al., 2010; Viola, et al., 2011; Zhang, et al., 2010; Zhang, et al., 2011). Furthermore it has been reported that after attenuation of CI artifacts, individual differences were reasonably well reconstructed, as evidenced by a high correlation between age and AEP amplitudes (Viola, et al., 2011).

However, one significant limitation of the ICA approach is the laborious selection of the ICs representing electrical CI artifact (Viola, et al., 2011). This process is subjective and time consuming, since it requires extensive visual inspection of all ICs by a trained operator. Although automatic methods have been developed that reasonably well identify ICs representing conventional EEG artifacts (Mognon, et al., 2010; Nolan, et al., 2010; Viola, et al., 2011), they are not optimal to identify components representing electrical CI artifacts, which have a particular signature in the spatial and temporal domain as illustrated in Figure 6.1.

Accordingly we aimed at developing and validating a novel, automatic and user-friendly algorithm that screens the temporal and spatial properties of ICs and identifies the components representing the CI artifact. The Cochlear Implant Artifact Correction (CIAC) tool presented here provides a faster and, more importantly, more objective CI artifact attenuation, and thus facilitates the reconstruction of AEPs. In a first step the CIAC approach was validated using a published AEP study from 18 adult CI users. In

this study IC classification was performed manually by a well-trained researcher (FCV) (Viola, et al., 2011), and the resulting AEPs served as a reference for the development of CIAC. In a second step, an unpublished set of EEG recordings from a subgroup of the same CI users (N = 12) presented with different auditory stimuli and recorded 12 months earlier was evaluated. CI artifacts were attenuated based on the selection performed by CIAC and by another well-trained expert (PS) with several years of experience in using ICA for the evaluation of AEPs from CI users (Sandmann, et al., 2009; Sandmann, et al., 2010). For both studies the AEPs after automatic selection with CIAC were evaluated. We adjusted CIAC parameters on study 1, aiming for high sensitivity and specificity, and hoping that it would work for a wide range data. Since data were available for a subgroup of this sample we also explored whether AEPs reconstructed after CIAC selection would show good temporal stability.

6.3. Methods

6.3.1. CIAC description

ICs can be characterized by their properties both in the temporal and in the spatial domain and different criteria can be defined to distinguish between brain related and CI artifact related components. In the spatial domain the residual variance (RV) between the actual IC topography and the model projection for the equivalent dipole to the same electrode montage can be used as a differentiation criterion (Gramann, et al., 2010; Onton, et al., 2006), since brain related ICs are dipolar and thus have a much lower RV (Figure 6.1, top row). Contrary to several conventional types of EEG artifacts, which are represented by ICs with similar topographies across subjects (Viola, et al., 2009), the topographies of the CI artifact related ICs are less dipolar and, partly reveal information about the location of the internal components of the CI device, as can be seen in Figure 6.1, top row. Accordingly across individuals the CI artifact topographies can be substantially different. On the other hand, for the same CI user, the topographies of the ICs reflecting the artifact may share a substantial degree of similarity. When inspecting the temporal properties of the CI related ICs from different CI users it is evident that they share very similar profiles. The largest activity takes place during the onset and/or offset of the artifact as can be seen both for the ERP and its first temporal derivative (Figure 6.1, middle and bottom rows). On the other hand, ICs representing for instance late auditory cortex related activity usually have largest deflections in the time window corresponding to the N1-P2 responses (100-250 ms) as illustrated in Figure 6.1.

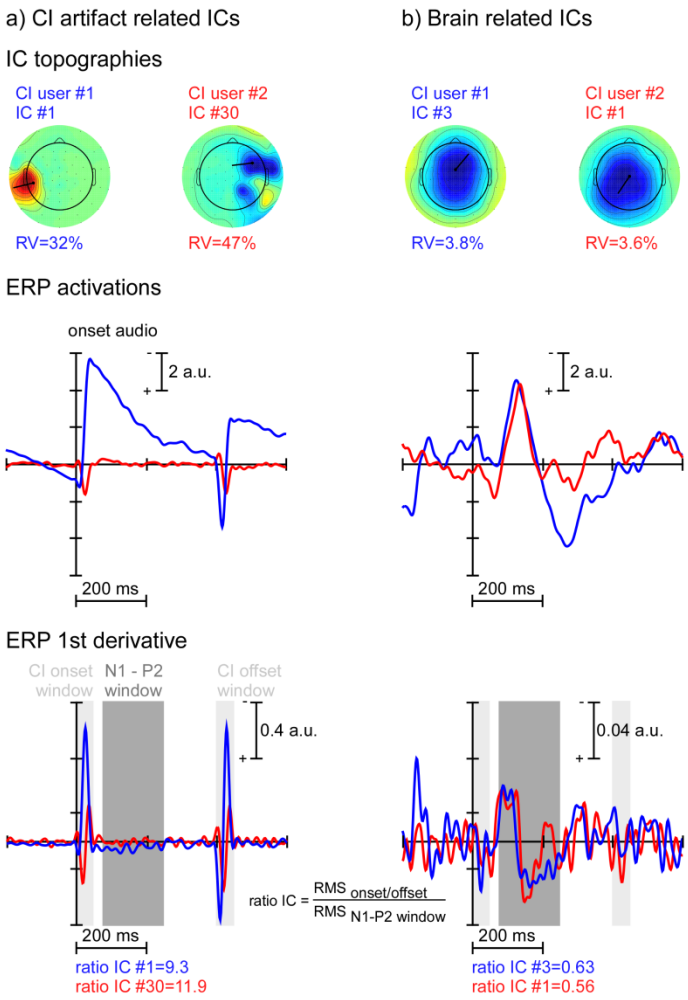

Figure 6.1 *Properties of independent components (ICs). Column a) shows two ICs representing the cochlear implant (CI) artifact for user #1, implanted on the left side, (blue) and user #2, implanted on the right side (red). Column b) shows another two ICs representing brain related activity for the same CI users. The top row shows the ICs topographies and the respective residual variance (RV) in % after dipole fitting. 2-D projections of dipole location and orientation are indicated in black on top of the topographic maps. The middle row shows the ERP for each IC. Zero ms represents auditory onset and amplitude values are expressed in arbitrary units (a.u.). The bottom row shows the temporal derivative of the ERP for each IC. The time windows corresponding to the onset of the CI artifact are displayed in light grey, whereas the time window representing activity of interest (N1-P2 peaks) is displayed in dark grey. For each IC the ratio between the root mean square (RMS) amplitude in the onset/offset window and the RMS amplitude in the time window of interest was calculated (ratio IC).*

Based on these observations we implemented an algorithm that combines spatial and temporal information and selects CI related ICs using three steps and three thresholds. Figure 6.2 shows a schematic flow chart of the cochlear implant artifact correction (CIAC) algorithm. As a starting point three user inputs are required: 1) ICs from one or

more EEG dataset, epoched to the auditory stimuli of interest; 2) the duration of the auditory stimuli; 3) a time window of interest for the AEP response. In the first step CIAC selects the ICs with RV larger than a pre-defined threshold (*RV* > *Thr_rv*). In the second step the temporal derivative of the ERP is calculated for each of the ICs which are part of the subset selected in the first step. Then the ratio is computed between the root mean square (RMS) amplitude of the IC temporal derivative in the artifact onset/offset time window (derived from the duration of the auditory stimuli – user input) and the RMS amplitude for the time window where the responses of interest are expected (user input). The IC with the largest ratio is selected as a topographical template for that particular CI user, since it is the one reflecting the strongest artifact profile, and its topography is then going to be correlated with all other topographies. In the third step ICs are selected if at least one of these two criteria is met: having a ratio larger than a pre-defined threshold (*ratio* > *Thr_deriv*) or the correlation between topography and the CI artifact template being above a pre-defined threshold (*correlation* > *Thr_corr*). After CIAC performed these three steps, visual representations are presented to the user, displaying the topographies of the selected ICs as well as the original AEP and the corrected AEP. The user is thus provided with a visual representation of the degree of CI artifact attenuation that could be achieved. In case of an unsatisfactory result CIAC could be re-run using different, user-defined thresholds.

For the residual variance threshold we experienced consistently good results using values between 15% < *Thr_rv* < 25%. By default CIAC uses *Thr_rv* = 20%, which is close to residual variance thresholds for the evaluation of IC quality as described in other studies (Gramann, et al., 2010; Onton, et al., 2006). The recommended values for the derivative ratio threshold are 1.5 < *Thr_deriv* < 3.5 and the default is in between this range (*Thr_deriv* = 2.5). This range is motivated by a previous study (Viola, et al., 2011) where the ICs manually labeled as CI artifact were characterized by a ratio range between 1.5 and 12. For the correlation threshold the recommended values are 0.85 < *Thr_corr* < 0.95, which represents a rather conservative range. Since in our experience ICs reflecting CI artifact have either very similar or uncorrelated topographies, the default value was set to *Thr_corr* = 0.95.

To validate the CIAC algorithm EEG recordings from CI users comprising two study sets were evaluated. In section 6.3.2 we report the results of a study with environmental sounds and henceforth we refer to it as Environmental Sounds Study (ESS). In section 6.3.3 we report the results of a study with tonal and noise stimulation and henceforth labeled this as Tones and Noise Study (TNS). Note that, chronologically, the TNS study

was recorded first and the ESS study recorded approximately 12 month later, but, because the ESS data were already available (Viola, et al., 2011), they were used for the development of CIAC and thus are reported first.

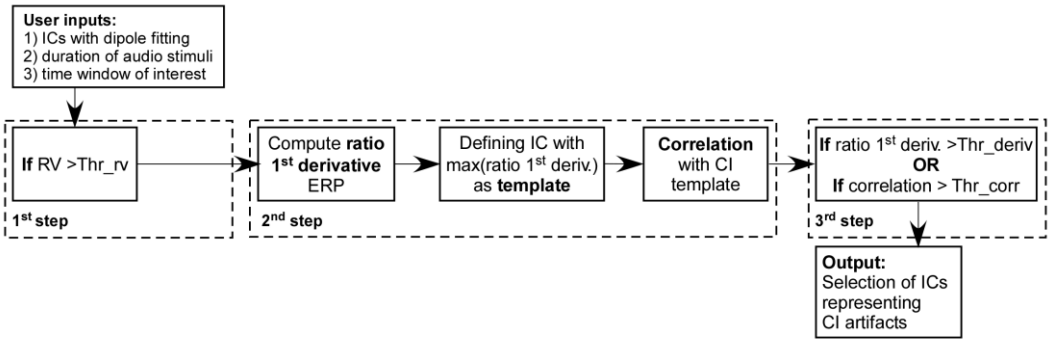

Figure 6.2 *Schematic flow chart of the cochlear implant artifact correction (CIAC) algorithm. The main inputs are the independent components (ICs) after and corresponding information from dipole fitting, the duration of the auditory stimuli used and a time window of interest that should contain the auditory evoked responses. In the first step a sub group of ICs is selected based in the residual variance (RV) obtained after dipole modeling and using a pre-defined threshold (Thr_rv). In the second step the first temporal derivative of the evoked response potential (ERP) of these ICs is computed and a ratio (ratio deriv.) between the root mean square (RMS) in the time window of the onset/offset of the artifact (derived from the duration of the auditory stimuli) and the time window of interest is calculated. The IC with the highest ratio deriv. is selected as a template and its topography map is correlated with all other ICs maps. In the third step ICs with a ratio deriv. or a correlation with the template larger than pre-defined thresholds (Thr_deriv and Thr_corr, respectively), are selected as representing the CI artifact.*

6.3.2. Environmental Sounds Study (ESS)

6.3.2.1. Subjects

Eighteen post-lingually deafened, adult CI users (10 females, *M* = 59.89, *SD* = 13.06 years) were recruited from the South of England Cochlear Implant Centre in Southampton, UK. All CI users were right-handed and had no history of neurological or psychiatric disorders and had normal or corrected to normal vision. All but one CI user were unilaterally implanted and all CI users had at least 6 months experience with the implant (CI experience: *M* = 40.22, *SD* = 36.60 months). Details about the clinical profile of the CI users have been described elsewhere (Viola, et al., 2011). Procedures were approved by the local ethics committee and conformed to the declaration of Helsinki.

6.3.2.2. Stimuli and Task

CI users were stimulated with 80 environmental sounds with 400 ms duration and a sampling rate of 22 kHz via two loudspeakers (Quad L12) positioned at an azimuth of 45°/135° in front of the participant. Sounds were presented at a comfortable level adjusted individually for each participant using a five level loudness comfort rating scale varying from 60 to 80 dB SPL in steps of 5 dB SPL. The environmental sounds were used as primes in a semantic priming paradigm (Viola, et al., 2011).

6.3.2.3. Electrophysiology recordings

CI users were seated in an electrically shielded, sound attenuated and dimly lit booth (Industrial Acoustics, Winchester, UK) and EEG data were recorded from 68 channels using a high-input impedance amplifier system (Compumedics Neuroscan, Charlotte, NC, USA) and a customized, infracerebral electrode cap with an equidistant electrodes lay-out (Easycap, Herrsching, Germany). Data were recorded with a sampling rate of 1000 Hz using the nose-tip as reference, and were analogue filtered between 0.1 and 200 Hz. Electrode impedances were maintained below 20 kΩ prior to data acquisition.

6.3.2.4. Data processing

EEG data were processed using custom scripts and EEGLAB (Delorme & Makeig, 2004) running in the MATLAB (Mathworks, Natick, MA) environment. Data were filtered offline from 1 to 40 Hz using sinc FIR filters windowed with a Hann window (courtesy of A. Widmann: www.uni-leipzig.de/~biocog/content/widmann/eeglab-plugins/). Data were then down-sampled to 500 Hz and pruned of unique, non-stereotyped artifacts using the EEGLAB function *jointprob.m* (Delorme, et al., 2007a). Extended infomax ICA as implemented in EEGLAB was then applied to the remaining data in order to achieve a reliable decomposition (Debener, et al., 2010). Independent components (ICs) representing eye-blinks and electrocardiographic artifacts were semi-automatically identified using CORRMAP (Viola, et al., 2009) and then corrected from all datasets. Since one of the parameters assessed in the CIAC algorithm is the residual variance (RV) equivalent current dipole modeling was then computed for the remaining ICs using a four-shell spherical head model and procedures implemented in the EEGLAB DIPFIT toolbox (Oostenveld & Oostendorp, 2002). Afterwards all datasets were segmented into epochs from -200 to 600 ms relative to sound onset. AEPs were obtained by time-domain averaging and the pre-stimulus interval (-200 to 0 ms) was used for baseline subtraction.

6.3.2.5. Automatic identification of CI artifact related ICs using CIAC

CIAC was tested using the following input parameters: ICs from 18 EEG datasets recorded from the CI users, 400 ms for the duration of the auditory stimuli and the interval from 80 to 250 ms (corresponding to the N1-P2 responses) was selected as time window of interest. The default threshold values were used: *Thr_rv* = 20%; *Thr_deriv* = 2.5; *Thr_corr* = 0.95. After automatic attenuation of CI artifacts, AEPs at missing electrodes were interpolated with the EEGLAB function *eeg_interp.m*, which implements a smoothed inverse distance approach. The sensitivity and specificity of CIAC were evaluated, taking as "gold standard" the manual selection previously performed by an expert (Viola, et al., 2011). Sensitivity was defined as the ratio between the number of ICs selected both by CIAC and by the expert (Hits) divided by the sum of Hits and Misses, the latter corresponds to the ICs identified only by the expert. Specificity was defined as the ratio between the number of ICs not selected both by the expert and CIAC (Correct Rejects) divided by the sum of Correct Rejects and False Alarms, the latter corresponds to the ICs selected by CIAC only.

6.3.2.6. Auditory evoked potential quantification

AEP amplitude and latency analyses were performed for the fronto-central channel closed to Fcz, showing the largest grand average N1 amplitude. AEP peak amplitudes and latencies were determined using a semi-automatic procedure as implemented in *peakdet.m* (www.billauer.co.il/peakdet.html). The N1 and P2 peak amplitudes and latencies obtained after manual and automatic selection of CI related ICs were compared.

6.3.3. Tones and Noise Study (TNS)

6.3.3.1. Subjects

Twelve post-lingually deafened cochlear implant (CI) users (5 females, *M* = 61.75, *SD* = 13.46 years) implanted unilaterally were recruited from the South of England Cochlear Implant Centre in Southampton, UK. All CI users were right-handed and had no history of neurological or psychiatric disorders and had normal or corrected to normal vision. Procedures were approved by the local ethics committee and conformed to the declaration of Helsinki. All CI users had at least 6 months experience with the implant (CI experience: *M* = 41.75, *SD* = 37.69 months). The CI users participated also in the Environmental Sounds Study (ESS) approximately one year later (Interval between recordings: *M* = 12.33, *SD* = 0.98 months).

6.3.3.2. Stimuli and Task

The procedures were the same as described for the single case previously reported (Debener, et al., 2008a). Stimuli were 1-kHz tones and white noise, 220 ms long with 10 ms rise and fall time, sampled at 44.1 kHz and presented at 70 dB SPL. The stimuli were presented using two loudspeakers (Quad L12) as described in the ESS, while the participants watched a silent movie.

6.3.3.3. Electrophysiology recordings

The procedure used was the same as described for the ESS (section 6.3.2.3).

6.3.3.4. Data Analysis

EEG data were processed the same way as described for the ESS (section 6.3.2.4).

6.3.3.5. Automatic identification of CI artifact related ICs using CIAC

CIAC was applied to the twelve CI user datasets using as input parameters 220 ms for the duration of the auditory stimuli and the interval from 54 to 180 ms (corresponding to the P1-N1 responses) for the time window of interest. After running CIAC with the thresholds used in the ESS it was observed that some of the reconstructed AEPs were still contaminated by a large CI artifact. The thresholds were then adjusted (*Thr_rv* = 20%; *Thr_deriv* = 1.5; *Thr_corr* = 0.9) within the range proposed above and CIAC was run again. It is worth noting that the *Thr_deriv* is largely dependent on the strength of the CI artifact present in the data, which can vary depending on the type of stimuli and stimulus presentation details. The ICs selected automatically were corrected and the AEPs were reconstructed for all datasets. AEPs at missing electrodes were interpolated with the EEGLAB function *eeg_interp.m*, which implements a smoothed inverse distance approach. The sensitivity and specificity of CIAC were again evaluated, taking as "gold standard" the manual selection performed by an independent expert that was not involved neither in data collection and processing or development of the algorithm (PS).

6.3.3.6. Auditory evoked potential quantification

AEP amplitude and latency parametrization was performed as described in the ESS. Since the stimuli used in the TNS had the duration of 220 ms, for some CI users the P2 response was contaminated by residual offset CI artifact. Therefore the focus of the analysis was on the P1-N1 time window with a particular focus on the N1 response, which could be identified for all CI users.

6.3.4. Statistical Analysis

All variables were tested for normality using Shapiro-Wilk tests. For the ESS comparisons between manual and automatic CI artifact selection N1 and P2 peak amplitudes and latencies were evaluated using two-tailed paired t-tests. For four out of the eighteen CI users it was not possible to identify a P2 component in the AEPs after automatic attenuation, similar to previous observations (Viola, et al., 2011). For these participants P2 amplitude was taken as 0 μV and P2 latency as the mean value of the other CI users (245 ms). In order to investigate if the automatic selection of CI related ICs would preserve the individual differences found for the manually corrected datasets (Viola, et al., 2011), the Spearman correlation, indicated with r_S, between age and N1-P2 peak-to-peak amplitude was calculated. For the TNS study the Spearman correlation between age and N1 amplitude was computed. The same correlation was calculated for the ESS using only the datasets from the 12 CI users that participated in both studies. For all tests differences were considered significant when $p < .05$.

6.3.5. Test-retest reliability

The test-retest reliability was also assessed by computing the coefficient of determination (R^2) for the correlation between N1 peak amplitudes and latencies in the TNS (first test) and in the ESS (retest). It is worth noting that the studies were not planned as retests and therefore different stimuli and paradigms were used. In addition, since the participants had at least 6 months experience with the CI device prior to taking part in either of the studies reported here, we assumed that the auditory system would have re-organized to a substantial extent and AEPs would have been established (Pantev, et al., 2006). Thus, we predicted that, given careful artifact attenuation, the AEP N1 response should be characterized by a reasonable temporal stability.

6.4. Results

6.4.1. Environmental Sounds Study (ESS)

After running CIAC, the reconstructed AEPs were similar to the ones obtained after manual selection of CI artifacts. Figure 6.3 shows the individual AEPs for a fronto-central electrode, as well as the grand average AEP and the N1 and P2 peak topographies. No significant differences were found for the N1 peak latency obtained after manual (MAN) and automatic (AUTO) selection ($t(17) = 1.27$, n.s.). The P2 peak latency was also not significantly different ($t(17) = 0.81$, n.s.). When comparing the N1-P2 peak-to-peak amplitude, no significant differences were found ($t(17) = -1.42$, n.s.). Table 6.1 shows a summary of these comparisons. Interestingly, CIAC revealed a mean sensitivity

of 91.7 % ± 0.12 and a mean specificity of 92.3 % ± 0.07, when its performance was compared to the manual selection. The correlation between age and N1-P2 peak-to-peak amplitude after the two types of CI artifact selection is shown in Figure 6.3-c. A significant negative correlation between age and peak-to-peak amplitude was found after automatic selection (AUTO: r_S = -0.67, p = .002), replicating previous findings (MAN: r_S = -0.70, p =.001) (Viola, et al., 2011).

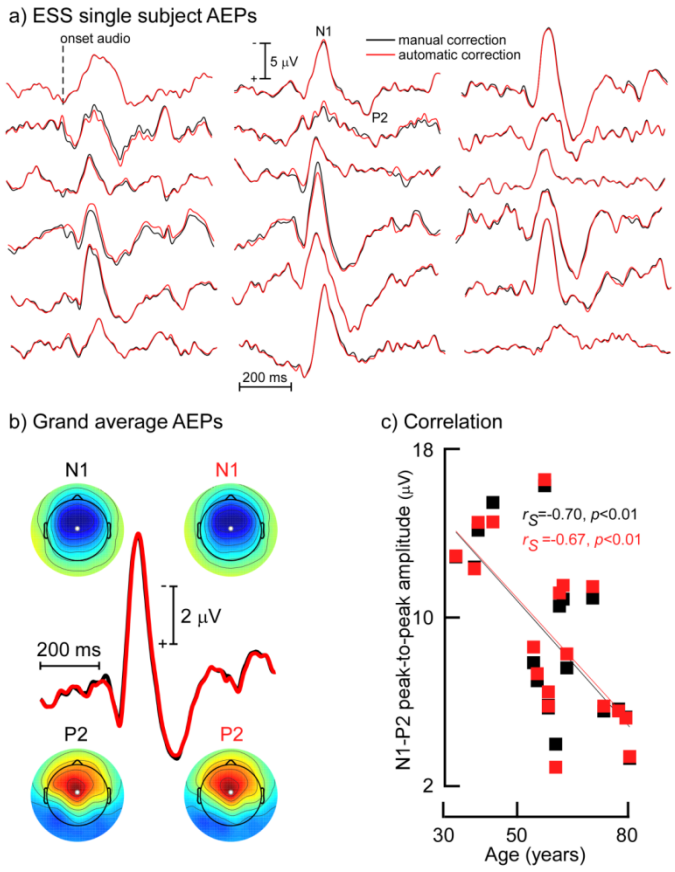

Figure 6.3 *Summary of the auditory evoked potentials (AEPs) for the Environmental Sounds Study (ESS). a) Comparison of single subject AEPs reconstructed after manual (black) and automatic (red) attenuation of cochlear implant artifacts. A fronto-central channel is shown. b) Grand average AEPs after manual (black) and automatic (red) CI artifact attenuation and respective N1 and P2 peak topographies. c) Correlation between age (years) and N1-P2 peak-to-peak amplitude (µV) for data corrected manually (black) and automatically (red).*

Table 6.1 *Mean N1-P2 peak-to-peak amplitude and N1 and P2 peak latencies for datasets where cochlear implant artifact related independent components (ICs) were selected by an expert (manual) and by CIAC algorithm (automatic) for the Environmental Sounds Study (ESS). All results are presented as Mean ± 1 SD.*

		ESS Latency [ms]	
ICs selection	ESS N1-P2 peak-to-peak amplitude [μV]	N1	P2
manual	9.0 ± 4.1	132.3 ± 13.7	244.9 ± 27.6
automatic	9.1 ± 4.1	130.8 ± 13.2	244.7 ± 28.0

6.4.2. Tones and Noise Study (TNS)

After running CIAC, AEPs were reconstructed for the 12 CI users. The residual artifacts in this study were larger than when the same CI users were stimulated with environmental sounds. Figure 6.4 shows the AEPs for a fronto-central electrode after automatic attenuation of CI artifacts for the two studies (ESS, left and TNS, right), as well as the grand average and respective N1 and P2 (ESS) and the P1 and N1 peak topographies (TNS). Age and N1 amplitude were systematically correlated in both studies (ESS: r_S = -0.48, p =.12; TNS: r_S = -0.52, p =.09) but failed to reach significance.

In this study CIAC revealed a mean sensitivity of 87.3 % ± 0.13 and a mean specificity of 65.6 % ± 0.10, when its performance was compared to the manual selection performed by an independent expert. The specificity was lower than in the previous study. After investigating the properties of the ICs selected by the algorithm and the ones selected by the expert, it was found that the expert seemed to be more conservative, while the algorithm selected also noise related ICs affected by residual CI artifact.

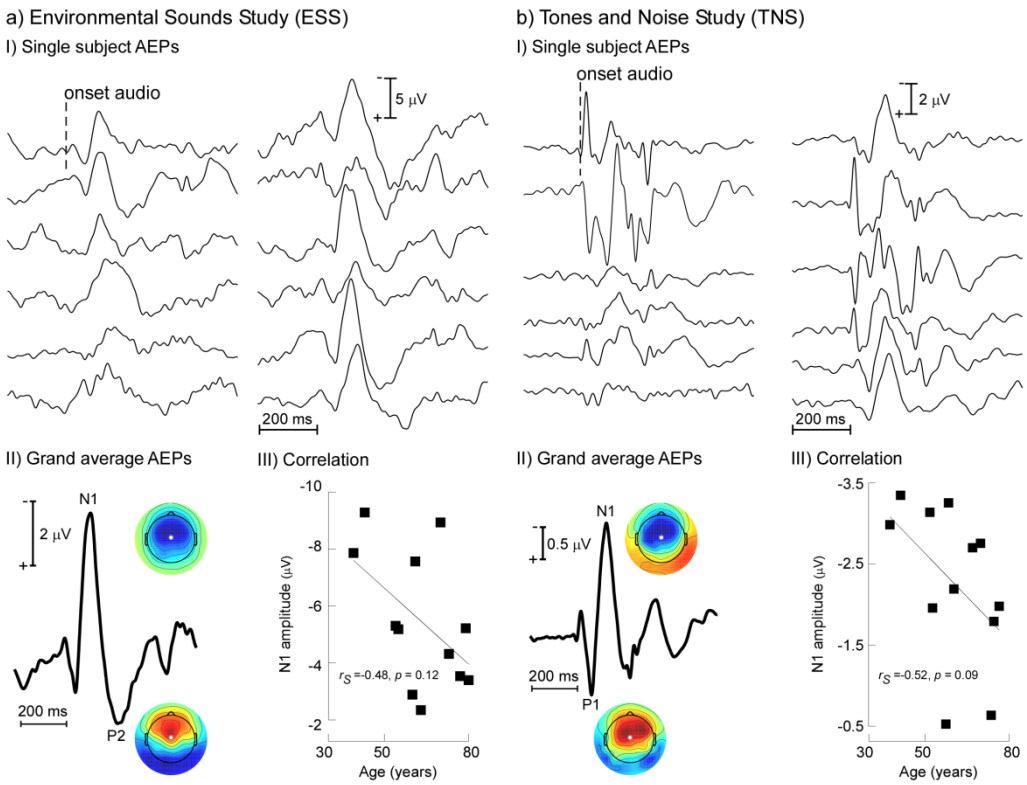

Figure 6.4 *Comparison of auditory evoked potentials (AEPs) reconstructed for the Environmental Sounds Study (ESS) (Column a) and for the Tones and Noise Study (TNS) (Column b) after automatic attenuation of cochlear implant artifacts. I) Single subject AEPs for a fronto-central channel. II) Grand average AEPs and respective N1 and P2 peak topographies (ESS) and P1 and N1 peak topographies (TNS). III) Correlation between age (years) and N1 peak amplitude (µV).*

6.4.3. Test-retest reliability

In order to investigate test-retest reliability, the coefficient of determination was computed for N1 peak amplitudes and latencies, as shown in Figure 6.5. In line with what was reported in previous studies where normal hearing individuals with a broad age range were assessed (Walhovd & Fjell, 2002), a high test-retest reliability was found for N1 latencies (r_S = 0.77; R^2 = 0.59) and for N1 amplitudes (r_S = 0.69; R^2 = 0.48), suggesting that both parameters were reliably reconstructed in both studies.

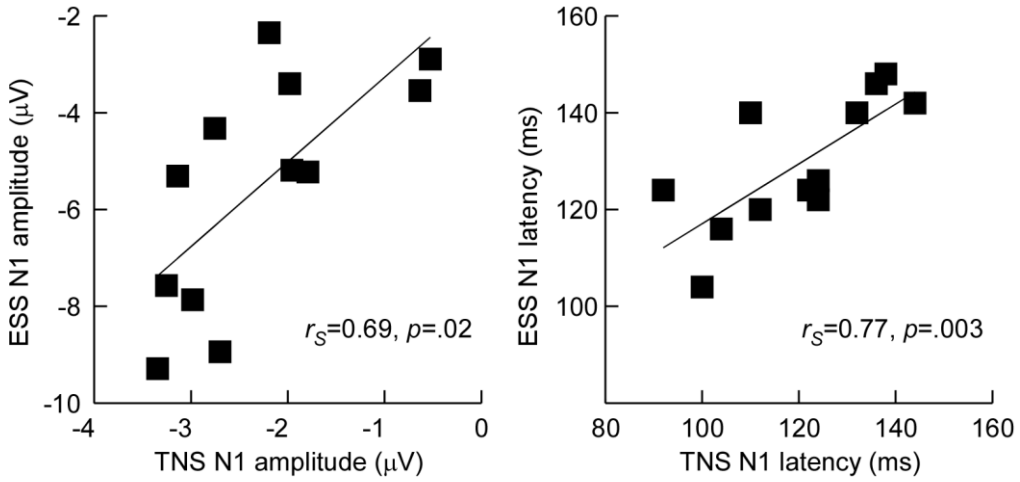

Figure 6.5 *Test-retest reliability for the N1 peak amplitude and latency. Left: correlation for the N1 amplitude expressed in μV for the Tones and Noise Study (TNS) and the Environmental Sounds Study (TNS). Right: correlation for the N1 peak latency expressed in ms for the TNS and the ESS.*

6.5. Discussion

CIAC is a tool that automatically selects ICs representing CI artifacts, thus aiming for a more objective and efficient attenuation of electrical CI artifacts and facilitating the reconstruction of AEPs in CI users. The algorithm was optimized taking into account known properties of the ICs representing CI artifacts. We also aimed at reducing the number of computational steps and thresholds to a minimum. As a result we consider the selection of CI artifacts with CIAC a quick, comprehensive procedure.

The performance of CIAC was evaluated using a total of 30 EEG recording from 18 adult CI users using different types of CI devices, and which were stimulated in two studies with either environmental sounds or tones and noise, separated in time approximately one year. CIAC revealed a high sensitivity and a good specificity when compared to the results of classification by two experts. It is worth noting that the ability of automatically identifying CI artifact related ICs relies mainly on the general quality of the ICA decomposition, which depends on EEG preprocessing and other aspects not covered here (Debener, et al., 2010). The existence of ICs where the artifact is not well disentangled from brain activity (or other types of artifact) may present some challenges. One example is the case when the offset of the auditory stimuli coincides with an AEP response of interest. This was the case in the TNS data where the P2 responses were difficult to reconstruct for some CI users. Accordingly the duration of the auditory stimuli used

should be longer than the cortical response interval of interest, in order to enlarge the probability to reconstruct good quality AEPs. When it comes to the comparison between CIAC and experts, the results should be considered preliminary, since only two experts participated in the validation procedure. Given the large number of decisions necessary (approximately number of electrodes x number of individuals) it is likely that users show some degree of inconsistency, thus limiting the reliability of the resulting AEPs. Different experts may also apply different criteria. For instance, it is our experience that experts may ignore noise related ICs contaminated with residual CI artifact since these normally explain a small amount of variance in the AEPs. Moreover experts could be biased by their past experience, if they, for instance, only had experience with datasets collected from CI users using devices from a specific manufacturer or collected with a particular electrode montage. It is also worth noting that the number of researchers experienced with the selection of CI artifact related ICs is likely small, which hinders the wider use of AEPs for the assessment of auditory rehabilitation. Accordingly a comparison of CIAC with more than two experts, as provided for the CORRRMAP plug-in for instance, would have not been feasible (Viola, et al., 2009).

In terms of data quality, after automatic selection of CI artifacts, AEPs with reasonable quality could be reconstructed. However for the TNS study the amount of residual artifact was larger than in the ESS. One reason could be the fact that in the TNS study the CI users performed a passive listening task. For this and other reasons it is likely the resulting AEPs were of a lower signal-to-noise ratio, which may cause more difficulty for ICA in separating AEPs from artifact.

When comparing manual and automatic selection no significant differences were found between AEP N1 and P2 peak amplitudes and latencies for datasets from the ESS. We also found a high correlation between age and the N1-P2 peak-to-peak amplitude, corroborating previously reported results that the attenuation of the CI artifact does not eliminate potentially informative individual differences in the AEPs (Viola, et al., 2011). Age and N1 amplitude were also correlated in the sub-group of 12 CI users, showing that the individual differences between users were conserved independent of the type of stimuli. As this sub-group was evaluated at two different points of time after implantation, it was possible to evaluate the test-retest reliability of the AEPs. As predicted, a high test-retest reliability was observed for both N1 peak amplitude and latency. The amplitude reliability was comparable to values reported in a comparable study from young and old normal hearing listeners that were re-tested after one year (Walhovd & Fjell, 2002). Our reliability results accordingly suggest that by measuring

standard AEP markers such as the N1 peak amplitude and latency, insights could be obtained about the rehabilitation state of the auditory system, in particular within the first few months after implant device switch on (Pantev, et al., 2006). We consider important that, despite the electrical artifact that can be orders magnitude larger than the auditory cortex response (e.g., Debener, et al., 2008a), AEPs can be reliably reconstructed with ICA, and thus be used in the context of investigating auditory rehabilitation from CI users as proposed previously (Kileny, 2007; McNeill, et al., 2009).

Our work is in line with a broader field of research that has been moving towards the objective and automatic correction of artifacts in EEG recordings (Mognon, et al., 2010; Nolan, et al., 2010; Viola, et al., 2009) using ICA as the main pre-processing method. The development of CIAC opens new doors in the use of EEG as a routine tool to assess auditory cortical function in CI users, since the types of auditory stimuli, as well as the experimental design do not need to be strongly conditioned in order to minimize CI artifacts. In the context of CI rehabilitation further research is needed to evaluate the value of late AEPs, for instance in helping with the CI fitting procedure, or in response to speech sounds in patient groups that cannot voluntarily report their electrical hearing experience, such as early implanted children (Kileny, 2007). Accordingly we envision that measures of auditory cortex function as assessed with late AEPs can be of use in CI configuration from initial setup to the long-term monitoring of rehabilitation progress. We fully agree with the view that developing the ability of the brain to learn how to use an implant may be as important as further improvements of CI device technology (Moore & Shannon, 2009). In this context CIAC may be an improvement, as it facilitates the investigation of auditory cortex functions in CI users.

6.6. Conclusion

The CIAC algorithm reported here provides a fast, user-friendly and objective method to correct electrical CI artifacts from AEP recordings. We hope that this freely available tool will support research investigating auditory cortex reorganization during CI adaptation and rehabilitation, since it is a significant step towards the objective and efficient study of late AEPs. As CIAC will be provided as an open source plugin to be used with the popular EEGLAB toolbox, we hope that other researchers will contribute to its further development, validation and, ultimately, its clinical application.

7. General Discussion

7.1. Summary

This work consisted of three empirical studies, which had as a common goal the evaluation and improvement of the signal processing tools that need to be applied when using multi-channel EEG and AEPs to investigate auditory cortical rehabilitation in CI users. New ICA-based tools were developed, in order to objectively identify biological and CI artifacts in EEG recordings. Moreover, the ability of ICA in attenuating the CI artifact while preserving the AEPs was evaluated and the quality of reconstructed AEPs was assessed.

In *Study 1* a tool called CORRMAP was developed. This tool identifies ICs related to eye blinks, lateral eye movements, and the heartbeat. The rationale is that these biological artifacts give rise to ICs with scalp topography maps across subjects that are highly correlated. Therefore a template-correlation based approach was successful in selecting ICs objectively. The validation procedure consisted of comparing the performance of CORRMAP with the performance of 11 raters who were familiar with ICA. For eye-related artifacts, a very high degree of overlap between raters, and between raters and CORRMAP was observed. For heartbeat artifact ICs lower degrees of association were found both, between users and between users and CORRMAP. Overall the results showed that CORRMAP helps to use ICA efficiently for the removal of biological artifacts.

In *Study 2* effects of CI artifact attenuation on AEP quality were investigated in a sample of 18 adult post-lingually deafened individuals, stimulated with environmental sounds and pictures of natural scenes. AEPs were reconstructed after an ICA-based attenuation approach. The ability of ICA in attenuating the CI artifact while preserving the AEPs, i.e. the specificity, was evaluated using two approaches. One was a simulation study where NH datasets were initially contaminated with CI artifacts, and the other was the evaluation of VEPs from CI users. The simulation study revealed very high spatial correlations between original and recovered normal hearing AEPs. Moreover the differences between VEPs before and after ICA-based attenuation were also minimal. The combination of these two approaches provided strong evidence of high specificity. Furthermore the quality of the AEPs was evaluated with an SNR measure. It was found that AEPs from CI users were systematically correlated with age, demonstrating that individual differences were well preserved. CI users with large SNR AEPs were characterized by a significantly shorter duration of deafness. Overall the results confirm

that after ICA, good quality AEPs can be recovered, facilitating the objective, noninvasive study of auditory cortex function in CI users.

In *Study 3* an approach combining temporal and spatial properties of ICs was implemented, in order to find objectively those ICs representing the CI artifact. The algorithm, named CIAC, was validated using the EEG study set from *Study 2* and another independent study set. The validation procedure consisted of comparing the performance of the tool with the selections of two experienced raters. Results from this comparison revealed that CIAC has a good sensitivity and specificity. AEPs to environmental sounds reconstructed after automatic selection of ICs related to the CI artifact were compared with the AEPs evaluated in *Study 2*. A high correlation between age and N1-P2 peak-to-peak amplitudes was observed in the AEPs, replicating the findings from *Study 2*. Moreover when comparing AEPs from the two EEG study sets, the test-retest reliability for N1 amplitudes and latencies was significant. This suggested that CIAC based attenuation reliably preserves plausible individual response characteristics. Overall CIAC enabled the objective and efficient attenuation of the CI artifact in EEG recordings, as it provided a reasonable reconstruction of individual AEPs.

The combination of the two tools was shown to be successful at attenuating artifacts in EEG recordings. The reconstruction of AEPs was facilitated and the attenuation of artifacts was more objective, quicker, and systematic. CIAC in particular is a significant step towards the objective and efficient study of late AEPs. Therefore it is expected that it will support research investigating auditory cortex reorganization during CI adaptation and rehabilitation. In the case of CORRMAP, it is expected that its application will become very popular among EEG researchers in general, since it deals with common biological artifacts prominent in almost all research environments. In conclusion CORRMAP and CIAC open new doors in the use of EEG as a routine tool to assess auditory cortical function in CI users.

7.2. Towards automatic identification of artifacts in EEG using ICA

EEG recordings are contaminated by different types of biological and non-biological artifacts. ICA has been proven to be successful in attenuating several types of artifacts (e.g. Debener, et al., 2008a; Debener, et al., 2008b; Hoffmann & Falkenstein, 2008; Mennes, et al., 2010). The interest of using this technique to process multi-channel EEG data has increased in the last years as is shown by the increasing number of peer-reviewed publications where ICA was used (www.ncbi.nlm.nih.gov/pubmed). The ICA-based attenuation approach has the advantage of avoiding the rejection of trials contaminated

for instance with ocular artifacts. This can be of particular importance when recording sessions need to be short and the amount of EEG data collected is minimal, as for instance is the case when testing clinical populations or children. Furthermore ICA allows the disentanglement of time-locked artifacts from brain signals, as in the case of CI artifacts in AEPs and heartbeat artifacts in heartbeat evoked potentials (HEPs) (Terhaar, Viola, Baer, & Debener, under revision).

However the selection of artifact-related ICs is still challenging. The visual inspection is time-consuming, requires expertise and involves subjective decisions. In this work two new user-friendly tools, CORRMAP (cf. Chapter 4) and CIAC (cf. Chapter 6), were developed with the aim of overcoming the challenge of selecting ICs related to artifacts. An important goal was to develop robust tools where the number of input and user-defined parameters is minimal. This was achieved by tailoring each tool to a particular class of artifacts that has a specific signature. Other authors have developed methods to identify both biological and non-biological artifacts, which require the combination of multiple features (Mognon, et al., 2010; Nolan, et al., 2010). In this work another approach was taken. Thus CORRMAP was tailored to identify only ICs related to common biological artifacts, and CIAC only to ICs related to CI artifacts.

In *Study 1* the target was ICs representing eye blinks, lateral movements, and heartbeat artifacts. In this case it was possible to develop a method based on a single feature: the ICA inverse weights or IC scalp maps. In *Study 3* an approach similar to CORRMAP would have been insufficient, because the scalp maps of ICs related to the CI artifact differ between CI users. The differences are related not only to the side of implantation but also to the type of implant. Therefore in this case it was necessary to use a combination of temporal and spatial properties. CIAC requires a small number of inputs but operates in only three steps.

The validation procedures applied consisted of comparing the performance of the algorithms with the performance of researchers familiar with ICA. In the case of CORRMAP the validation procedure consisted of three EEG study sets, recorded with different montages in different laboratories. Moreover 11 raters familiar with ICA were requested to select manually the ICs related with the three target artifacts. Thus it was possible to compare both inter-rater-reliability and CORRMAP-rater overlap, which provided comprehensive validation results. It was found that CORRMAP is robust and performs equally well independently of the type of EEG montage.

To validate CIAC two EEG study sets were used. It is important to highlight that in this case it was not possible to use datasets recorded with different montages in different laboratories. This is due to the fact that few laboratories use multi-channel EEG to assess CI users. A similar limitation occurred when recruiting researchers familiar with inspecting ICA decompositions from CI users. Only two raters participated in the validation procedure, thus inter-rater-reliability was not assessed. The raters' selection was used as the "*gold standard*" when calculating the sensitivity and specificity of CIAC. The validation procedure also included the comparison of AEPs reconstructed after manual and automatic selection of ICs representing the CI artifact. In both cases correlation patterns between age and N1-P2 peak-to-peak amplitude were observed. Moreover since a subset of the datasets included in the two EEG study sets were collected for the same CI users, it was also possible to compare test-retest reliability of AEPs reconstructed after automatic selection of CI artifact-related ICs. The systematic pattern of individual differences in N1 amplitudes and latencies observed with different stimuli at different time points after implantation, strongly suggests that CIAC can overcome the electrical artifact problem. Nevertheless the generalization of CIAC as standard pre-processing tool awaits further validation. It is important to evaluate the tool using data collected with different EEG montages and with other types of auditory stimulation.

In summary CORRMAP and CIAC are objective, user-friendly tools that facilitate the use of an ICA-based approach to attenuate biological and CI artifacts, respectively. The performance of the tools was comparable to the performance of trained researchers. The fact that each tool was tailored to a particular class of artifacts has the advantage that the number of inputs and user-decisions is reduced. This allows the quick processing of multiple EEG datasets, since both tools run semi-automatically. CORRMAP and CIAC were developed as documented plug-ins for the EEGLAB toolbox (Delorme & Makeig, 2004) and are freely available online (www.debener.de). Both tools can also be used to teach new researchers how to evaluate ICA decompositions and can contribute to establish guidelines when attenuating artifacts in EEG recordings.

Nevertheless it is important to highlight that the success of both tools relies on the quality of the ICA decomposition. It is known that the degree of independence achieved may differ for different data sets and also for different ICA algorithms applied to the same dataset (Makeig & Onton, 2011). Infomax-based ICA provides a "complete" decomposition, i.e. data contributions from numbers of sources beyond the number of available data channels will be mixed into some or all of the resulting components. In practice even in good quality decompositions three main types of ICs can be found. One

type consists of ICs related to biological artifacts or other known artifacts. Another type consists of ICs related to brain sources. The third type consists of spatially irregular ICs of unknown origin ("noisy" ICs), whose signal strength is small and possibly represent mixtures of multiple source areas (Onton, et al., 2006).

It has been observed that scalp maps of ICs that tend to account for ERP features are nearly dipolar, whereas "noisy" ICs are typically non-dipolar and tend to contribute less to overall EEG dynamic changes time-locked to significant task events (Onton, et al., 2006). This is consistent with a working assumption that dipolar ICs are those generated in one (or two) patch(es) of cortex, whereas non-dipolar ICs, if not accounting for non-brain artifacts, may account for mixtures of small source processes or aspects of processes not fitting the spatial source stationarity assumption (Onton, et al., 2006).

There are several scenarios that may contribute to the violation of the ICA assumptions. The presence of bad channels in the data may increase the risk of nonstationary. The spatial stationarity would also be violated in the case of dislocation of electrodes. This may occur if the electrode cables are pulled or if participants move their heads abruptly during the recording. It is recommended that these portions of data should be pruned before using ICA (cf. Debener, et al., 2010).

The amount of data influences the quality of the ICA decomposition and guidelines have been described in the literature (Debener, et al., 2010; Makeig & Onton, 2011). It has also been suggested that high-pass filtering the data may improve the ICA decomposition. This procedure is going to eliminate drifts that may be caused for instance by sweating artifacts. These drifts are often spatially unstable and fluctuate substantially over time, contributing then with spatially nonstationary signals to the EEG (cf. Debener, et al., 2010).

In conclusion the success of ICA depends on several factors. It is important to keep in mind that this technique has limitations and relies on various assumptions. The quality of the recorded data, as well as the pre-processing, influences the quality of the decomposition. Nevertheless it is expected that new algorithms and better validation criteria will be developed. Although these advances are not yet available, ICA can be expected to continue providing a significant contribution to cognitive brain research (Debener, et al., 2010).

7.3. Investigation of auditory rehabilitation after cochlear implantation

Cochlear implants are regarded as one of the great achievements of modern medicine (Wilson & Dorman, 2008) with the number of implanted devices worldwide exceeding 220,000 units (Cosetti & Waltzman, 2011). The advances in CI technology have made it possible that many of these CI users recover a large range of auditory functions. There are reports of CI users able to have telephone conversations (eg., Debener, et al., 2008a; Migirov, Taitelbaum-Swead, Drendel, Hildesheimer, & Kronenberg, 2010; Oyanguren, Gomes, Tsuji, Bento, & Brito Neto, 2010) or to enjoy music (Migirov, et al., 2010). However the range of satisfaction and performance with the implant is broad. This variability in outcomes does not seem to be explained by CI technology alone. It is likely influenced by the degree of cortical adaptation to the electrical stimulation provided by the implant (Moore & Shannon, 2009; Wilson & Dorman, 2008a). Researchers have then become interested in using neurophysiological or functional imaging measurements to investigate auditory cortical function in CI users.

Several authors have used AEPs to investigate for instance neural correlates of speech perception in CI users (e.g. Henkin, et al., 2009; Kelly, et al., 2005). One advantage is that AEPs can be easily recorded both in clinical and in research settings. The combination of three electrodes - one active electrode placed in the vertex, plus the ground and the reference - is sufficient to measure N1 responses. On the other hand AEPs are corrupted by an electrical artifact caused by the CI device.

It is not yet established which method is the best to attenuate CI artifacts. The results from *Study 2* and *Study 3* favor the use of ICA. It was shown that it was possible to reconstruct AEPs with small residual CI artifact, providing evidence that ICA has high sensitivity. In *Study 2* a combination of simulated NH AEPs results and analysis of VEPs from CI users also provided indirect but strong evidence of ICA specificity, which further validates the application of this method in the context of CI artifact attenuation.

AEPs from CI users had a large variability in terms of component morphology, amplitude, and latency. CI users had smaller N1 amplitudes. Nevertheless individual features of the population such as aging effects that are evident in NH participants were preserved in the recovered AEPs in both studies. This result strongly suggests that the ICA-based CI artifact-attenuation procedure did not eliminate individual differences.

Moreover it was also observed that CI user AEPs can have N1 SNR values similar to NH AEPs. It was found that the CI users with larger SNR, that is, more robust N1 responses, had been deaf for significantly shorter periods. These results are in accordance with

previous studies which have shown evidence that the duration of deafness may be a key clinical parameter in auditory rehabilitation (Green, et al., 2005; Sandmann, et al., 2010; van Dijk, et al., 1999). Taken together, these findings may imply that the longer the auditory cortex was deprived of sensory input, the more difficult auditory rehabilitation with a CI becomes. However it is still not clear which parameters are the best predictors of outcome after implantation.

In summary it has been shown that good quality AEPs can be acquired, even when using complex sounds with long durations. This opens up the possibility of using stimuli with high frequency resolution, complexity, and ecological validity. Challenging aspects for CI users such as music or emotion perception, which require stimuli with longer durations, could then be investigated. Moreover high test-retest reliability was observed for both N1 peak amplitude and latency. These results suggest that by measuring standard AEP markers such as the N1 peak amplitude and latency, insights could be obtained about the rehabilitation state of the auditory system. It is then expected that EEG may become a routine tool to assess auditory cortical function in CI users, since the types of auditory stimuli, as well as the experimental design do not need to be strongly conditioned in order to minimize CI artifacts.

In order to better understand auditory rehabilitation after implantation, it seems important to investigate not only auditory cortical function, but also other sensory modalities, in particular vision. It is known that during sensory deprivation the auditory cortex undergoes plasticity, and can be recruited during the processing of visual stimuli (Finney, Clementz, Hickok, & Dobkins, 2003; Finney, Fine, & Dobkins, 2001). After implantation the deafened auditory cortex needs to adapt to the electrical stimulation provided by the CI, i.e. to undergo plasticity. PET studies have shown evidence of cross-modal reorganization in adult CI users, who recruited visual cortex when hearing words. The recruitment of visual cortex was positively correlated with speech perception measures and lip-reading scores (Giraud, et al., 2001a). Moreover it has been shown in a sample of children that cortical activity during rest measured with PET pre-implantation was correlated with performance in speech recognition tests: hypometabolism of the auditory cortex was predictive of better speech perception post-implantation (Lee, et al., 2007). VEP studies have also suggested that auditory cortex from CI users may be recruited during the processing of specific visual stimuli (Doucet, et al., 2006). Other authors have reported an association between VEP N1 responses and speech perception performance in individuals with pre-lingual onset, but not in individuals with a post-lingual onset, of severe to profound SNHL (Buckley & Tobey, 2010).

In *Study 2* CI users were stimulated using a semantic priming paradigm that included environmental sounds (primes) and pictures of natural scenes (targets). The participants were asked if the objects shown in the pictures were big or small. Sounds and pictures were arranged either as congruent or incongruent pairs. The hypothesis is that users that perform well with the CI would show a semantic priming effect, i.e. quicker and more accurate responses for targets preceded by a congruent sound. To best to my knowledge this is the first attempt to study AEPs and VEPs together in a sample of CI users. Preliminary results have shown that word recognition and environmental sound identification are correlated (Reed & Delhorne, 2005). However it is not yet well understood how CI users perceive environmental sounds (Reed & Delhorne, 2005). It is expected that this ongoing combined investigation of behavior results, AEPs, and VEPs may provide insights into auditory rehabilitation after implantation.

7.4. Outlook

In this section two main topics are discussed. The first is the implementation and validation of ICA-based tools to select objectively ICs. The second comprises future directions for AEP studies with CI samples.

The tools described in this work are in line with a broader field of research that has been moving towards the objective and automatic correction of artifacts in EEG recordings using ICA as the main pre-processing method (Mognon, et al., 2010; Nolan, et al., 2010). As the different tools are provided as open-source plugins to be used with the popular EEGLAB toolbox, researchers can contribute to its further development, validation and, ultimately, its clinical application. It would be interesting to compare the performance of the different tools, since the ones developed here were tailored to specific artifacts while others were designed with other goals. For instance, only one approach evaluated the correction of myogenic artifacts (Nolan, et al., 2010). The attenuation of this type of biological artifact is still particularly challenging. Although it has been reported that the ICA-based approach is successful in attenuating artifacts during walking and running (Gwin, et al., 2010), other authors have reported a much less complete separation between myogenic artifacts and brain-related activity (McMenamin, et al., 2010).

Due to the current popularity of ICA, it is expected that the number of researchers wanting to use these tools may increase. This may provide further validation, and consequently evidence of the advantages, and possible drawbacks of each method. It could also be the case that a combination of methods would be beneficial to better attenuate artifacts and this aspect should also be evaluated.

Guidelines based on the current ICA-based methods should be created, in order to assure standardized analyses across laboratories. This may contribute to the standardization of event-related EEG research in general, and in the attenuation of artifacts in particular. Nevertheless it is important to highlight that the application of ICA to EEG research is not limited to the attenuation of artifacts.

Several researchers have used ICA to separate the activities of individual brain sources that contribute to the scalp data (eg. Debener, et al., 2005a; Makeig, et al., 2004b; Makeig, et al., 2002). This line of research considers that the ERP responses are not invariant across trials and that trial-by-trial fluctuations should not be regarded as irrelevant background-noise (cf. Spencer, 2005). Indeed it has been shown that the single-trial variation of an ERP is a highly informative index of cortical activity (Debener, et al., 2006; Eichele, Juvodden, Ullsperger, & Eichele, 2010). Furthermore single-trial ERP information can be used to perform an EEG-informed fMRI analysis when data has been collected simultaneous. Thus brain regions whose hemodynamic activity is associated with the amplitude of certain ERPs can be identified (Debener, et al., 2006; Debener, et al., 2005b; Eichele, et al., 2005). The simultaneous recording of EEG and BOLD responses has been reviewed in the literature (Herrmann & Debener, 2008).

ICs related to different ERP components or different EEG phenomena have been selected based on the visual screening of the component properties. Similarly to the selection of ICs related to artifacts this procedure is prone to subjective decisions and is time-consuming. To facilitate IC clustering in this context a new tool - COMPASS - was developed. This tool receives as single input a time-range that is used to define a topographic map derived from the ERP. In the following steps clear-cut inferential statistics on both temporal and spatial information are used to identify ICs that significantly contribute to a certain ERP (Wessel & Ullsperger, 2011). It is expected that the tools to select ICs mentioned here may contribute to the achievement of higher-quality output in the EEG research field.

In the particular case of CORRMAP and CIAC, the number of reports describing their applicability to other EEG/ERP studies is still limited. Nevertheless in February 2011 CORRMAP became part of the official EEGLAB distribution. This may increase the popularity of this tool among other researchers. As of August 2011, the article describing CORRMAP has been cited 15 times. This is a strong indication that the tool may be already relevant to other EEG/ERP researchers. For instance CORRMAP was used to semi-automatically identify ocular artifact-related ICs in a study investigating pain

processing in depressed patients (Terhaar et al., 2011). It was also shown that CORRMAP can identify efficiently ICs representing heartbeat artifacts. The attenuation of this artifact made it possible to reconstruct HEP that provided an objective measurement of interoception in a sample of depressed patients (Terhaar, et al., under revision). Furthermore the use of CORRMAP has been recommended as a pre-processing step before using COMPASS (Wessel & Ullsperger, 2011). In the case of CIAC, it is envisioned that this tool may become also popular in the context of CI research using AEPs. New directions of research in this field are discussed below.

Several authors have emphasized that it is likely that the degree of auditory cortical rehabilitation plays an important role in explaining the variability of implantation outcomes observed (Moore & Shannon, 2009; Wilson & Dorman, 2008). This large variability is not well understood and makes the prediction of outcomes very difficult for clinicians (Peterson, et al., 2010). Moreover the candidacy criteria have also been expanded, and nowadays the samples of implanted individuals tend to be even more heterogeneous (Cosetti & Waltzman, 2011). Studies using imaging techniques, such as PET (e.g. Coez, et al., 2008; Lee, et al., 2007), and multi-channel EEG (e.g. Gilley, et al., 2008; Sandmann, et al., 2010), have contributed to the output of CI research. However most results are still preliminary, as the CI samples tested have been small and the findings await replication.

Current CI technology enables very satisfactory speech perception in quiet (Peterson, et al., 2010; Wilson & Dorman, 2008a; Zeng, et al., 2008). However there are still many challenges in daily life that could be aided by electrical hearing. Typical examples include: hearing in noise, music perception, talker identification, and emotion detection (Zeng, et al., 2008). It is important that new research studies will investigate other types of auditory stimulation than speech sounds.

Simulation studies with NH listeners can also provide important information about electrical hearing. Several authors have investigated the effects of perceptual learning using CI simulations (vocoder) of speech and environmental sounds (Loebach & Pisoni, 2008; Shafiro, 2008a, 2008b). Other authors have used this type of simulation to investigate voice-discrimination (Massida et al., 2011). It would be interesting to complement these behavioral findings with AEPs.

It is known that the auditory system experiences loss of acuity due to aging which may culminate in severe hearing impairment (Roth, et al., 2011). Changes in AEPs due to aging have also been characterized (Kerr, et al., 2011; Schiff, et al., 2008). In the last

years the cochlear implantation candidacy criteria have been broadened and patients with an age range between 70 and 90 years have been implanted (Carlson, et al., 2010; Williamson, et al., 2009). Several studies with elderly CI samples have reported significant hearing benefits after implantation reflected in an improvement in speech perception (Budenz et al., 2011; Carlson, et al., 2010; Haensel, Ilgner, Chen, Thuermer, & Westhofen, 2005; Migirov, et al., 2010; Oyanguren, et al., 2010; Williamson, et al., 2009). For some elderly CI users the benefit was so significant that they could even use the telephone (Migirov, et al., 2010; Oyanguren, et al., 2010). Moreover a study comparing outcomes for elderly (>65 years old) and younger (mean age = 37 years) CI users have found no differences in terms of speech perception (Haensel, et al., 2005). However other authors have suggested that the side of implantation may influence speech perception outcomes in elderly patients (Budenz, et al., 2011). AEPs studies may be relevant to better understand cortical plasticity in elderly individuals.

Another relevant topic is the comparison between unilateral and bilateral implantation outcomes. The number of bilateral implantations has increased, but benefits are not yet well understood. Behavior studies have shown evidence of improved speech perception in noise, as well as practical benefits in daily activities both for bilateral implanted children (Galvin, Mok, & Dowell, 2007) and adults (Laske et al., 2009). Another study has shown evidence that bilateral implanted children have better sound localization abilities (Murphy, Summerfield, O'Donoghue, & Moore, 2011). However is not easy to predict if a unilaterally-implanted CI user would benefit from a second CI (Galvin, et al., 2007). The number of imaging studies addressing this question is very limited (Green, Julyan, Hastings, & Ramsden, 2011). The influence of factors such as the delay between implantations (Laske, et al., 2009), or altered hemispheric asymmetries should be further investigated. It is also noteworthy that several studies have provided evidence that unilateral implantation is cost-effective (Bond et al., 2009; UK CI Study Group, 2004) but cost-effectiveness of bilateral implantation is still not yet confirmed (Bond, et al., 2009; Summerfield, Marshall, Barton, & Bloor, 2002).

EEG and AEPs studies can contribute to the investigation of these and other open questions. The use of multi-channel EEG recordings allows the computation of source localization methods, which complement the evidence provided by high time resolution (Debener, et al., 2008a; Gilley, et al., 2008). This can be an important alternative to high-spatial resolution techniques such as PET, which are invasive and involve higher costs. The development of objective methods that improve and facilitate the processing of multi-channel EEG data will likely contribute to an increase in the number and the

quality of AEP studies. It is envisioned that AEP research may play a relevant role in the future of CI research. In the long run AEPs may possibly contribute to the identification of candidates at risk of a suboptimal outcome, and to the planning of appropriate interventions in advance (Peterson, et al., 2010). Generally AEP studies will contribute to extend our basic knowledge of the auditory system and how it interacts with other sensory and cognitive systems (Peterson, et al., 2010).

It is my personal hope that the tools developed in this work will contribute to further improvements in the processing of multi-channel EEG data. The fact that CORRMAP has been incorporated in the official EEGLAB distribution is for me an important personal achievement. I believe that CIAC would be also successful and become popular in the context of CI research. It is also my personal view that: *"The success of these implants is due mainly to the cleverness of the brain, not the implant."* (Rosenzweig, et al., 2005, page 267). Therefore I hope that the development of CIAC may be a small contribution for other researchers wanting to use AEPs to investigate the plasticity of the auditory system.

References

Anemuller, J., Duann, J. R., Sejnowski, T. J., & Makeig, S. (2006). Spatio-temporal dynamics in fMRI recordings revealed with complex independent component analysis. *Neurocomputing, 69*(13-15), 1502-1512.

Bauer, P. W., Sharma, A., Martin, K., & Dorman, M. (2006). Central auditory development in children with bilateral cochlear implants. *Arch Otolaryngol Head Neck Surg, 132*(10), 1133-1136.

Bear, M. F., Connors, B. W., & Paradiso, M. A. (2007). *Neuroscience : exploring the brain* (3rd ed.). Philadelphia ; London: Lippincott Williams & Wilkins.

Bell, A. J., & Sejnowski, T. J. (1995). An information-maximization approach to blind separation and blind deconvolution. *Neural computation, 7*(6), 1129-1159.

Berg, P., & Scherg, M. (1991). Dipole models of eye movements and blinks. *Electroencephalography and clinical neurophysiology, 79*(1), 36-44.

Beynon, A. J., Snik, A. F., & van den Broek, P. (2002). Evaluation of cochlear implant benefit with auditory cortical evoked potentials. *International journal of audiology, 41*(7), 429-435.

Bond, M., Mealing, S., Anderson, R., Elston, J., Weiner, G., Taylor, R. S., Hoyle, M., Liu, Z., Price, A., & Stein, K. (2009). The effectiveness and cost-effectiveness of cochlear implants for severe to profound deafness in children and adults: a systematic review and economic model. *Health technology assessment, 13*(44), 1-330.

Brix, R., & Gedlicka, W. (1991). Late cortical auditory potentials evoked by electrostimulation in deaf and cochlear implant patients. *European archives of oto-rhino-laryngology : official journal of the European Federation of Oto-Rhino-Laryngological Societies, 248*(8), 442-444.

Buckley, K. A., & Tobey, E. A. (2010). Cross-Modal Plasticity and Speech Perception in Pre- and Postlingually Deaf Cochlear Implant Users. *Ear Hear*.

Budenz, C. L., Cosetti, M. K., Coelho, D. H., Birenbaum, B., Babb, J., Waltzman, S. B., & Roehm, P. C. (2011). The effects of cochlear implantation on speech perception in older adults. *Journal of the American Geriatrics Society, 59*(3), 446-453.

Burkard, R. F., Eggermont, J. J., & Don, M. (2007). *Auditory evoked potentials : basic principles and clinical application*. Philadelphia, Pa.: London : Lippincott Williams & Wilkins.

Cardoso, J.-F., & Souloumiac, A. (1994). Blind beamforming for non-gaussian signals. . *IEE Proc. F*(140), 362-370.

Carlson, M. L., Breen, J. T., Gifford, R. H., Driscoll, C. L., Neff, B. A., Beatty, C. W., Peterson, A. M., & Olund, A. P. (2010). Cochlear implantation in the octogenarian and nonagenarian. *Otology & neurotology : official publication of the American Otological Society, American Neurotology Society [and] European Academy of Otology and Neurotology, 31*(8), 1343-1349.

Champoux, F., Lepore, F., Gagne, J. P., & Theoret, H. (2009). Visual stimuli can impair auditory processing in cochlear implant users. *Neuropsychologia, 47*(1), 17-22.

Chatelin, V., Kim, E. J., Driscoll, C., Larky, J., Polite, C., Price, L., & Lalwani, A. K. (2004). Cochlear implant outcomes in the elderly. *Otol Neurotol, 25*(3), 298-301.

Chawla, M. P., Verma, H. K., & Kumar, V. (2008). Artifacts and noise removal in electrocardiograms using independent component analysis. *International journal of cardiology, 129*(2), 278-281.

Coez, A., Zilbovicius, M., Ferrary, E., Bouccara, D., Mosnier, I., Ambert-Dahan, E., Bizaguet, E., Syrota, A., Samson, Y., & Sterkers, O. (2008). Cochlear implant benefits in deafness rehabilitation: PET study of temporal voice activations. *J Nucl Med, 49*(1), 60-67.

Cohen, J. (1988). *Statistical power analysis for the behavioral sciences* (2nd ed. Vol. Hillsdale). NJ: Lawrence Earlbaum Associates.

Comon, P. (1994). Independent component analysis: A new concept? *Signal Processing, 36*(3), 287-341.

Comon, P., & Jutten, C. (2010). *Handbook of blind source separation : independent component analysis and applications*. Amsterdam; London; Oxford: Elsevier;Academic Press.

Cone-Wesson, B., & Wunderlich, J. (2003). Auditory evoked potentials from the cortex: audiology applications. *Curr Opin Otolaryngol Head Neck Surg, 11*(5), 372-377.

Cosetti, M., & Roland, J. T., Jr. (2010). Cochlear implantation in the very young child: issues unique to the under-1 population. *Trends in amplification, 14*(1), 46-57.

Cosetti, M. K., & Waltzman, S. B. (2011). Cochlear implants: current status and future potential. *Expert review of medical devices, 8*(3), 389-401.

Cox, R. M., & Alexander, G. C. (1995). The abbreviated profile of hearing aid benefit. *Ear and hearing, 16*(2), 176-186.

Crane, B. T., Gottschalk, B., Kraut, M., Aygun, N., & Niparko, J. K. (2010). Magnetic resonance imaging at 1.5 T after cochlear implantation. *Otology & neurotology : official publication of the American Otological Society, American Neurotology Society [and] European Academy of Otology and Neurotology, 31*(8), 1215-1220.

Croft, R. J., & Barry, R. J. (2000). EOG correction: which regression should we use? *Psychophysiology, 37*(1), 123-125.

Davis, P. A. (1939). Effects of acoustic stimuli on the waking human brain. *Neurophysiology, 2*, 494-499.

Debener, S., Hine, J., Bleeck, S., & Eyles, J. (2008a). Source localization of auditory evoked potentials after cochlear implantation. *Psychophysiology, 45*(1), 20-24.

Debener, S., Makeig, S., Delorme, A., & Engel, A. K. (2005a). What is novel in the novelty oddball paradigm? Functional significance of the novelty P3 event-related potential as revealed by independent component analysis. *Brain Res Cogn Brain Res, 22*(3), 309-321.

Debener, S., Mullinger, K. J., Niazy, R. K., & Bowtell, R. W. (2008b). Properties of the ballistocardiogram artefact as revealed by EEG recordings at 1.5, 3 and 7 T static magnetic field strength. *Int J Psychophysiol, 67*(3), 189-199.

Debener, S., Strobel, A., Sorger, B., Peters, J., Kranczioch, C., Engel, A. K., & Goebel, R. (2007). Improved quality of auditory event-related potentials recorded simultaneously with 3-T fMRI: removal of the ballistocardiogram artefact. *Neuroimage, 34*(2), 587-597.

Debener, S., Thorne, J., Schneider, T. R., & Viola, F. C. (2010). Using ICA for the Analysis of Multi-Channel EEG Data. In M. Ullsperger & S. Debener (Eds.), *Simultaneous EEG and fMRI* (pp. 121-135). New York: Oxford University Press.

Debener, S., Ullsperger, M., Siegel, M., & Engel, A. K. (2006). Single-trial EEG-fMRI reveals the dynamics of cognitive function. *Trends in Cognitive Sciences, 10*(12), 558-563.

Debener, S., Ullsperger, M., Siegel, M., Fiehler, K., von Cramon, D. Y., & Engel, A. K. (2005b). Trial-by-trial coupling of concurrent electroencephalogram and functional magnetic resonance imaging identifies the dynamics of performance monitoring. *Journal of Neuroscience, 25*(50), 11730-11737.

Delorme, A., & Makeig, S. (2004). EEGLAB: an open source toolbox for analysis of single-trial EEG dynamics including independent component analysis. *Journal of Neuroscience Methods, 134*(1), 9-21.

Delorme, A., Sejnowski, T., & Makeig, S. (2007a). Enhanced detection of artifacts in EEG data using higher-order statistics and independent component analysis. *NeuroImage, 34*(4), 1443-1449.

Delorme, A., Westerfield, M., & Makeig, S. (2007b). Medial prefrontal theta bursts precede rapid motor responses during visual selective attention. *Journal of Neuroscience, 27*(44), 11949-11959.

DiPietroPaolo, D., Muller, H. P., Nolte, G., & Erne, S. N. (2006). Noise reduction in magnetocardiography by singular value decomposition and independent component analysis. *Medical & biological engineering & computing, 44*(6), 489-499.

Donaldson, G. S., Chisolm, T. H., Blasco, G. P., Shinnick, L. J., Ketter, K. J., & Krause, J. C. (2009). BKB-SIN and ANL predict perceived communication ability in cochlear implant users. *Ear & Hearing, 30*(4), 401-410.

Dorman, M. F., & Wilson, B. S. (2004). The design and function of cochlear implants. *American Scientist, 92*, 436-445.

Doucet, M. E., Bergeron, F., Lassonde, M., Ferron, P., & Lepore, F. (2006). Cross-modal reorganization and speech perception in cochlear implant users. *Brain, 129*(Pt 12), 3376-3383.

Eichele, H., Juvodden, H. T., Ullsperger, M., & Eichele, T. (2010). Mal-adaptation of event-related EEG responses preceding performance errors. *Frontiers in human neuroscience, 4*.

Eichele, T., Specht, K., Moosmann, M., Jongsma, M. L., Quiroga, R. Q., Nordby, H., & Hugdahl, K. (2005). Assessing the spatiotemporal evolution of neuronal activation with single-trial event-related potentials and functional MRI. *Proceedings of the National Academy of Sciences of the United States of America, 102*(49), 17798-17803.

Escudero, J., Hornero, R., Abasolo, D., Fernandez, A., & Lopez-Coronado, M. (2007). Artifact removal in magnetoencephalogram background activity with independent component analysis. *IEEE transactions on bio-medical engineering, 54*(11), 1965-1973.

Fallon, J. B., Irvine, D. R., & Shepherd, R. K. (2008). Cochlear implants and brain plasticity. *Hearing Research, 238*(1-2), 110-117.

Feige, B., Scheffler, K., Esposito, F., Di Salle, F., Hennig, J., & Seifritz, E. (2005). Cortical and subcortical correlates of electroencephalographic alpha rhythm modulation. *Journal of Neurophysiology, 93*(5), 2864-2872.

Finney, E. M., Clementz, B. A., Hickok, G., & Dobkins, K. R. (2003). Visual stimuli activate auditory cortex in deaf subjects: evidence from MEG. *Neuroreport, 14*(11), 1425-1427.

Finney, E. M., Fine, I., & Dobkins, K. R. (2001). Visual stimuli activate auditory cortex in the deaf. *Nature Neuroscience, 4*(12), 1171-1173.

Friesen, L. M., & Picton, T. W. (2010). A method for removing cochlear implant artifact. *Hearing Research, 259*(1-2), 95-106.

Galvin, K. L., Mok, M., & Dowell, R. C. (2007). Perceptual benefit and functional outcomes for children using sequential bilateral cochlear implants. *Ear & Hearing, 28*(4), 470-482.

Garrido, M. I., Kilner, J. M., Stephan, K. E., & Friston, K. J. (2009). The mismatch negativity: a review of underlying mechanisms. *Clinical Neurophysiology, 120*(3), 453-463.

Gifford, R. H., Shallop, J. K., & Peterson, A. M. (2008). Speech recognition materials and ceiling effects: considerations for cochlear implant programs. *Audiology & Neurootology, 13*(3), 193-205.

Gilley, P. M., Sharma, A., Dorman, M., Finley, C. C., Panch, A. S., & Martin, K. (2006). Minimization of cochlear implant stimulus artifact in cortical auditory evoked potentials. *Clinical Neurophysiology, 117*(8), 1772-1782.

Gilley, P. M., Sharma, A., & Dorman, M. F. (2008). Cortical reorganization in children with cochlear implants. *Brain Research, 1239*, 56-65.

Giraud, A. L., & Lee, H. J. (2007). Predicting cochlear implant outcome from brain organisation in the deaf. *Restorative Neurololgy and Neuroscience, 25*(3-4), 381-390.

Giraud, A. L., Price, C. J., Graham, J. M., Truy, E., & Frackowiak, R. S. (2001a). Cross-modal plasticity underpins language recovery after cochlear implantation. *Neuron, 30*(3), 657-663.

Giraud, A. L., & Truy, E. (2002). The contribution of visual areas to speech comprehension: a PET study in cochlear implants patients and normal-hearing subjects. *Neuropsychologia, 40*(9), 1562-1569.

Giraud, A. L., Truy, E., & Frackowiak, R. (2001b). Imaging plasticity in cochlear implant patients. *Audiology & Neurootology, 6*(6), 381-393.

Gramann, K., Onton, J., Riccobon, D., Mueller, H. J., Bardins, S., & Makeig, S. (2010). Human brain dynamics accompanying use of egocentric and allocentric reference frames during navigation. *Journal of Cognitive Neuroscience, 22*(12), 2836-2849.

Green, K. M., Julyan, P. J., Hastings, D. L., & Ramsden, R. T. (2005). Auditory cortical activation and speech perception in cochlear implant users: effects of implant experience and duration of deafness. *Hearing Research, 205*(1-2), 184-192.

Green, K. M., Julyan, P. J., Hastings, D. L., & Ramsden, R. T. (2008). Auditory cortical activation and speech perception in cochlear implant users. *Journal of Laryngology & Otology, 122*(3), 238-245.

Green, K. M., Julyan, P. J., Hastings, D. L., & Ramsden, R. T. (2011). Cortical activations in sequential bilateral cochlear implant users. *Cochlear implants international, 12*(1), 3-9.

Groppe, D. M., Makeig, S., & Kutas, M. (2009). Identifying reliable independent components via split-half comparisons. *NeuroImage, 45*(4), 1199-1211.

Guiraud, J., Besle, J., Arnold, L., Boyle, P., Giard, M. H., Bertrand, O., Norena, A., Truy, E., & Collet, L. (2007). Evidence of a tonotopic organization of the auditory cortex in cochlear implant users. *Journal of Neuroscience, 27*(29), 7838-7846.

Gwin, J. T., Gramann, K., Makeig, S., & Ferris, D. P. (2010). Removal of movement artifact from high-density EEG recorded during walking and running. *Journal of Neurophysiology, 103*(6), 3526-3534.

Haensel, J., Ilgner, J., Chen, Y. S., Thuermer, C., & Westhofen, M. (2005). Speech perception in elderly patients following cochlear implantation. *Acta oto-laryngologica, 125*(12), 1272-1276.

Handy, T. C. (2005). *Event-related potentials : a methods handbook*. Cambridge, Mass.: MIT Press.

Hari, R., Pelizzone, M., Makela, J. P., Hallstrom, J., Huttunen, J., & Knuutila, J. (1988). Neuromagnetic responses from a deaf subject to stimuli presented through a multichannel cochlear prosthesis. *Ear & Hearing, 9*(3), 148-152.

Heller, J. W., Brackmann, D. E., Tucci, D. L., Nyenhuis, J. A., & Chou, C. K. (1996). Evaluation of MRI compatibility of the modified nucleus multichannel auditory brainstem and cochlear implants. *The American Journal of Otology, 17*(5), 724-729.

Henkin, Y., Kileny, P. R., Hildesheimer, M., & Kishon-Rabin, L. (2008). Phonetic processing in children with cochlear implants: an auditory event-related potentials study. *Ear & Hearing, 29*(2), 239-249.

Henkin, Y., Kishon-Rabin, L., Tatin-Schneider, S., Urbach, D., Hildesheimer, M., & Kileny, P. R. (2004). Low-resolution electromagnetic tomography (LORETA) in children with cochlear implants: a preliminary report. *International Journal of Audiology, 43 Suppl 1*, S48-51.

Henkin, Y., Tetin-Schneider, S., Hildesheimer, M., & Kishon-Rabin, L. (2009). Cortical neural activity underlying speech perception in postlingual adult cochlear implant recipients. *Audiology & Neurootology, 14*(1), 39-53.

Herrmann, C. S., & Debener, S. (2008). Simultaneous recording of EEG and BOLD responses: a historical perspective. *International Journal of Psychophysiology, 67*(3), 161-168.

Himberg, J., Hyvarinen, A., & Esposito, F. (2004). Validating the independent components of neuroimaging time series via clustering and visualization. *NeuroImage, 22*(3), 1214-1222.

Hine, J., & Debener, S. (2007). Late auditory evoked potentials asymmetry revisited. *Clinical Neurophysiology, 118*(6), 1274-1285.

Hine, J., Thornton, R., Davis, A., & Debener, S. (2008). Does long-term unilateral deafness change auditory evoked potential asymmetries? *Clinical Neurophysiology, 119*(3), 576-586.

Hochmair, E. S. (2001). MRI safety of Med-El C40/C40+ cochlear implants. *Cochlear implants international, 2*(2), 98-114.

Hoffmann, S., & Falkenstein, M. (2008). The correction of eye blink artefacts in the EEG: a comparison of two prominent methods. *Public Library of Science One, 3*(8), e3004.

Hoke, M., Pantev, C., Lutkenhoner, B., Lehnertz, K., & Surth, W. (1989). Magnetic fields from the auditory cortex of a deaf human individual occurring spontaneously or evoked by stimulation through a cochlear prosthesis. *Audiology 28*(3), 152-170.

Hood, L. J., Berlin, C. I., & Allen, P. (1994). Cortical deafness: a longitudinal study. *Journal of the American Academy of Audiology, 5*(5), 330-342.

Hoth, S. (1998). [Measuring late electrically evoked potentials of the auditory system in cochlear implant patients]. *HNO, 46*(8), 739-747.

Humes, L. E., Kewley-Port, D., Fogerty, D., & Kinney, D. (2010). Measures of hearing threshold and temporal processing across the adult lifespan. *Hearing Research, 264*(1-2), 30-40.

Hyde, M. (1997). The N1 response and its applications. *Audiology & Neurootology, 2*(5), 281-307.

Hyvärinen, A., Karhunen, J., & Oja, E. (2001). *Independent component analysis*. New York ; Chichester: Wiley.

Hyvarinen, A., & Oja, E. (2000). Independent component analysis: algorithms and applications. *Neural networks, 13*(4-5), 411-430.

Ito, K., Momose, T., Oku, S., Ishimoto, S., Yamasoba, T., Sugasawa, M., & Kaga, K. (2004). Cortical activation shortly after cochlear implantation. *Audiology & Neurootology, 9*(5), 282-293.

James, C. J., & Demanuele, C. (2010). Space-time independent component analysis: the definitive BSS technique to use in biomedical signal processing? *Conference proceedings : Annual International Conference of the IEEE Engineering in Medicine and Biology Society, 2010*, 1898-1901.

Jezzard, P., Matthews, P. M., & Smith, S. M. (2001). *Functional MRI : an introduction to methods*. New York: Oxford University Press.

Joyce, C. A., Gorodnitsky, I. F., & Kutas, M. (2004). Automatic removal of eye movement and blink artifacts from EEG data using blind component separation. *Psychophysiology, 41*(2), 313-325.

Jung, T. P., Makeig, S., Humphries, C., Lee, T. W., McKeown, M. J., Iragui, V., & Sejnowski, T. J. (2000a). Removing electroencephalographic artifacts by blind source separation. *Psychophysiology, 37*(2), 163-178.

Jung, T. P., Makeig, S., Westerfield, M., Townsend, J., Courchesne, E., & Sejnowski, T. J. (2000b). Removal of eye activity artifacts from visual event-related potentials in normal and clinical subjects. *Clinical Neurophysiology, 111*(10), 1745-1758.

Jung, T. P., Makeig, S., Westerfield, M., Townsend, J., Courchesne, E., & Sejnowski, T. J. (2001). Analysis and visualization of single-trial event-related potentials. *Human brain mapping, 14*(3), 166-185.

Kaga, K., Nakamura, M., Takayama, Y., & Momose, H. (2004). A case of cortical deafness and anarthria. *Acta oto-laryngologica, 124*(2), 202-205.

Kappenman, E. S., & Luck, S. J. (2010). The effects of electrode impedance on data quality and statistical significance in ERP recordings. *Psychophysiology, 47*(5), 888-904.

Kelley, M. W. (2006). Regulation of cell fate in the sensory epithelia of the inner ear. *Nature reviews. Neuroscience, 7*(11), 837-849.

Kelly, A. S., Purdy, S. C., & Thorne, P. R. (2005). Electrophysiological and speech perception measures of auditory processing in experienced adult cochlear implant users. *Clinical Neurophysiology, 116*(6), 1235-1246.

Kerr, C. C., Rennie, C. J., & Robinson, P. A. (2011). Model-based analysis and quantification of age trends in auditory evoked potentials. *Clinical Neurophysiology 122*(1), 134-147.

Kileny, P. R. (2007). Evoked potentials in the management of patients with cochlear implants: research and clinical applications. *Ear & Hearing, 28*(2 Suppl), 124S-127S.

Kileny, P. R., Boerst, A., & Zwolan, T. (1997). Cognitive evoked potentials to speech and tonal stimuli in children with implants. *Otolaryngology-head and neck surgery, 117*(3 Pt 1), 161-169.

Koelsch, S., Wittfoth, M., Wolf, A., Muller, J., & Hahne, A. (2004). Music perception in cochlear implant users: an event-related potential study. *Clinical Neurophysiology, 115*(4), 966-972.

Kotchoubey, B. (2006). Event-related potentials, cognition, and behavior: a biological approach. *Neuroscience & Biobehavioral Reviews, 30*(1), 42-65.

Kraus, N., Micco, A. G., Koch, D. B., McGee, T., Carrell, T., Sharma, A., Wiet, R. J., & Weingarten, C. Z. (1993). The mismatch negativity cortical evoked potential elicited by speech in cochlear-implant users. *Hearing Research, 65*(1-2), 118-124.

Kubo, T., Yamamoto, K., Iwaki, T., Matsukawa, M., Doi, K., & Tamura, M. (2001). Significance of auditory evoked responses (EABR and P300) in cochlear implant subjects. *Acta oto-laryngologica, 121*(2), 257-261.

Laske, R. D., Veraguth, D., Dillier, N., Binkert, A., Holzmann, D., & Huber, A. M. (2009). Subjective and objective results after bilateral cochlear implantation in adults. *Otology & neurotology : official publication of the American Otological Society, American Neurotology Society [and] European Academy of Otology and Neurotology, 30*(3), 313-318.

Lazard, D. S., Giraud, A. L., Truy, E., & Lee, H. J. (2011). Evolution of non-speech sound memory in postlingual deafness: implications for cochlear implant rehabilitation. *Neuropsychologia, 49*(9), 2475-2482.

Lazeyras, F., Boex, C., Sigrist, A., Seghier, M. L., Cosendai, G., Terrier, F., & Pelizzone, M. (2002). Functional MRI of auditory cortex activated by multisite electrical stimulation of the cochlea. *NeuroImage, 17*(2), 1010-1017.

Lee, D. S., Lee, J. S., Oh, S. H., Kim, S. K., Kim, J. W., Chung, J. K., Lee, M. C., & Kim, C. S. (2001). Cross-modal plasticity and cochlear implants. *Nature, 409*(6817), 149-150.

Lee, H. J., Giraud, A. L., Kang, E., Oh, S. H., Kang, H., Kim, C. S., & Lee, D. S. (2007). Cortical activity at rest predicts cochlear implantation outcome. *Cerebral Cortex, 17*(4), 909-917.

Lee, T. W., Girolami, M., & Sejnowski, T. J. (1999). Independent component analysis using an extended infomax algorithm for mixed subgaussian and supergaussian sources. *Neural computation, 11*(2), 417-441.

Loebach, J. L., & Pisoni, D. B. (2008). Perceptual learning of spectrally degraded speech and environmental sounds. *Journal of the Acoustical Society of America, 123*(2), 1126-1139.

Lonka, E., Kujala, T., Lehtokoski, A., Johansson, R., Rimmanen, S., Alho, K., & Naatanen, R. (2004). Mismatch negativity brain response as an index of speech perception recovery in cochlear-implant recipients. *Audiology & Neurootology, 9*(3), 160-162.

Lopes da Silva, F. H. (2010). EEG: Origin and Measurement. In C. Mulert & L. Lemieux (Eds.), *EEG-fMRI : physiological basis, technique, and applications* (pp. 19 - 38). Heidelberg: Springer.

Lorente de No, R. (1947). Action potential of the motoneurons of the hypoglossus nucleus. *Journal of cellular physiology, 29*(3), 207-287.

Luck, S. J. (2005). *An introduction to the event-related potential technique*. Cambridge, Ma. ; London: MIT Press.

Majdani, O., Rau, T. S., Gotz, F., Zimmerling, M., Lenarz, M., Lenarz, T., Labadie, R., & Leinung, M. (2009). Artifacts caused by cochlear implants with non-removable magnets in 3T MRI: phantom and cadaveric studies. *European Archives of Oto-Rhino-Laryngology*.

Makeig, S., Debener, S., Onton, J., & Delorme, A. (2004a). Mining event-related brain dynamics. *Trends in Cognitive Sciences, 8*(5), 204-210.

Makeig, S., Delorme, A., Westerfield, M., Jung, T. P., Townsend, J., Courchesne, E., & Sejnowski, T. J. (2004b). Electroencephalographic brain dynamics following manually responded visual targets. *Public Library of Science Biology, 2*(6), e176.

Makeig, S., Jung, T. P., Bell, A. J., Ghahremani, D., & Sejnowski, T. J. (1997). Blind separation of auditory event-related brain responses into independent components. *Proceedings of the National Academy of Sciences of the United States of America, 94*(20), 10979-10984.

Makeig, S., & Onton, J. (2011). ERP Features and EEG Dynamics: An ICA Perspective. In S. J. Luck & E. S. Kappenman (Eds.), *Oxford Handbook of Event-Related Potential Components* (pp. [Epub ahead of print]). New York: Oxford University Press.

Makeig, S., Westerfield, M., Jung, T. P., Covington, J., Townsend, J., Sejnowski, T. J., & Courchesne, E. (1999). Functionally independent components of the late positive event-related potential during visual spatial attention. *Journal of Neuroscience, 19*(7), 2665-2680.

Makeig, S., Westerfield, M., Jung, T. P., Enghoff, S., Townsend, J., Courchesne, E., & Sejnowski, T. J. (2002). Dynamic brain sources of visual evoked responses. *Science, 295*(5555), 690-694.

Makhdoum, M. J., Groenen, P. A., Snik, A. F., & van den Broek, P. (1998). Intra- and interindividual correlations between auditory evoked potentials and speech perception in cochlear implant users. *Scandinavian Audiology, 27*(1), 13-20.

Mantini, D., Franciotti, R., Romani, G. L., & Pizzella, V. (2008). Improving MEG source localizations: an automated method for complete artifact removal based on independent component analysis. *NeuroImage, 40*(1), 160-173.

Martin, B. A. (2007). Can the acoustic change complex be recorded in an individual with a cochlear implant? Separating neural responses from cochlear implant artifact. *Journal of the American Academy of Audiology, 18*(2), 126-140.

Martin, B. A., Tremblay, K. L., & Korczak, P. (2008). Speech evoked potentials: from the laboratory to the clinic. *Ear & Hearing, 29*(3), 285-313.

Massida, Z., Belin, P., James, C., Rouger, J., Fraysse, B., Barone, P., & Deguine, O. (2011). Voice discrimination in cochlear-implanted deaf subjects. *Hearing Research, 275*(1-2), 120-129.

May, P. J., & Tiitinen, H. (2010). Mismatch negativity (MMN), the deviance-elicited auditory deflection, explained. *Psychophysiology, 47*(1), 66-122.

McKeown, M. J., Jung, T. P., Makeig, S., Brown, G., Kindermann, S. S., Lee, T. W., & Sejnowski, T. J. (1998a). Spatially independent activity patterns in functional

MRI data during the stroop color-naming task. *Proceedings of the National Academy of Sciences of the United States of America, 95*(3), 803-810.

McKeown, M. J., Makeig, S., Brown, G. G., Jung, T. P., Kindermann, S. S., Bell, A. J., & Sejnowski, T. J. (1998b). Analysis of fMRI data by blind separation into independent spatial components. *Human brain mapping, 6*(3), 160-188.

McMenamin, B. W., Shackman, A. J., Greischar, L. L., & Davidson, R. J. (2010). Electromyogenic Artifacts and Electroencephalographic Inferences Revisited. *NeuroImage, 54*, 4-9.

McNeill, C., Sharma, M., & Purdy, S. C. (2009). Are cortical auditory evoked potentials useful in the clinical assessment of adults with cochlear implants? *Cochlear Implants International, 10*, 78-84.

Mennes, M., Wouters, H., Vanrumste, B., Lagae, L., & Stiers, P. (2010). Validation of ICA as a tool to remove eye movement artifacts from EEG/ERP. *Psychophysiology, 47*(6), 1142-1150.

Migirov, L., Taitelbaum-Swead, R., Drendel, M., Hildesheimer, M., & Kronenberg, J. (2010). Cochlear implantation in elderly patients: surgical and audiological outcome. *Gerontology, 56*(2), 123-128.

Mognon, A., Jovicich, J., Bruzzone, L., & Buiatti, M. (2010). ADJUST: An automatic EEG artifact detector based on the joint use of spatial and temporal features. *Psychophysiology*.

Moore, D. R., & Shannon, R. V. (2009). Beyond cochlear implants: awakening the deafened brain. *Nature Neuroscience, 12*(6), 686-691.

Most, T., Shrem, H., & Duvdevani, I. (2010). Cochlear implantation in late-implanted adults with prelingual deafness. *American journal of otolaryngology, 31*(6), 418-423.

Muller, H. P., Nolte, G., Paolo, D. D., & Erne, S. N. (2006). Using independent component analysis for noise reduction of magnetocardiographic data in case of exercise with an ergometer. *Journal of medical engineering & technology, 30*(3), 158-165.

Murphy, J., Summerfield, A. Q., O'Donoghue, G. M., & Moore, D. R. (2011). Spatial hearing of normally hearing and cochlear implanted children. *International journal of pediatric otorhinolaryngology, 75*(4), 489-494.

Naatanen, R., Gaillard, A. W., & Mantysalo, S. (1978). Early selective-attention effect on evoked potential reinterpreted. *Acta psychologica, 42*(4), 313-329.

Naatanen, R., & Picton, T. (1987). The N1 wave of the human electric and magnetic response to sound: a review and an analysis of the component structure. *Psychophysiology, 24*(4), 375-425.

Nolan, H., Whelan, R., & Reilly, R. B. (2010). FASTER: Fully Automated Statistical Thresholding for EEG artifact Rejection. *Journal of Neuroscience Methods, 192*(1), 152-162.

Onton, J., Delorme, A., & Makeig, S. (2005). Frontal midline EEG dynamics during working memory. *NeuroImage, 27*(2), 341-356.

Onton, J., & Makeig, S. (2009). High-frequency Broadband Modulations of Electroencephalographic Spectra. *Frontiers in Human Neuroscience, 3*, 61.

Onton, J., Westerfield, M., Townsend, J., & Makeig, S. (2006). Imaging human EEG dynamics using independent component analysis. *Neuroscience and Biobehavioral Reviews, 30*(6), 808-822.

Oostenveld, R., & Oostendorp, T. F. (2002). Validating the boundary element method for forward and inverse EEG computations in the presence of a hole in the skull. *Human brain mapping, 17*(3), 179-192.

Otten, L. J., & Rugg, M. D. (2005). Interpreting Event-Related Brain Potentials. In T. C. Handy (Ed.), *Event-related potentials : a methods handbook* (pp. 3-16). Cambridge, Mass.: MIT Press.

Oyanguren, V., Gomes, M. V., Tsuji, R. K., Bento, R. F., & Brito Neto, R. (2010). Auditory results from cochlear implants in elderly people. *Brazilian journal of otorhinolaryngology, 76*(4), 450-453.

Pantev, C., Dinnesen, A., Ross, B., Wollbrink, A., & Knief, A. (2006). Dynamics of auditory plasticity after cochlear implantation: a longitudinal study. *Cerebral Cortex, 16*(1), 31-36.

Peterson, N. R., Pisoni, D. B., & Miyamoto, R. T. (2010). Cochlear implants and spoken language processing abilities: review and assessment of the literature. *Restorative Neurology and Neuroscience, 28*(2), 237-250.

Phelps, M. E. (2006). *PET : physics, instrumentation, and scanners*. New York: Springer.

Picton, T. W., Bentin, S., Berg, P., Donchin, E., Hillyard, S. A., Johnson, R., Jr., Miller, G. A., Ritter, W., Ruchkin, D. S., Rugg, M. D., & Taylor, M. J. (2000). Guidelines for using human event-related potentials to study cognition: recording standards and publication criteria. *Psychophysiology, 37*(2), 127-152.

Picton, T. W., Lins, O. G., & Scherg, M. (1995). The recording and analysis of event-related potentials. In F. Boller & J. Grafman (Eds.), *Handbook of neuropsychology* (Vol. 10, pp. 3-73). Amsterdam ; New York: Elsevier.

Polich, J. (2007). Updating P300: an integrative theory of P3a and P3b. *Clinical Neurophysiology 118*(10), 2128-2148.

Reed, C. M., & Delhorne, L. A. (2005). Reception of environmental sounds through cochlear implants. *Ear & Hearing, 26*(1), 48-61.

Rosenthal, R. (1991). *Meta-analytic procedures for social research* (Vol. Newbury Park). CA: Sage.

Rosenzweig, M. R., Breedlove, S. M., Leiman, A. L., & Watson, N. V. (2005). *Biological psychology : an introduction to behavioral, cognitive, and clinical neuroscience* (4th ed.). Sunderland, Mass.: Sinauer.

Roth, T. N., Hanebuth, D., & Probst, R. (2011). Prevalence of age-related hearing loss in Europe: a review. *European Archives of Oto-Rhino-Laryngology*

Rouger, J., Lagleyre, S., Demonet, J. F., Fraysse, B., Deguine, O., & Barone, P. (2011). Evolution of crossmodal reorganization of the voice area in cochlear-implanted deaf patients. *Human brain mapping*.

Rouger, J., Lagleyre, S., Fraysse, B., Deneve, S., Deguine, O., & Barone, P. (2007). Evidence that cochlear-implanted deaf patients are better multisensory integrators. *Proceedings of the National Academy of Sciences of the United States of America, 104*(17), 7295-7300.

Rubinstein, J. T. (2004). How cochlear implants encode speech. *Current opinion in otolaryngology & head and neck surgery, 12*(5), 444-448.

Sandmann, P., Eichele, T., Buechler, M., Debener, S., Jancke, L., Dillier, N., Hugdahl, K., & Meyer, M. (2009). Evaluation of evoked potentials to dyadic tones after cochlear implantation. *Brain, 132*(Pt 7), 1967-1979.

Sandmann, P., Kegel, A., Eichele, T., Dillier, N., Lai, W., Bendixen, A., Debener, S., Jancke, L., & Meyer, M. (2010). Neurophysiological evidence of impaired musical sound perception in cochlear-implant users. *Clinical Neurophysiology, 121*(12), 2070-2082.

Santarelli, R., De Filippi, R., Genovese, E., & Arslan, E. (2008). Cochlear implantation outcome in prelingually deafened young adults. A speech perception study. *Audiology & neuro-otology, 13*(4), 257-265.

Schaul, N. (1998). The fundamental neural mechanisms of electroencephalography. *Electroencephalography and clinical neurophysiology, 106*(2), 101-107.

Schiff, S., Valenti, P., Andrea, P., Lot, M., Bisiacchi, P., Gatta, A., & Amodio, P. (2008). The effect of aging on auditory components of event-related brain potentials. *Clinical Neurophysiology, 119*(8), 1795-1802.

Schimmel, H. (1967). The (±) reference: accuracy of estimated mean components in average response studies. *Science, 157*(784), 92-94.

Schneider, T. R., Debener, S., Oostenveld, R., & Engel, A. K. (2008a). Enhanced EEG gamma-band activity reflects multisensory semantic matching in visual-to-auditory object priming. *NeuroImage, 42*(3), 1244-1254.

Schneider, T. R., Engel, A. K., & Debener, S. (2008b). Multisensory identification of natural objects in a two-way crossmodal priming paradigm. *Experimental Psychology, 55*(2), 121-132.

Sevy, A. B., Bortfeld, H., Huppert, T. J., Beauchamp, M. S., Tonini, R. E., & Oghalai, J. S. (2010). Neuroimaging with near-infrared spectroscopy demonstrates speech-evoked activity in the auditory cortex of deaf children following cochlear implantation. *Hearing Research, 270*(1-2), 39-47.

Shafiro, V. (2008a). Development of a large-item environmental sound test and the effects of short-term training with spectrally-degraded stimuli. *Ear & Hearing 29*(5), 775-790.

Shafiro, V. (2008b). Identification of environmental sounds with varying spectral resolution. *Ear & Hearing 29*(3), 401-420.

Shallop, J. K. (1993). Objective electrophysiological measures from cochlear implant patients. *Ear & Hearing, 14*(1), 58-63.

Sharma, A., Dorman, M. F., & Kral, A. (2005). The influence of a sensitive period on central auditory development in children with unilateral and bilateral cochlear implants. *Hearing Research, 203*(1-2), 134-143.

Sharma, A., Dorman, M. F., & Spahr, A. J. (2002). A sensitive period for the development of the central auditory system in children with cochlear implants: implications for age of implantation. *Ear & Hearing, 23*(6), 532-539.

Shipp, S. (2007). Structure and function of the cerebral cortex. *Current Biology 17*(12), R443-449.

Siesler, H. W. (2002). *Near-infrared spectroscopy : principles, instruments, applications*. Weinheim: Wiley-VCH.

Singh, S., Liasis, A., Rajput, K., Towell, A., & Luxon, L. (2004). Event-related potentials in pediatric cochlear implant patients. *Ear & Hearing, 25*(6), 598-610.

Slotnick, S. D. (2005). Source Localization of ERP Generators. In T. C. Handy (Ed.), *Event-related potentials : a methods handbook* (pp. 149-166). MIT Press.

Spencer, K. M. (2005). Averaging, Detection, and Classification of Single-Trial ERPs In T. C. Handy (Ed.), *Event-related potentials : a methods handbook* (pp. 209-227). Cambridge, Mass.: MIT Press.

Stone, J. V. (2004). *Independent component analysis : a tutorial introduction*. Cambridge, Mass. ; London: MIT Press.

Strelnikov, K., Rouger, J., Demonet, J. F., Lagleyre, S., Fraysse, B., Deguine, O., & Barone, P. Does brain activity at rest reflect adaptive strategies? Evidence from speech processing after cochlear implantation. *Cereb Cortex, 20*(5), 1217-1222.

Strelnikov, K., Rouger, J., Demonet, J. F., Lagleyre, S., Fraysse, B., Deguine, O., & Barone, P. (2010). Does brain activity at rest reflect adaptive strategies? Evidence from speech processing after cochlear implantation. *Cerebral Cortex, 20*(5), 1217-1222.

Summerfield, A. Q., Marshall, D. H., Barton, G. R., & Bloor, K. E. (2002). A cost-utility scenario analysis of bilateral cochlear implantation. *Archives of otolaryngology--head & neck surgery, 128*(11), 1255-1262.

Talsma, D., & Woldorff, M. G. (2005). Methods for the Estimation and Removal of Artifacts and Overlap in ERP Waveforms. In T. C. Handy (Ed.), *Event-related potentials : a methods handbook* (pp. 115-148). Cambridge, Mass.: MIT Press.

Teplan, M. (2002). Fundamentals of EEG measurement. *Measurement Science Review, 2*, 1 -11.

Terhaar, J., Viola, F. C., Baer, K., & Debener, S. (under revision). Neural correlates of altered body perception in depressed patients.

Terhaar, J., Viola, F. C., Franz, M., Berger, S., Bar, K. J., & Weiss, T. (2011). Differential processing of laser stimuli by Adelta and C fibres in major depression. *Pain, 152*(8), 1796-1802.

Theunissen, M., Swanepoel de, W., & Hanekom, J. (2009). Sentence recognition in noise: Variables in compilation and interpretation of tests. *International journal of audiology, 48*(11), 743-757.

Uhler, K., Yoshinaga-Itano, C., Gabbard, S. A., Rothpletz, A. M., & Jenkins, H. (2011). Longitudinal infant speech perception in young cochlear implant users. *Journal of the American Academy of Audiology, 22*(3), 129-142.

UK CI Study Group. (2004). Criteria of candidacy for unilateral cochlear implantation in postlingually deafened adults II: cost-effectiveness analysis. *Ear & Hearing, 25*(4), 336-360.

van Dijk, J. E., van Olphen, A. F., Langereis, M. C., Mens, L. H., Brokx, J. P., & Smoorenburg, G. F. (1999). Predictors of cochlear implant performance. *Audiology, 38*(2), 109-116.

Viola, F. C., Thorne, J., Edmonds, B., Schneider, T., Eichele, T., & Debener, S. (2009). Semi-automatic identification of independent components representing EEG artifact. *Clinical Neurophysiology, 120*(5), 868-877.

Viola, F. C., Thorne, J. D., Bleeck, S., Eyles, J., & Debener, S. (2011). Uncovering auditory evoked potentials from cochlear implant users with independent component analysis. *Psychophysiology*, in press.

Walhovd, K. B., & Fjell, A. M. (2002). One-year test-retest reliability of auditory ERPs in young and old adults. *International journal of psychophysiology : official journal of the International Organization of Psychophysiology, 46*(1), 29-40.

Watson, D. R., Titterington, J., Henry, A., & Toner, J. G. (2007). Auditory sensory memory and working memory processes in children with normal hearing and cochlear implants. *Audiology & neuro-otology, 12*(2), 65-76.

Wessel, J. R., & Ullsperger, M. (2011). Selection of independent components representing event-related brain potentials: a data-driven approach for greater objectivity. *Neuroimage, 54*(3), 2105-2115.

Williamson, R. A., Pytynia, K., Oghalai, J. S., & Vrabec, J. T. (2009). Auditory performance after cochlear implantation in late septuagenarians and octogenarians. *Otology & neurotology : official publication of the American Otological Society, American Neurotology Society [and] European Academy of Otology and Neurotology, 30*(7), 916-920.

Wilson, B. S., & Dorman, M. F. (2008a). Cochlear implants: A remarkable past and a brilliant future. *Hearing Research, 242*(1-2), 3-21.

Wilson, B. S., & Dorman, M. F. (2008b). Cochlear implants: current designs and future possibilities. *Journal of rehabilitation research and development, 45*(5), 695-730.

Winer, J. A., & Schreiner, C. (2010). *The auditory cortex : fundamental neuroscience*. London: Springer.

Wong, D. D., & Gordon, K. A. (2009). Beamformer suppression of cochlear implant artifacts in an electroencephalography dataset. *IEEE Transactions in Biomedical Engineering, 56*(12), 2851-2857.

Zeng, F. G., Rebscher, S., Harrison, W. V., Sun, X., & Feng, H. (2008). Cochlear Implants:System Design, Integration and Evaluation. *IEEE reviews in biomedical engineering, 1*, 115-142.

Zhang, F., Anderson, J., Samy, R., & Houston, L. (2010). The adaptive pattern of the late auditory evoked potential elicited by repeated stimuli in cochlear implant users. *International Journal of Audiology, 49*(4), 277-285.

Zhang, F., Hammer, T., Banks, H. L., Benson, C., Xiang, J., & Fu, Q. J. (2011). Mismatch negativity and adaptation measures of the late auditory evoked potential in cochlear implant users. *Hearing Research, 275*(1-2), 17-29.

Curriculum vitae

Name: Filipa Alexandra Campos Viola
Address: Osterkampsweg 30
26131 Oldenburg, Germany
Email: filipaviola@gmail.com
Telephone: +49 1577-3934428
Date of Birth: 01.01.1982
Place of Birth: Beja, Portugal
Citizenship: Portuguese

Employment history

01.2010 – Present Researcher, PhD Candidate at Carl von Ossietzky University, Dept. of Psychology, Oldenburg, Germany, under the supervision of Prof. Dr. Stefan Debener. Tasks: Project management, writing scientific publications, training and supervision of students, organization of workshops, lecturing in workshops, networking. (Graduating: Fall 2011).

01.2009 – 12.2009 Researcher, PhD Candidate at Biomagnetic Center, Dept. of Neurology, University Hospital Jena, Germany, under the supervision of Prof. Dr. Stefan Debener. Tasks: Electroencephalography recording and analysis, project management, writing of scientific publications, training of students, organization of workshops, lecturing in workshops, networking.

01.2008 – 12.2008 Researcher, PhD Candidate at MRC Institute of Hearing Research, Southampton, UK, under the supervision of Dr. Stefan Debener and Prof. Roger Thornton. Tasks: Electroencephalography recording and analysis, project management, networking.

01.2007 – 12.2007 Research Assistant, MRC Institute of Hearing Research, Southampton, UK. Research topics: Electroencephalography recording and analysis.

09.2003 – 07.2006 Internship at GoLP-CFP (Laser and Plasma Group – Plasma Physics Centre), Instituto Superior Técnico, Lisbon, Portugal. Research topics: optics, interferometry diagnostics for gas jets, image processing, optical aberrations.

Education

09.2006 – 07.2007 Instituto Superior Técnico, Lisbon, Portugal; Masters in Biomedical Engineering; final grade 17/20.

09.2001 – 07.2006 Instituto Superior Técnico, Lisbon, Portugal; Degree in Biomedical Engineering; final grade 16/20.

Awards

01.2008 – Present PhD Studentship from FCT – Fundação para a Ciência e Tecnologia, Ministry of Science and Technology, Portugal (SFRH/BD/37662/2007).

List of Publications

Peer reviewed articles

Viola, F.C., De Vos, M., Hine, J., Sandmann, P., Bleeck, S., Eyles, J., Debener, S. Automatic attenuation of cochlear implant artifacts for the evaluation of late auditory evoked potentials. *Under revision*.

Terhaar, J., Viola, F.C., Israel, A.K., Baer, K.J., Debener S. Neural correlates of altered body perception in depressed patients. *Under revision*.

Viola, F.C., Thorne, J.D., Bleeck, S., Eyles, J., Debener, S. (2011). Uncovering auditory evoked potentials from cochlear implant users with independent component analysis. Psychophysiology (*in press*).

Terhaar, J., Viola, F.C., Franz, M., Berger, S., Baer, K.J., Weiss, T. (2011). Differential processing of laser stimuli by Adelta- and C-fibres in major depression. *Pain, 152*(8), 1796-1802.

Thorne, J.D., Vos, M.D., Viola, F.C., Debener, S. (2011). Cross-modal phase reset predicts auditory task performance in humans. *Journal of Neuroscience*, 31(10), 3853-61.

Viola, F.C., Thorne, J., Edmonds, B., Schneider, T., Eichele, T. & Debener S. (2009). Semi-automatic identification of independent components representing EEG artifact. *Clinical Neurophysiology*, 120, 868-77.

Lemos, N., Lopes, N., Dias, J.M., & Viola, F. (2009). Design and characterization of supersonic nozzles for wide focus laser-plasmas interactions. *Review of Scientific Instruments*, 80, 103301.

Book chapters

Debener, S., Thorne, J., Schneider, T.R. & Viola, F.C. (2010). Using ICA for the Analysis of Multi-Channel EEG data. In: M. Ullsperger & S. Debener (Eds.), Integration of EEG and fMRI: Recording, Analysis, and Application (pp. 121-135). New York: Oxford University Press.